Regulation of cell wall glycopolymers in *Staphylococcus aureus*

Dissertation

der Mathematisch-Naturwissenschaftlichen Fakultät

der Eberhard Karls Universität Tübingen

zur Erlangung des Grades eines

Doktors der Naturwissenschaften

(Dr. rer. nat.)

vorgelegt von

Daniela Keinhörster

aus Essen

Tübingen

2019

Gedruckt mit Genehmigung der Mathematisch-Naturwissenschaftlichen Fakultät der Eberhard Karls Universität Tübingen.

Tag der mündlichen Qualifikation:	19.09.2019
Dekan:	Prof. Dr. Wolfgang Rosenstiel
1. Berichterstatter:	Prof. Dr. Christiane Wolz
2. Berichterstatter:	Prof. Dr. Andreas Peschel

Meiner Familie

Contents

Summary

The human pathogen *Staphylococcus aureus* is a leading cause of bacterial infections worldwide and a growing threat due to the development of antibiotic resistances. A special concern is the emergence of highly pathogenic community-associated methicillin-resistant *S. aureus* (CA-MRSA). While there is not much known about the molecular basis for their enhanced virulence, it likely involves upregulation of several virulence factors. As such, this thesis focusses on the regulation of the cell wall glycopolymers wall teichoic acids (WTA) and capsular polysaccharide (CP) and their impact on CA-MRSA virulence. For WTA, we were able to show that an increased WTA amount in the cell wall contributes to enhanced virulence of CA-MRSA. This is mediated by increased *tarH* expression as a result of enhanced Agr activity and derepression of *tarH* by the Agr antagonist Rot. CP is important for immune evasion due to its anti-phagocytic properties. However, since it simultaneously inhibits adherence by masking the underlying adhesins, both the presence and the absence of CP has been reported to be advantageous for *S. aureus*. While there are several acapsular strains emerging due to mutations in the capsular biosynthesis gene cluster (*capA-capP*) or the promoter region (P_{cap}), CP synthesis can also be switched off in response to environmental conditions via a complex regulatory network. Furthermore, CP expression has been shown to be strictly temporal and only present in a subset of stationary phase cells. We could show that on the transcriptional level this peculiar expression pattern is the consequence of direct SigB-dependent regulation and interference of *cap* repressors such as Rot, CodY and SaeR with the P_{cap} upstream region. Interestingly, this part of the promoter also contains a weak SigA-dependent promoter. Next to transcriptional regulation, there are post-transcriptional mechanisms involved to avoid conflict between precursor usage by the different cell wall glycopolymer biosynthesis machineries in growing bacterial cells. Of note, strains from the prominent CA-MRSA USA300 lineage are usually acapsular. This could be one strategy to ensure the high precursor amounts needed for increased WTA biosynthesis and to avoid possible opposing functions of CP and WTA in regard of adhesion. Elucidating the regulation of WTA and CP biosynthesis contributes to increase their potential as antigen in vaccine development and as prospective target for novel anti-infective strategies.

Zusammenfassung

Der humanpathogene Erreger *Staphylococcus aureus* ist Hauptverursacher bakterieller Infektionen weltweit und stellt durch die Entwicklung von Antibiotikaresistenzen eine wachsende Bedrohung dar. Besonders besorgniserregend ist das Aufkommen hoch pathogener ambulant erworbener Methicillin-resistenter *S. aureus* (CA-MRSA). Deren erhöhte Virulenz ist unter anderem Folge einer verstärkten Expression verschiedener Virulenzfaktoren. Im Rahmen dieser Arbeit sollte daher die Regulation der beiden Zellwand-Glykopolymere Wandteichonsäuren (WTA) und Kapselpolysaccharid (CP) untersucht und ihr Beitrag zur CA-MRSA Virulenz bestimmt werden. Wir konnten zeigen, dass ein erhöhter WTA-Gehalt in den Zellwänden von CA-MRSA zu deren gesteigerten Virulenz beiträgt. Dies geschieht durch vermehrte *tarH* Expression als Folge verstärkter Agr-Aktivität und damit einhergehender Derepression von *tarH* durch Rot. CP spielt durch seine anti-phagozytischen Eigenschaften eine wichtige Rolle bei der Immunevasion, maskiert jedoch gleichzeitig darunterliegenden Adhäsine. Somit ist auch der Verlust von CP durch Mutationen in den Biosynthesegenen (*capA-capP*) oder in der Promotorregion (P_{cap}) vorteilhaft für manche *S. aureus* Stämme. Darüber hinaus kann die Kapselsynthese je nach äußeren Bedingungen durch ein komplexes regulatorisches Netzwerk ausgeschaltet werden. Generell ist die Kapselexpression streng temporär und heterogen, sodass nur ein Teil der Stationär-Phasen-Zellen kapselpositiv ist. Wir konnten zeigen, dass dieses Expressionsmuster auf transkriptioneller Ebene eine Folge direkter SigB-Regulation und der Interaktion zahlreicher *cap* Repressoren wie Rot, CodY und SaeR mit der oberen P_{cap}-Region ist. Interessanterweise enthält diese Promotorregion auch einen schwachen SigA- Promotor. Neben der transkriptionellen Regulation sind auch post-transkriptionelle Mechanismen vorhanden, um eine sinnvolle Verteilung des gemeinsamen Grundbausteins der verschiedenen Glykopolymere in wachsenden bakteriellen Zellen zu gewährleisten. Es ist zu erwähnen, dass der bekannte CA-MRSA Vertreters USA300 einen kapselnegativen Phänotyp aufweist. Dies könnte dazu dienen hohe Mengen des gemeinsamen Grundbausteins für die erhöhte WTA-Biosynthese sicherzustellen und mögliche gegensätzliche Funktionen der beiden Glykopolymere in Bezug auf Adhäsion zu verhindern. Die Aufklärung der Regulation der WTA- und CP-Biosynthese erhöht das Potential dieser Strukturen als Antigen in der Impfstoffentwicklung und als zukünftiges Ziel neuer anti-infektiver Strategien.

List of publications

Accepted manuscripts

1. **Wall teichoic acids mediate increased virulence in *Staphylococcus aureus***
   Stefanie Wanner, Jessica Schade, Daniela Keinhörster, Nicola Weller, Shilpa E. George, Larissa Kull, Jochen Bauer, Timo Grau, Volker Winstel, Henriette Stoy, Dorothee Kretschmer, Julia Kolata, Christiane Wolz, Barbara M. Bröker and Christopher Weidenmaier
   Nature Microbiology (2017), Volume 2, Article number: 16257

2. **Revisiting the regulation of the capsular polysaccharide biosynthesis gene cluster in *Staphylococcus aureus***
   Daniela Keinhörster, Andrea Salzer, Alejandra Duque-Jaramillo, Shilpa E. George, Gabriella Marincola, Jean C. Lee, Christopher Weidenmaier and Christiane Wolz
   Molecular Microbiology (2019), in press

3. **Function and regulation of *Staphylococcus aureus* wall teichoic acids and capsular polysaccharides**
   Daniela Keinhörster, Shilpa E. George, Christopher Weidenmaier and Christiane Wolz
   International Journal of Medical Microbiology (2019), in press

Contribution to publications

Accepted manuscripts

1. **Wall teichoic acids mediate increased virulence in *Staphylococcus aureus***

   To this research article I contributed by isolating RNA and performing quantitative real-time PCR (qRT-PCR) to determine the expression of *tarM* and *tarS*. I also analyzed the expression of RNAIII*, dltA* and *tarH* via qRT-PCR in the USA500 background and isolated the WTA of this strain. Furthermore, I developed and performed the gel shift assay to show direct binding of Rot to the *tarH* and *hla* promoters. In addition, I helped with the performance of the animal experiments and was involved in data evaluation and interpretation, as well as proofreading of the manuscript.

2. **Revisiting the regulation of the capsular polysaccharide biosynthesis gene cluster in *Staphylococcus aureus***

   For this research article, I have made major contributions to the conception and the design of the study and the corresponding experiments. Furthermore, I planned and was involved in creating almost all new mutants, promoter fusion constructs and protein expression vectors. In addition, I performed RNA isolation, 5‘Rapid amplification of cDNA endings (5’RACE), many promoter activity assays and I supervised protein expression and purification, electrophoretic mobility shift assays (EMSAs) and immunofluorescence (IF) experiments. I was also involved in data analysis and interpretation, as well as figure design, writing and editing the manuscript.

3. **Function and regulation of *Staphylococcus aureus* wall teichoic acids and capsular polysaccharides**

   For this review, I was involved in conception of the article and contributed by writing large parts of the manuscript (Abstract, Introduction, Function and Regulation of CP, Conclusions). Together with Christiane Wolz, I was also responsible for editing the manuscript to its final version. Furthermore, I designed Figure 3 and helped with the creation of Figure 1.

Introduction

Staphylococcus aureus and its clinical relevance

The human pathogen *Staphylococcus aureus* is a leading cause of bacterial infections worldwide, ranging from moderately severe infections like minor skin, soft tissue or respiratory infections to dramatic and life-threatening forms of disease manifestations like necrotizing fasciitis or necrotizing pneumonia [1-3]. However, *S. aureus* is also a commensal organism and inhabits the nostrils of about 30% of healthy individuals [1]. This asymptomatic colonization constitutes a major risk for subsequent infection [1].

Antibiotic resistance has become a major complication when treating *S. aureus* infections [3]. Already two years after the clinical introduction of the first antibiotic penicillin, penicillin-resistant *S. aureus* was detected. Today, most infectious *S. aureus* isolates show resistance towards penicillin [3]. To overcome this problem the semisynthetic methicillin was created. However, the first methicillin-resistant *S. aureus* (MRSA) was identified only one year after methicillin was first clinically used [3,4]. Nowadays, MRSA is spread all over the world and is endemic in most hospitals and healthcare facilities in industrialized countries, where it makes up to 50% of infectious *S. aureus* isolates [3]. Next to healthcare-associated MRSA (HA-MRSA) infections, which normally require predisposing risk factors or illnesses, there are now community-associated MRSA (CA-MRSA) emerging with the capacity to infect healthy individuals with no history of hospitalization [1,3]. This suggests that these bacterial strains have greater virulence than the traditional HA-MRSA [1].

Virulence regulation in *S. aureus*

Virulence of *S. aureus* is multi-factorial and depends on a series of toxins, adhesins, immune evasion factors and other virulence determinants [3,5-7]. Regulation of these different virulence factors is very complex and involves several two-component systems (TCS), transcription factors and the alternative sigma factor B (SigB) [8]. Usually the expression of virulence genes is not just controlled by a single regulator but by a network of various interacting regulators. Two well-studied virulence regulators in *S. aureus* are the TCS Agr and Sae, which allow the bacteria to sense and respond to environmental signals by activation and repression of genes. TCS

generally consist of a sensor kinase that is auto-phosphorylated upon activation by a certain signal. The phosphate group is then transferred to a response regulator that activates or represses transcription of the target genes [9].

The histidine sensor kinase SaeS of the Sae system was shown to be activated in response to human neutrophil peptides [10]. The corresponding phosphorylated response regulator SaeR impacts target gene expression by direct binding to their promoters [11]. Of note, activation or inhibition of the Sae system often seem to be strain dependent, especially as several SaeS variants exist which differ in their kinase activity [12,13].

As a quorum sensing system the Agr system encodes a typical auto-activation circuit [14]. Thereby the two proteins AgrA and AgrC constitute a classical two-component signaling module, whereas AgrB and AgrD combine to generate the activating ligand, the autoinducing peptide [14]. This signal molecule binds to and activates the sensor histidine kinase AgrC, which activates the response regulator AgrA, upregulating the promoter of the *agrBDCA* operon and leading to transcription of the RNAIII effector molecule [14]. Agr exerts many of its effects via repression of the transcription factor Rot [15,16]. This is mediated by the annealing of RNAIII to *rot* mRNA, resulting in repression of translation initiation and derepression of Rot-regulated target genes (Fig. 1A) [17]. With increasing activity towards higher cell densities, the Agr system is known for the growth phase-dependent regulation of adhesins and exoproteins [14,18].

An important example of a transcription factor in *S. aureus* is CodY, which is known to regulate several metabolic and virulence genes by direct DNA binding. Of note binding is influenced by the presence of the branched chain amino acids and GTP, making CodY most active under conditions of nutrient excess [19].

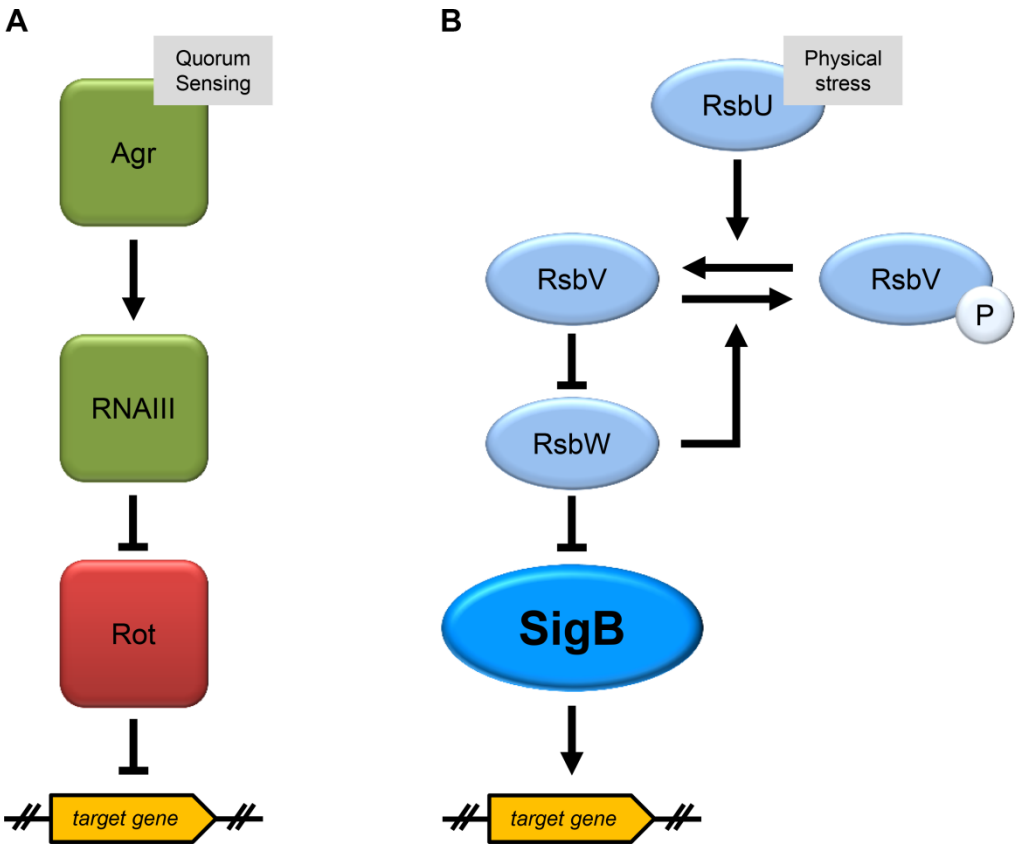

Fig. 1 Mechanism of target gene regulation by the Agr system and the alternative sigma factor B (SigB). (A) The quorum sensing system Agr controls gene expression in a cell density-dependent manner. Upon activation of Agr its effector molecule RNAIII is expressed. RNAIII anneals to *rot* mRNA which results in repression of translation inititation and derepression of Rot-regulated target genes. Thus, Agr and RNAIII function as gene activators (green) and Rot as gene repressor (red). (B) In its inactive state SigB is bound by the anti-sigma factor RsbW, which in addition is able to phosphorylate the anti-sigma factor antagonist RsbV. Upon stress the phosphatase RsbU becomes activated and dephosphorylates the inactive anti-sigma factor antagonist RsbV-P. Unphosphorylated RsbV can interact and complex with RsbW, thereby releasing SigB which is then able to aggregate with the RNA polymerase and form an active holoenzyme for transcription of its target genes.

SigB is involved in the general stress response of *S. aureus* and was shown to regulate many virulence genes and other global virulence regulators [21,22]. SigB is activated upon environmental conditions like acid stress [23], heat stress, salt stress, alkaline stress [20,24] or antibiotic exposure [25] and towards stationary growth phase [24]. Regulation of SigB itself in *S. aureus* primarily occurs on the post-translational level, involving the anti-sigma factor RsbW, the anti-sigma factor antagonist RsbV as well as the phosphatase RsbU (Fig. 1B) [20]. On the transcriptional level the *rsbUVWsigB* operon is controlled by three distinct promoters [20]. Of note, the cold shock protein CspA was shown to bind and stabilize the *rsbVWsigB* transcript [26], thereby increasing the expression of *sigB* and SigB-dependent genes [27-29].

Role of virulence regulation in CA-MRSA

For CA-MRSA it was observed that enhanced virulence was accompanied by more efficient evasion of the host defence systems, likely determining their increased virulence potential [4,30]. While *S. aureus* has developed several strategies for immune evasion, the most crucial is likely the production of toxins that kill human leukocytes [4]. Therefore, a specific toxin repertoire or enhanced toxin production seems to be the basis for enhanced CA-MRSA virulence [30]. While on the one hand additional toxins can be expressed due to the acquisition of novel genes, on the other hand toxins encoded on the core genome can be upregulated by differential gene expression [1,3,4,30]. Recent findings suggest that the Agr system has a strong impact on CA-MRSA virulence by controlling all *S. aureus* toxins involved in immune evasion [31]. Thus, high expression of Agr may contribute to the increased expression of these virulence factors in CA-MRSA [4,30]. However, Agr does not only upregulate immune evasion toxins but is also involved in the regulation of surface binding proteins and other virulence factors like secondary cell wall glycopolymers [32-37].

Cell wall glycopolymers of *S. aureus*

Secondary cell wall glycopolymers are part of the cell envelope and as such involved in host cell interaction. Two prominent examples are wall teichoic acids (WTA) and capsular polysaccharide (CP), which are considered promising targets for anti-infective therapies and vaccines [7,38]. The following information is based on the accepted review article “Function and regulation of *Staphylococcus aureus* wall teichoic acids and capsular polysaccharides”, which can be found in the Appendix for further introduction. Of note, the review already contains results that are described and discussed in more detail in the Results and the Discussion sections.

Wall Teichoic Acids

WTA has multiple functions ranging from maintenance of cell wall biosynthesis, cellular physiology, phage interaction, host cell adhesion, antibiotic resistance and immune regulation [7,39,40]. It is present in all analysed *S. aureus* strains and in most clonal lineages consists of a polyribitol-phosphate backbone [7,41], which is modified with D-alanine and N-acetylglucosamine (GlcNAC) residues. Despite being a dominant surface epitope with multiple roles in host infection, little is known about WTA

regulation. This might be due to the fact that the genes involved in WTA biosynthesis (*tarO, tarAHGBXD, tarI'J'KFIJL, mnaA*) and modification (*dltXABCD, tarM, tarS, tarP*) are scattered throughout the genome. It could be shown that WTA chain length is determined by the Agr system which regulates expression of the RboP polymerase TarK [32]. Furthermore, it was demonstrated that WTA modification is sensitive to changing environmental conditions [42-44]. In particular, the *dlt* operon is regulated by the TCS ArlRS [43] and GraRS [45] as well as by the transcription factor MgrA [46] in response to different environmental stimuli.

Capsular Polysaccharide

Due to its anti-phagocytic properties CP is an essential virulence factor involved in immune evasion [47,48]. However, CP also inhibits adherence of the underlying adhesins so that the presence as well as the absence of CP has been reported to be advantageous for *S. aureus* [49,50]. Acapsular strains usually carry mutations in any of the capsular biosynthesis genes or in the promoter region [49,51]. In particular, strains from the USA300 lineage are CP-negative due to conserved mutations in the *cap5* locus [52]. However, a recent study suggests that USA300 strains might indeed produce CP during infection [53]. Of note, CP synthesis is also highly dependent on environmental conditions, generally low during exponential growth phase [33,34,54-57] and strongly heterogeneous in stationary growth phase [33,34,58-62].

The most prevalent CP serotypes are serotype 5 and 8 [50], which both consist of trisaccharide repeating units of D-N-acetyl mannosaminuronic acid, L-N-acetyl fucosamine, and D-N-acetyl fucosamine. Only the linkages between the sugars and the site of O-acetylation of the mannosaminuronic acid residues are different [63-66]. Regulation of both serotypes is also very similar as their corresponding biosynthesis gene clusters (*capA-capP*) are allelic [67] and share a highly conserved promoter region (P_{cap}) [68]. The operon is mainly transcribed as single large 17 kb transcript [69,70]. P_{cap} activity generally correlates with CP synthesis, indicating that regulation occurs predominantly on the transcriptional level [34,59,60,62,70]. However, the molecular mechanisms of *cap* regulation are elusive. A transcriptional start site (TSS) has been determined, which is not preceded by a classical sigma factor consensus sequence [70]; instead, there were several inverted and direct repeats identified in P_{cap}, amongst which a 10 bp inverted repeat (IR) was shown to be crucial for promoter activity [70]. The IR was proposed to function as an operator site for the *cap* activators

RbsR, which functions as repressor of the *rbsUDK* operon and is thus involved in ribose uptake [71], and MsaB [72], which is also annotated as cold shock protein CspA. In addition to these two regulators there were several other transcription factors (MgrA, CcpA, RpiR, SpoVG, CcpE, XdrA, CodY, Rot), TCS (Agr, ArlRS, KdpDE, AirRS, SaeRS) and SigB shown to be involved in regulation of *cap* expression [7,50]. However, it is not known how all these regulators modulate *cap* expression and how they contribute to the peculiar expression pattern.

Aim

Cell wall glycopolymers like WTA and CP are important virulence factors as they play a major role in *S. aureus* colonization, pathogenesis and bacterial evasion of the host immune defences. Thus, they are evaluated as targets for anti-infective therapies and vaccines. However, synthesis and modification of these molecules is highly variable and mechanisms involved in their regulation are only partially understood.

The first part of the thesis focusses on WTA which is known to play key roles in cellular physiology, colonization, pathogenesis and immune evasion of *S. aureus*. Being such a dominant molecule it is likely that WTA contributes to the increased virulence of highly pathogenic *S. aureus* strains. With highly virulent CA-MRSA strains on the rise, it is of great importance to understand how their increased virulence potential is generated in order to develop new approaches to controlling this important bacterial pathogen. Previous reports indicate that the ability of CA-MRSA to evade human host defence systems is one of the predominant factors assumed to be associated with enhanced virulence. However, the impact of cell wall components has not been studied so far. Here, I aimed to investigate the role of WTA in CA-MRSA virulence and to determine the molecular differences regarding WTA regulation in CA-MRSA versus HA-MRSA strains.

In the second part of the thesis the focus lies on CP regulation. Due to its anti-phagocytic properties which are important for immune evasion, but also the simultaneous inhibition of adherence by masking underlying adhesins, either the presence or absence of CP has been reported to be advantageous for *S. aureus*. In addition, CP expression has been shown to be strictly temporal and only present in a subset of stationary phase cells. Together, this might explain the failure in clinical trials when CP is used alone as antigen in vaccine development against *S. aureus*. Despite a lot of research on CP regulation, the mechanisms responsible for the peculiar expression pattern are still unknown. Here, I aimed to revisit the P_{cap} promoter architecture and to investigate the molecular interference of different regulatory elements involved in *cap* regulation in order to determine the molecular basis for the distinct CP expression pattern.

Results

Regulation of WTA biosynthesis

The results presented here are part of the accepted research article “Wall teichoic acids mediate increased virulence in *Staphylococcus aureus”*, which can be found in the Appendix.

Elevated WTA levels in the cell walls of CA-MRSA strains contribute to their enhanced virulence

To investigate whether there is a difference regarding WTA amounts in the cell walls of CA-MRSA and HA-MRSA and if this plays a role for the enhanced virulence of CA-MRSA we measured the WTA content of several strains using a colorimetric assay. We found that the CA-MRSA strains MW2 and USA300, as well as the clinical isolate 103 contained more WTA in their cell wall fractions in comparison to the non-CA-MRSA laboratory strain SA113 and the clinical isolate 331865. According to their WTA content the strains were grouped into WTA^{high} (MW2, USA300, 103) and WTA^{low} (SA113, 331865) strains (Fig. 2A). In addition, also the HA-MRSA strain USA500 was found to exhibit decreased WTA amounts and was thus classified as WTA^{low}. Of note, differences in WTA polymer length between WTA^{high} and WTA^{low} strains could not be observed.

As readout for virulence we tested the ability of the purified cell wall fractions as well as of live bacterial cells to induce abscess formation in mice. Interestingly, WTA^{high} strains and their cell wall fractions induced skin abscess formation more efficiently than WTA^{low} strains. To exclude that WTA modification contributes to cell wall mediated abscess formation we also analyzed D-alanine and GlcNAc amounts of the isolated WTA and expression of the corresponding modification enzymes via quantitative real-time PCR (qRT-PCR). We could not detect differences in D-alanine levels and *dlt* expression between WTA^{high} and WTA^{low} strains. Of note, in line with elevated *tarM* and *tarS* expression USA300 showed slightly increased GlcNAc amounts in its WTA. However, using cell wall fractions from USA300 lacking the two GlcNAc-transferases TarM and TarS, an impact of GlcNAc modification on abscess induction could not be detected. Thus, we concluded that the enhanced WTA content found in CA-MRSA strains contributes to increased virulence.

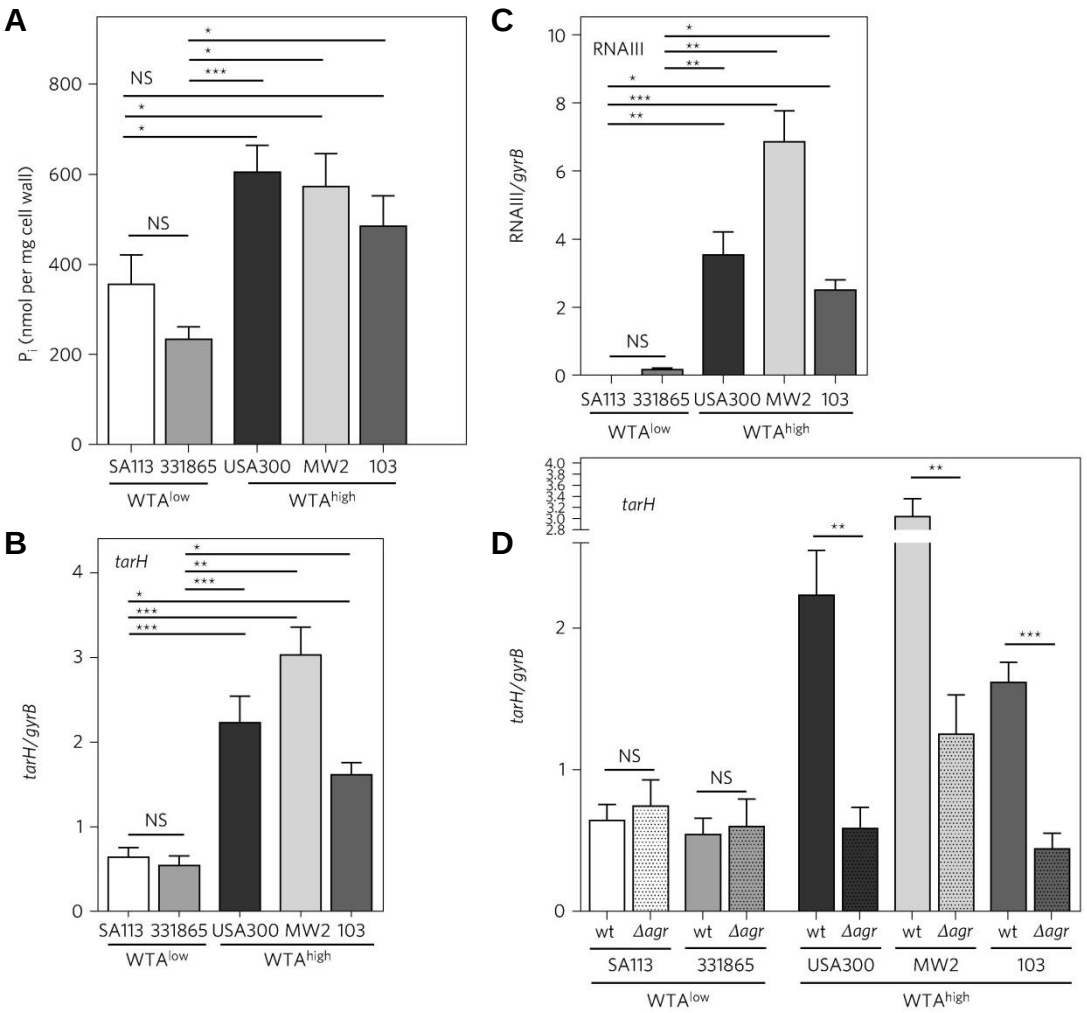

Fig. 2 Amounts of WTA in the cell wall fractions of *S. aureus* strains and transcriptional analysis by qRT–PCR (Figure and Figure legend modified from Figure 1, Wanner et al., 2017, Nature Microbiology). (A) The amount of WTA of different *S. aureus* strains is depicted as nmol inorganic phosphorus (Pi) per mg cell wall dry weight. Shown are means ± standard error of the mean (SEM) for n=8–11 independent WTA isolations. P values for multiple comparisons were determined by one-way ANOVA with Tukey's post-test. *P < 0.05, **P < 0.01, ***P < 0.0001. NS, not significant. (B) Transcriptional analysis of the WTA biosynthesis gene *tarH* and (C) RNAIII, the downstream regulator of the global virulence Agr regulon from *in vitro* cultures grown to stationary phase in WTA^{high} strains and WTA^{low} strains. The expression of transcripts was quantified relative to the transcription of gyrase. Shown are means ± SEM for n = 6 independent experiments. P values for multiple comparisons were determined by one-way ANOVA with Tukey's post-test. *P < 0.05, **P < 0.01, ***P<0.0001. (D) Transcriptional analysis of the WTA biosynthesis gene *tarH*. from *in vitro* cultures grown to stationary phase in WTA^{high}, WTA^{low} and their corresponding *Δagr* mutant strains. The expression of transcripts was quantified relative to the transcription of gyrase. Shown are means ± SEM for n = 6 independent experiments. Statistically significant differences between WTA^{high} and WTA^{low} and their respective mutant strains were determined by Student's t-test. *P < 0.05, **P < 0.01, ***P < 0.001.

The WTA^{high} phenotype is a consequence of *tarH* overexpression

With all analysed strains sharing the same ribitol-WTA structure and biosynthesis pathways we aimed to understand the underlying molecular mechanisms leading to the different WTA contents in WTA^{high} and WTA^{low} strains. Therefore, WTA biosynthesis gene expression of *in vitro* cultures was quantified at two distinct growth phases (logarithmic and stationary growth phase) using qRT-PCR. Of the analyzed

genes (*tarO, tarA, tarK, tarL, tarG* and *tarH*) only *tarH* transcription was significantly increased in WTA^{high} strains compared to WTA^{low} strains. However, this effect was only observed in stationary growth phase (Fig. 2B). The same result was observed for the USA500 strain. *tarH* encodes for the energizing ATPase subunit of the TarGH ABC transporter, which is responsible for the transport of mature WTA over the cytoplasmic membrane [7,73]. Hence, we wondered whether high *tarH* expression would increase WTA export and result in a WTA^{high} phenotype. Indeed, upon overexpression of *tarH* from a plasmid the WTA^{high} phenotype could be restored in WTA^{low} strains, whereas transformation with the empty plasmid did not affect WTA levels (Fig. 3B). Thus, WTA translocation likely constitutes the rate limiting step in WTA biosynthesis and determines WTA contents in the cell wall.

tarH overexpression is mediated by high Agr activity in WTA^{high} strains

The Agr system has previously been shown to be more active in CA-MRSA strains [30,31,74] and is known to affect expression of virulence factors during the transition from exponential to stationary growth phase *in vitro* [8]. With *tarH* being more expressed in WTA^{high} strains and only towards stationary growth phase it seems likely that *tarH* is Agr-controlled. To investigate whether Agr is differentially expressed in WTA^{high} and WTA^{low} strains we measured the expression of the Agr effector molecule RNAIII in stationary growth phase by qRT-PCR. Indeed, WTA^{high} strains revealed higher RNAIII levels than WTA^{low} strains (Fig. 2C). This was also true for the USA500 strain. Of note, the WTA^{low} strain SA113 is a naturally occurring *agr* deletion mutant for which no RNAIII expression could be detected. Next, we compared *tarH* expression in the different strain backgrounds and their corresponding *agr* mutants via qRT-PCR. While there was no difference in *tarH* expression between WTA^{low} wildtype and *agr* mutants, *tarH* expression was significantly decreased in *agr* mutants of WTA^{high} strains (Fig. 2D). Thus, it seems that the WTA^{high} phenotype depends on a highly active Agr system. To further proof this hypothesis, we quantified WTA content of WTA^{high} and WTA^{low} strains and their *agr* mutants using a colorimetric assay (Fig. 3A). In line with qRT-PCR results, mutation of *agr* in WTA^{low} strains had no effect on the WTA content in their cell wall. However, in WTA^{high} background the WTA content of *agr* mutants was significantly reduced to similar levels as in WTA^{low} wildype and *agr* mutants. Furthermore, WTA amounts followed Agr activity by increasing during logarithmic growth and peaking in stationary phase. Due to higher Agr activity this effect was more pronounced in WTA^{high} strains than in WTA^{low} strains and the WTA^{high} phenotype only

developed at the onset of stationary phase. Taken together, there is a clear correlation between Agr activity, *tarH* expression and WTA content. High Agr activity leads to increased *tarH* expression and enhanced WTA content in WTA^{high} strains, whereas WTA^{low} strains are characterized by reduced Agr activity and *tarH* expression.

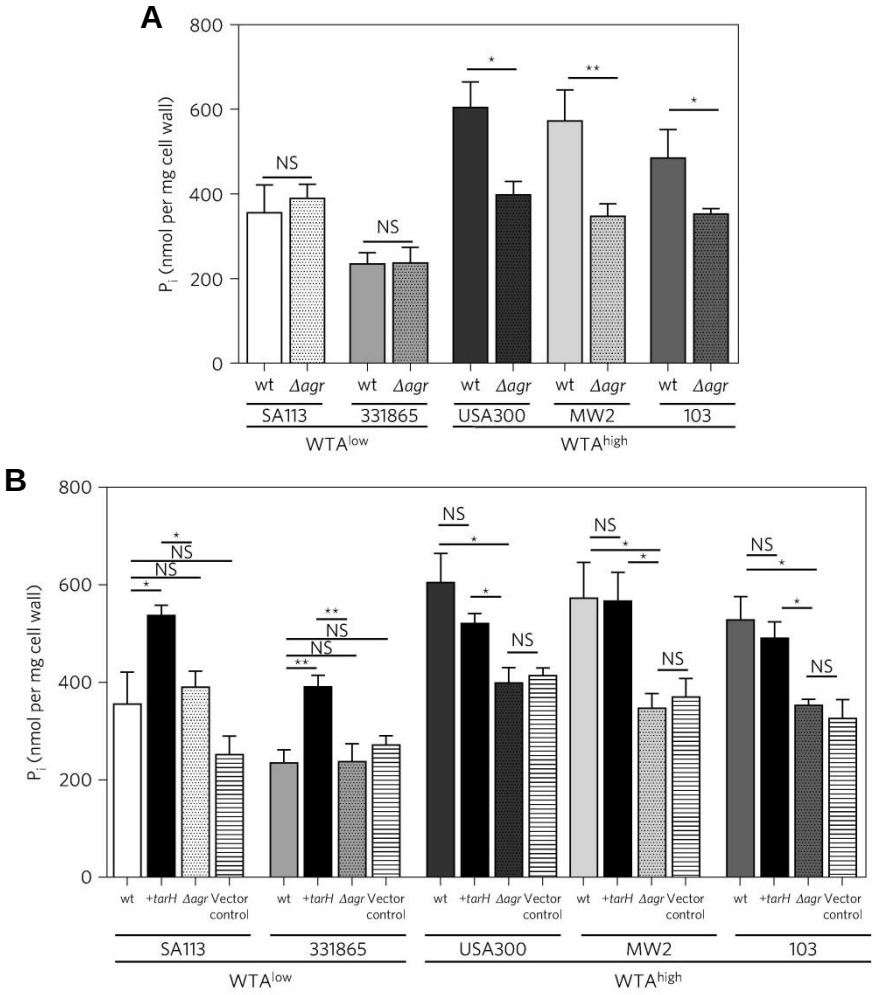

Fig. 3 Agr-dependent control of WTA content in the staphylococcal cell wall (Figure and Figure legend modified from Figure 2, Wanner et al., 2017, Nature Microbiology). (A) Content of WTA in the cell wall of WTA^{high}, WTA^{low} and their corresponding *Δagr* mutant strains. The amount of WTA is depicted as nmol inorganic phosphorus (Pi) per mg cell wall dry weight. Shown are means ± SEM for n=8–11 independent WTA isolations. Statistically significant differences between WTA^{high} and WTA^{low} and their respective *Δagr* mutant strains were determined by Student's t-test. *P < 0.05, **P < 0.01, ***P<0.001. (B) Content of WTA in the cell wall fractions of WTA^{high}, WTA^{low} and their corresponding *Δagr* mutant strains. In addition the WTA content of WTA^{high} and WTA^{low} strains after *tarH* overexpression or containing the empty expression vector (vector control) is shown. The amount of WTA is depicted as nmol inorganic phosphorus (Pi) per mg cell wall dry weight. Shown are means ± SEM for n=8–12 independent WTA isolations. P values for multiple comparisons were determined by one-way ANOVA with Tukey's post-test for each strain. *P < 0.05, **P < 0.01, ***P<0.001.

Rot links *tarH* overexpression with Agr activity

Many Agr effects are exerted via repression of the transcription factor Rot [15,16]. As a mechanism, RNAIII binds to *rot* mRNA, resulting in repression of translation initiation and derepression of Rot-regulated target genes [17]. Measuring *tarH* expression in WTA^{high} and WTA^{low} wildtype and *rot* mutants indeed revealed a significant repressive impact of *rot* on *tarH* expression (Fig. 4A). For example, *tarH* expression levels in a WTA^{low} *rot* mutant were similar to those in WTA^{high} wildtype. In addition, a WTA^{high} *rot agr* double mutant displayed similarly elevated *tarH* expression levels as a *rot* mutant alone, indicating that Agr influences *tarH* expression via Rot. The same could be observed when analysing the WTA content of these strains (Fig. 4B). Measuring RNAIII content in WTA^{high} wildtype and a *rot* mutant showed severely increased levels of RNAIII in the *rot* mutant (Fig. 4C), hinting at direct RNAIII-*rot* interaction and an altered steady state for RNAIII when *rot* is missing. With Rot being a DNA-binding protein, we wondered whether *tarH* repression occurs indeed by direct binding of Rot to the *tarH* promoter region (P_{tarH}). To address this question electrophoretic mobility shift assays (EMSAs) were performed using whole cell lysates. To ensure high Rot levels, cell extracts were isolated from an USA300 *agr* mutant. After incubation of the cell extracts with fluorescently labelled P_{tarH} DNA probe and separation in an agarose gel, a clear shift could be observed (Fig. 4D). In contrast, using cell extract from an isogenic *rot* mutant, such a shift was not detectable, and the promoter fragment was partially degraded. As a reference, the promoter of the Rot repressed *hla* gene (P_{hla}) [75,76] was used, showing a similar shift. Thus, we could clearly demonstrate that Rot directly represses *tarH* and that Agr-dependent *tarH* expression is mediated by derepression of Rot via RNAIII (Fig. 4E).

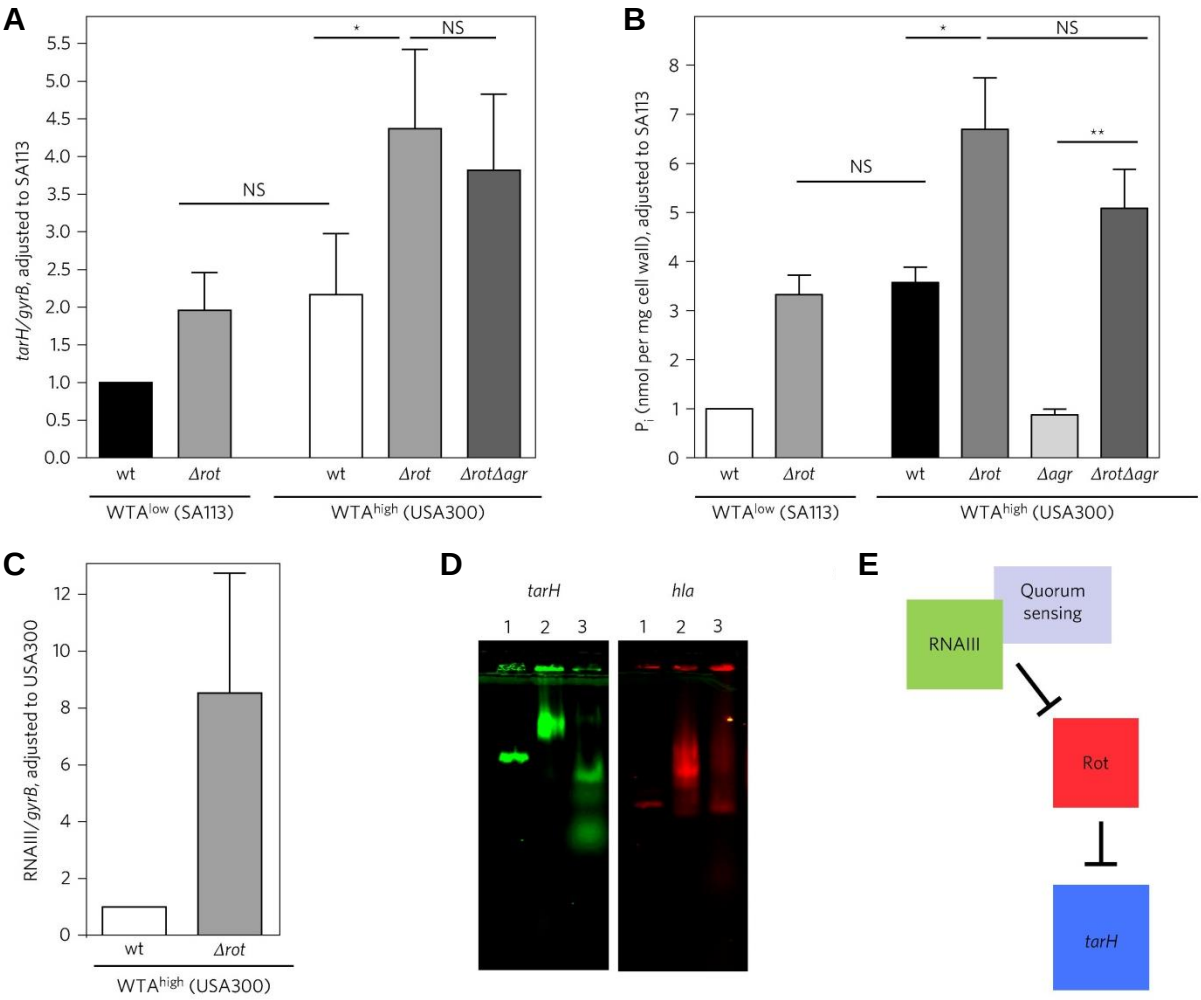

Fig. 4 Rot controls *tarH* expression and WTA biosynthesis downstream of RNAIII (Figure and Figure legend modified from Figure 3, Wanner et al., 2017, Nature Microbiology). (A) Transcription analysis of the WTA biosynthesis gene *tarH* from *in vitro* cultures grown to stationary phase. Expression of transcripts was quantified relative to the transcription of gyrase and adjusted to SA113. Shown are means ± SEM for n = 8 independent experiments. P values for multiple comparisons were determined by one-way ANOVA with Bonferroni's post-test. *P < 0.05. (B) Content of WTA in the cell wall of WTA^{high} (USA300), WTA^{high} *Δrot* mutant (USA300*Δrot*), WTA^{low} (SA113) and WTA^{low} *Δagr* mutant (SA113*Δagr*) strains. The amount of WTA is depicted as nmol inorganic phosphorus (Pi) per mg cell wall dry weight and adjusted to SA113. Shown are means ± SEM for n = 6 independent experiments. P values for multiple comparisons were determined by one-way ANOVA with Bonferroni's post-test. *P < 0.05, **P < 0.01. (C) Transcription analysis of RNAIII in USA300 and its corresponding *Δrot* mutant in stationary-phase cultures. Expression of the RNAIII transcript was quantified relative to the transcription of gyrase and adjusted to USA300. Shown are means ± SEM for n = 8 independent experiments. (D) LI-COR Odyssey-based gel shift assays with cell extracts and labelled *tarH* promoter. Rot binding to the promoter was visualized with cell extracts from a Rot-expressing USA300 strain lacking *agr* (lane 2) and an isogenic *rot* mutant (lane 3). Lane 1 contains the promoter fragment without cell extract as a control. The *hla* promoter (red) was used as a positive control. Rot binding to the *hla* promoter was visualized with cell extracts from a Rot-expressing USA300 strain lacking *agr* (lane 2) and an isogenic *rot* mutant (lane 3). Lane 1 contains the promoter fragment without cell extract as a control. Shown is a representative example of n = 3 independent experiments. (E) The *tarH* regulatory cascade; *tarH* is under negative control of a Rot. Rot mRNA stability is controlled by RNAIII and at high RNAIII levels Rot-mediated repression is relaxed.

Regulation of CP biosynthesis

The results presented here are part of the accepted manuscript “Revisiting the regulation of the capsular polysaccharide biosynthesis gene cluster in *Staphylococcus aureus*”, which can be found in the Appendix.

P_{cap} consists of a SigA- and a SigB promoter

In order to understand how the peculiar CP expression pattern (earlyOff/lateHeterogeneous) is mediated on the molecular level, we first analyzed the structure of the principal promoter P_{cap}. By applying 5’ Rapid Amplification of cDNA Endings (5’ RACE) we identified three putative TSS, two of which were preceded by conserved SigB and SigA consensus sequences, respectively (Fig. 5A). Among these the TSS preceded by the SigB motif was by far the most dominant. While the SigB-dependent promoter in P_{cap} consists of a conserved SigB -35 region, its -10 region contains three mismatches [77]. Interestingly, the SigB -35 region was located within the IR that was previously shown to be crucial for *cap* expression [70]. The identified TSS of the SigB-dependent promoter is in line with previous RNA Seq data of our group and whole genome analyses of TSS in *S. aureus* [78,79]. The TSS preceded by a SigA motif is located further upstream and is also in line with previous predictions [79]. Of note, the TSS described by Ouyang et al. was not detected [70]. However, the third putative TSS was located in close proximity to it but was not preceded by any sigma factor consensus sequence, questioning the presence of a functional promoter. Together, P_{cap} likely contains two promoters, one dominant SigB-dependent promoter and an additional SigA-dependent promoter further upstream.

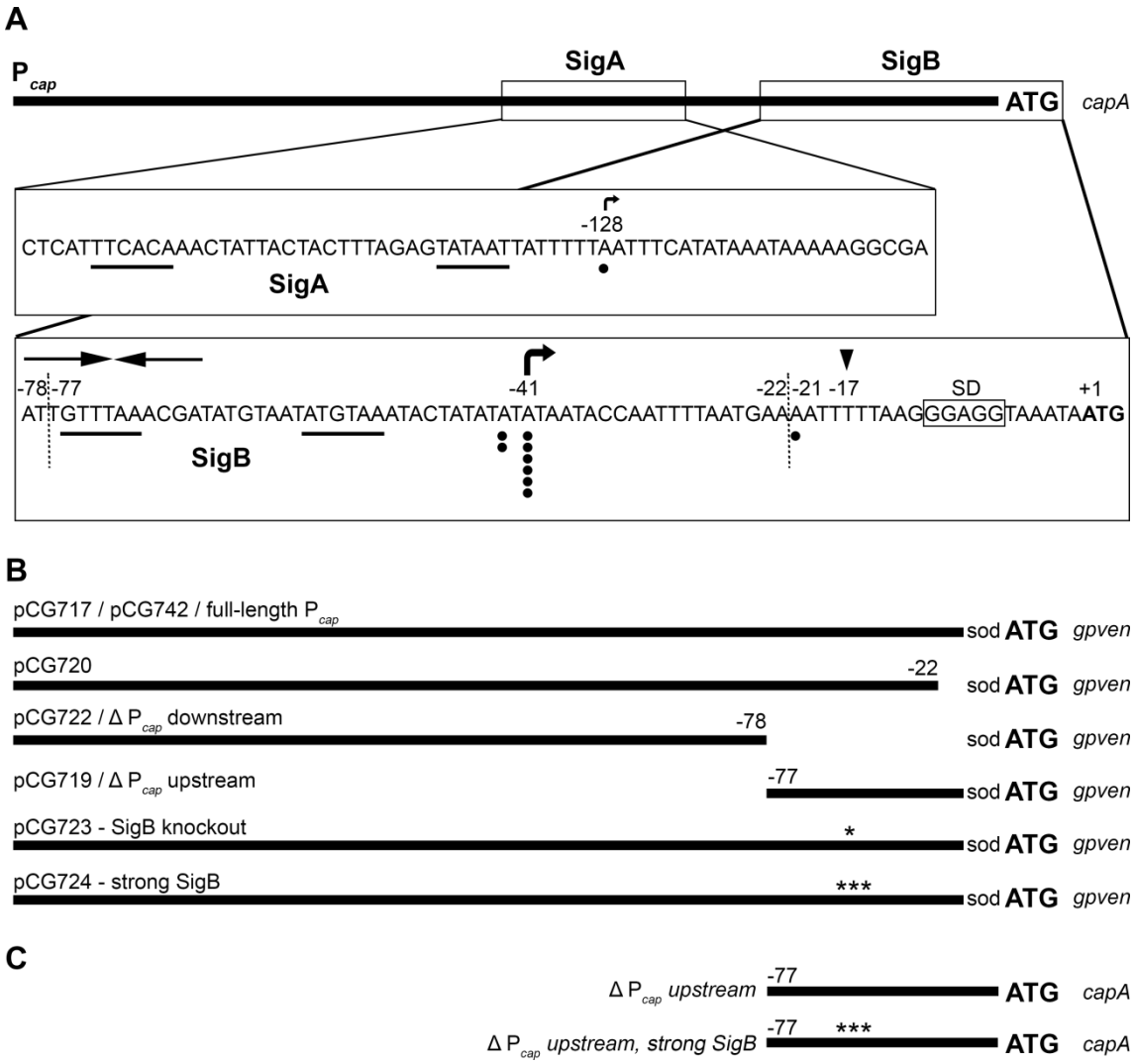

Fig. 5 P_{cap} promoter architecture and P_{cap} variants employed in this study (Figure and Figure legend modified from Figure 1, Keinhörster et al., 2019, Molecular Microbiology). (A) P_{cap} (344 bp) in front of *capA* with magnified SigA- and SigB-promoters. Black dots represent the putative transcriptional start sites (TSSs) suggested by 10 analyzed 5' RACE clones. Sigma factor -35 and -10 motifs are underlined, bent arrows indicate the corresponding TSSs. The TSS and inverted repeat (IR) structure proposed by Ouyang et al. (Ouyang et al., 1999) are marked as black triangle and opposing arrows, respectively. Vertical dashed lines indicate sites of promoter truncation. Numbers mark positions with reference to the ATG of *capA*. The native Shine Dalgarno (SD) sequence is labelled and indicated by a box. (B) P_{cap} promoter fusion variants in front of an artificial ribosomal binding site (sod) and *gpven* gene. Numbers show truncation sites and asterisks indicate point mutations (* -56:G→T; *** 58:A→G, 57:T→G, 52:A→T). (C) Genomic P_{cap} variants in front of *capA*. Numbers show truncation sites and asterisks indicate point mutations (*** 58:A→G, 57:T→G, 52:A→T).

cap expression is directly dependent on SigB activity

Functionality of the identified promoters was assessed by measuring promoter activities of various P_{cap}-*gpven* promoter fusion constructs [80], including deletions of the putative SigA- and SigB-dependent promoters. Deleting the putative TSSs described by Ouyang et al. [70] and the one we identified in close proximity to it did not influence promoter activity. This supports that there is no active promoter in this region. Instead, the putative TSSs may have been derived from RNA processing. When only

the SigA-dependent promoter was present, promoter activity drastically decreased, suggesting very weak promoter activity. In contrast, when the upstream region was deleted and the construct only contained the SigB-dependent promoter, activity was further increased in comparison to the full-length promoter. Thus, *cap* expression is indeed driven by dual promoter activities: a weak SigA-dependent promoter located in the upstream region plus a main SigB-dependent promoter further downstream. Interestingly, even though containing a functional SigA-dependent promoter the main function of the upstream region seems to be repressive. As additional controls to prove direct involvement of SigB in *cap* activation, promoter activity of the native P_{cap} promoter was determined in wildtype and a *rsbUVWsigB* mutant. Furthermore, promoter fusion constructs with mutations in the SigB consensus to either abolish or enhance SigB affinity were created. While deletion of *sigB* or a loss-of-function mutation in the SigB consensus sequence eliminated P_{cap} activity, a strong SigB consensus enhanced promoter activity compared to the native promoter. These results clearly indicate, that SigB is directly involved in and functions as main driver of *cap* expression.

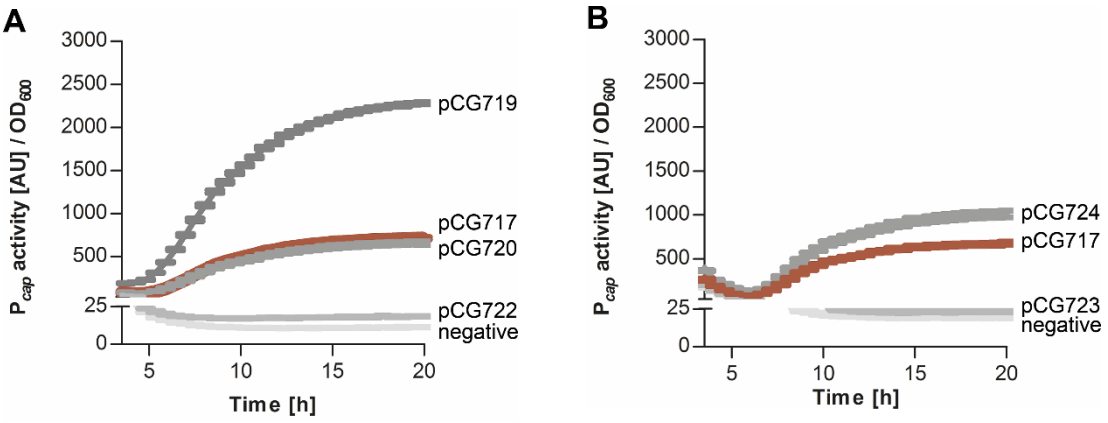

Fig. 6 SigB is the main driver of P_{cap} activity (Figure and Figure legend modified from Figure 2, Keinhörster et al., 2019, Molecular Microbiology). Promoter activities of different truncated (A) or mutated (B) P_{cap} fusions in Newman wildtype. The different promoter fusion constructs are described in Fig. 5B. The promoter activity of the full-length P_{cap} promoter fusion (pCG717) serves as reference and is marked in red. Mean gpVenus intensity per OD_{600} plus standard deviation of biological triplicates is shown over time.

MsaB/CspA contributes to *cap* activation by modulating SigB activity

Interestingly, the identified SigB -35 region was previously described as IR, functioning as a binding site for two putative *cap* activators RbsR and MsaB [71,72]. To determine if and how they interfere with the SigB-dependent promoter, the native P_{cap} promoter fusion was introduced and analyzed in *rbsR* and *msa* mutants. While we could not detect any effect of *rbsR* deletion on P_{cap} activity, in the *msa* mutant P_{cap} activity was

indeed decreased, supporting the finding that MsaB is a *cap* activator. However with MsaB being also annotated as the cold shock protein CspA which was shown to bind and stabilize the *rsbVWsigB* transcript [26], we hypothesized that MsaB/CspA activates *cap* by increasing SigB activity. To address this question, we made use of a dual promoter fusion construct to simultaneously determine P_{cap} and P_{asp23} activities. P_{asp23} is commonly used as readout for SigB activity [77,81,82] and was fused to *gpcer* [80]. With both promoters being directly controlled by SigB we found P_{cap} and P_{asp23} activity to be highly correlated. In the *msa* mutant, both promoters showed weaker activity compared to that in the wildtype. However, upon expression of *sigB* from a constitutive promoter in a *rsbUVWsigB* negative background to avoid post-translational regulation of SigB, *msa* deletion did no longer affect P_{cap} and P_{asp23} activity. This indicates, that *msa* indeed positively affects *cap* expression via modulation of SigB activity. In addition, we performed EMSAs with purified MsaB/CpsA and the full-length P_{cap} promoter, but even using high amounts of protein there was no shift of the labelled DNA probe. This also supports the finding that MsaB/CspA promotes *cap* expression by modulating SigB activity instead of directly binding to P_{cap}.

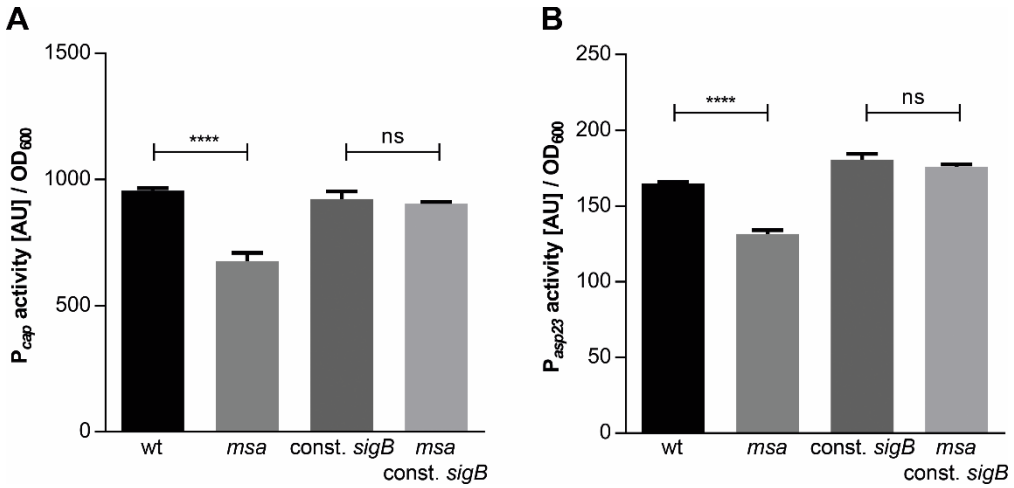

Fig. 7 MsaB/CspA activates *cap* expression by modulating SigB activity (Figure and Figure legend modified from Figure 3, Keinhörster et al., 2019, Molecular Microbiology). Promoter activity of full-length P_{cap}-*gpven* (A) and P_{asp23}-*gpcer* (B) dual promoter fusion (pCG742, see Fig. 5B) in Newman wildtype and a *msa* mutant with or without constitutive *sigB* expression (const. *sigB*). gpCerulean (P_{asp23}) and gpVenus (P_{cap}) intensities are given per OD_{600} after 16 h of growth. Experiments were performed in biological triplicates, error bars represent the standard deviation. Statistical significance was obtained by ordinary one-way ANOVA followed by Tukey's multiple comparison test (ns: not significant, ****: p<0.0001).

P_{cap} upstream region is of repressive function

To further investigate the repressive function of the P_{cap} upstream region we focused on the role of the three known *cap* repressors CodY, Rot and Sae. Therefore, full-length P_{cap} as well as upstream or downstream truncated promoter variants were introduced in *codY*, *rot* and *sae* single and triple mutants. Mutation of any of the three regulators led to a significant increase of promoter activity of full-length P_{cap}, confirming that they are indeed *cap* repressors. That their effects are additive could be observed by the fact, that in the triple mutant the promoter activity was even higher than in the single mutants. Interestingly, mutation of the repressors had no or only minor effects on promoter activity when the upstream region of P_{cap} was deleted, indicating that the repressors target this region to repress *cap*. Of note, promoter activity of the upstream truncated construct even exceeded that of the full-length promoter in the triple mutant. This suggests that next to CodY, Rot and Sae, the upstream region is also targeted by other repressors. When we additionally analyzed the effect of the repressors on the SigA-dependent promoter which is also located within the P_{cap} upstream region, we noticed that neither CodY nor Rot affected promoter activity. Only mutation of *sae* led to an increase of promoter activity of the SigA-dependent promoter, even though it remained weak compared to the full-length promoter. Thus, the three known *cap* repressors CodY Rot and Sae mediate their effects by targeting the P_{cap} upstream region thereby interfering with SigB-dependent promoter activity.

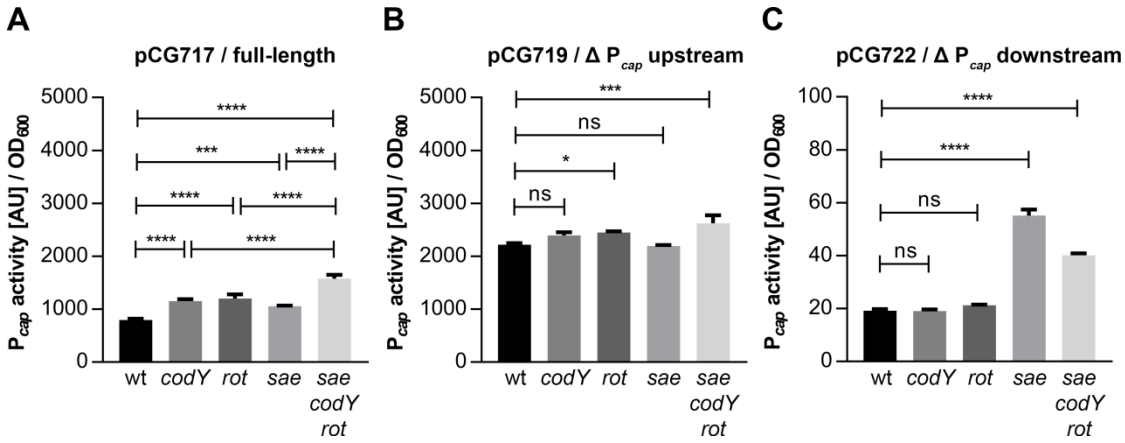

Fig. 8 CodY, Rot and Sae repress *cap* expression by interfering with the P_{cap} upstream region (Figure and Figure legend modified from Figure 4, Keinhörster et al., 2019, Molecular Microbiology). Promoter activity of different P_{cap} truncations in Newman wildtype, *codY*, *rot*, *sae* single and triple mutants (A-C). The different promoter fusion constructs are described in Fig. 5B. gpVenus intensity is given per OD_{600} after 16 h of growth. Experiments were performed in biological triplicates, error bars represent the standard deviation. Statistical significance was determined by ordinary one-way ANOVA followed by Dunnett's multiple comparison test (ns: not significant, *: p<0.1, ***: p<0.001, ****: p<0.0001).

CodY, Rot and Sae directly bind to the P_{cap} upstream region

Having shown that CodY Rot and Sae repress *cap* by targeting the P_{cap} upstream region, the question arises whether repression occurs through direct DNA binding. Therefore, we performed EMSAs with purified CodY, Rot and SaeR proteins. Of note, SaeR can only bind to DNA in its phosphorylated state [11]. Thus, we created a phosphomimetic SaeR harboring a D51E substitution. Incubating $SaeR^{D51E}$ with fluorescently labelled P_{cap} upstream region resulted in the formation of a protein-DNA complex. Such a protein-DNA complex could not be observed when unphosphorylated native SaeR was used. Binding of $SaeR^{D51E}$ to the P_{cap} upstream region is in line with a putative binding motif located in this region [12]. Also Rot and CodY were shown to bind specifically to the P_{cap} upstream region. Thus, the EMSA results are in line with finding described above, that the three repressors target the P_{cap} upstream region. Of note, CodY was previously shown to bind to the downstream region of P_{cap} reaching into the coding region of *capA* [83]. Using such a probe in our EMSAs we could confirm binding of CodY to the P_{cap} downstream region. Together, SaeR and Rot directly bind to the P_{cap} upstream region, whereas CodY binds two distinct sites, one in the P_{cap} upstream region and one further downstream reaching into the coding region of *capA*.

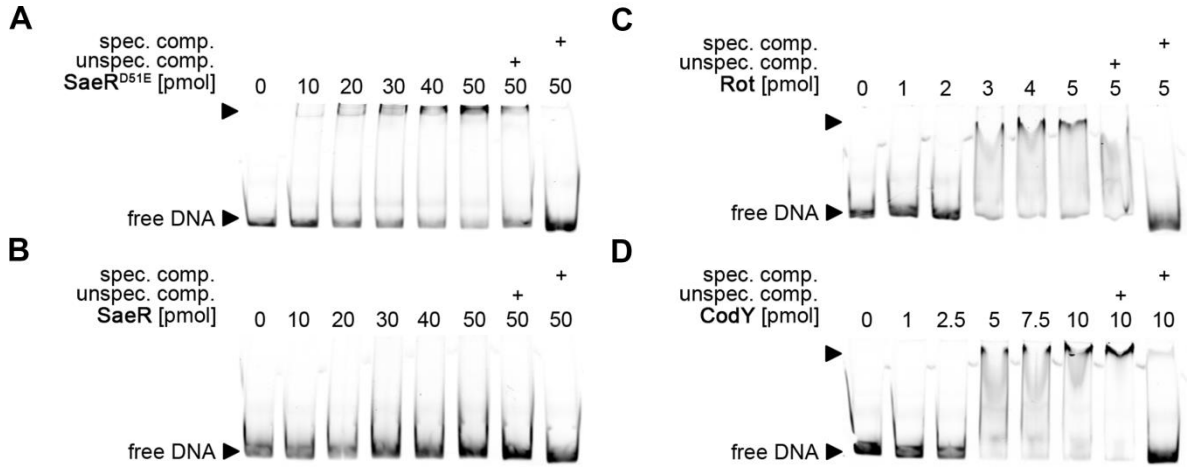

Fig. 9 CodY, Rot and SaeR bind directly to P_{cap} upstream region (Figure and Figure legend modified from Figure 5, Keinhörster et al., 2019, Molecular Microbiology). Electrophoretic mobility shift assays of purified $SaeR^{D51E}$ (A), SaeR (B), Rot (C) and CodY (D). Increasing amounts of protein were incubated with fluorescently labelled P_{cap} upstream region (-78 to -344 from *capA*, see Fig. 5A). As a control for specificity, shifts were subject to competition with the promoter of the 16 S rRNA gene (unspec. comp.) or unlabelled P_{cap} upstream region (-78 to -344 from *capA*, see Fig. 5A) (spec. comp.) in 100 fold excess. Representative pictures from at least three independently performed experiments are shown.

SigB activity and upstream repressors contribute to the peculiar CP expression

To confirm that all the promoter-based results described above indeed translate into CP production, we used immunofluorescence (IF) to detect CP. This also allowed us to determine the impact of our findings on temporal and heterogeneous CP synthesis. In order to ensure that all bacteria are actively dividing and do not contain residual CP from stationary phase we diluted the cultures thrice before proceeding with the IF experiment. CP production was investigated throughout growth at five different time points. In line with previous results, growing bacteria did not show CP production, but as soon as they reached stationary growth phase approximately 40% of the population became CP-positive [34]. With SigB being a known regulator of late genes [21,22,24,78] we wanted to investigate if SigB-dependent regulation determines growth phase-dependent *cap* expression. Indeed, detection of P_{cap} and P_{asp23} promoter activity on the single cell level via fluorescence microscopy showed the expected growth phase dependency with the two promoters reaching their maximum activities in stationary growth phase. Interestingly, P_{asp23} activity was already detectable in some bacteria from exponential growth phase which was not the case for P_{cap} activity. This indicates that also SigB activity itself is heterogeneous but is not sufficient to activate P_{cap} early in growth. We wondered if constitutive *sigB* expression would affect CP production. Expressing *sigB* from a constitutive promoter in a *rsbUVWsigB* negative background led to an earlier onset of CP production and 50% CP-positive cells in stationary phase. However, a bigger impact on CP synthesis was observed upon genomic deletion of the P_{cap} upstream region with an earlier onset of CP production and 83% CP-positive cells in stationary growth phase. In addition, in this background CP heterogeneity in stationary phase was strongly reduced and completely abolished in combination with constitutive *sigB* expression. Thus, it seems to be the combination of repression mediated by the upstream promoter region and SigB activity that is responsible for heterogeneous CP expression pattern in stationary growth phase. Of note, CP synthesis remained growth phase-dependent. To exclude that this was due to the rather weak SigB promoter in P_{cap}, we altered the SigB -10 region to match the conserved SigB consensus sequence on the chromosome of the upstream truncated strain. In combination with constitutive *sigB* expression this shifted the onset of CP production even further towards early growth but the majority of the population remained CP-negative in early growth.

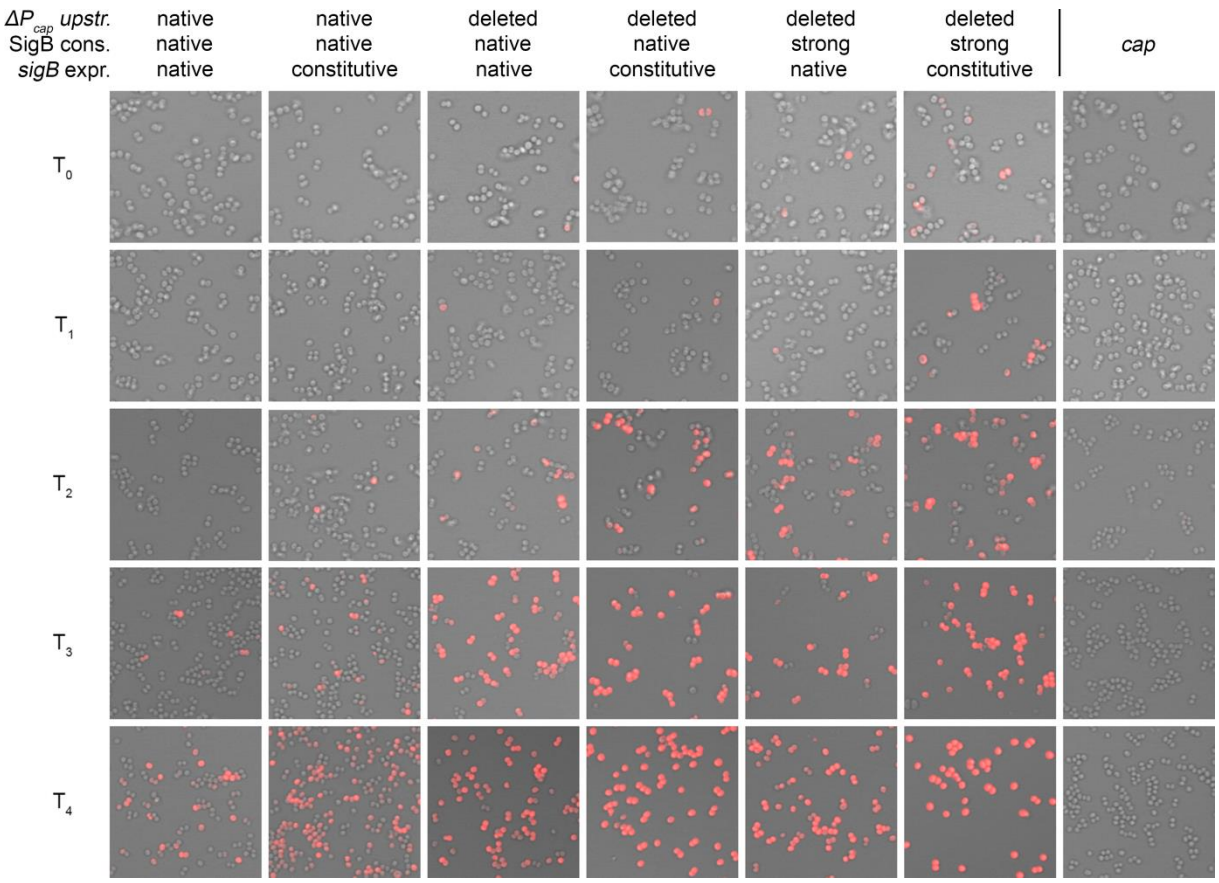

Fig. 10 SigB regulation and upstream repressors determine temporal and heterogeneous CP synthesis (Figure and Figure legend modified from Figure 6, Keinhörster et al., 2019, Molecular Microbiology). Detection of CP production by bacteria from different growth phases via immunofluorescence. The wildtype strain Newman was mutated in order to delete the upstream region (*ΔP$_{cap}$ upstr.*), to contain a strong SigB -10 consensus motif (SigB cons.) and/or constitutive *sigB* expression (*sigB* expr.) and grown to defined growth phase T_0 - T_4. The different genomic P$_{cap}$ variants are described in Fig. 5C. Representative pictures from at least three independent cultures are shown.

CP synthesis is additionally controlled on the post-transcriptional level

In order to investigate whether growth phase-dependent CP production in this strain correlates with *capA* transcript levels, we quantified *capA* mRNA via qRT-PCR and compared it with a corresponding wildtype. While the wildtype shows strongly repressed *capA* transcript levels in early growth phase, in the P$_{cap}$ upstream region truncated strain with strong SigB consensus sequence and constitutive *sigB* expression, *capA* mRNA was stronger and constitutively expressed. With CP production still being growth phase-dependent despite an active promoter, this suggests the existence of post-transcriptional mechanisms of CP regulation.

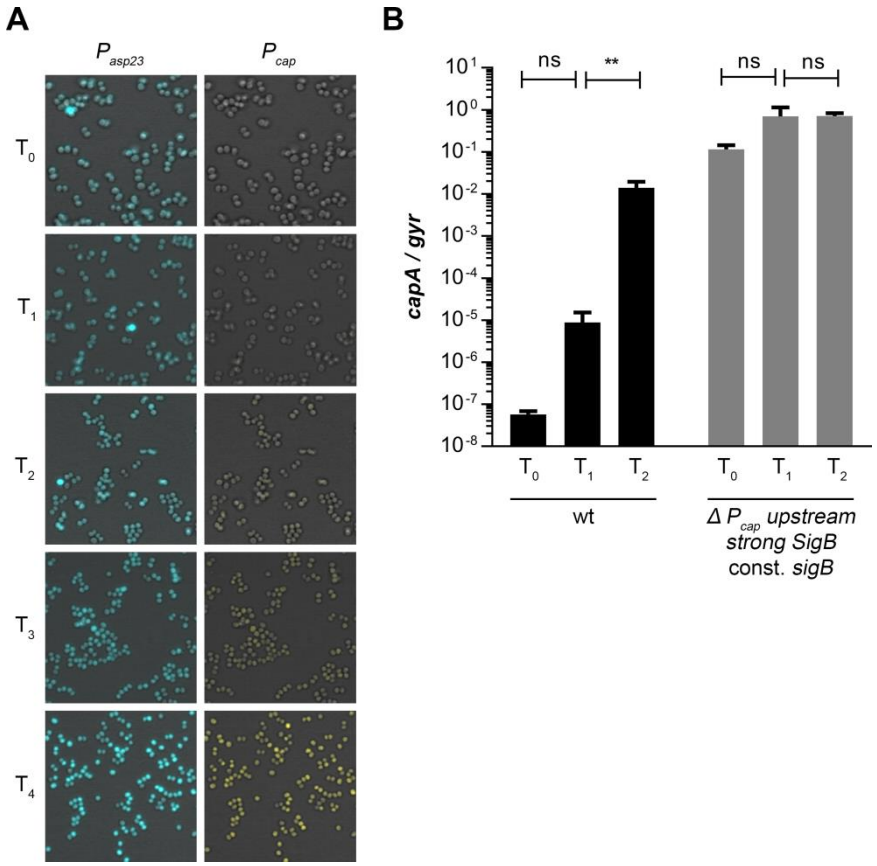

Fig. 11 *capA* transcription can be rendered constitutive (Figure and Figure legend modified from Figure 7, Keinhörster et al., 2019, Molecular Microbiology). (A) Promoter activities of P_{asp23}-*gpcer* and full-length P_{cap}-*gpven* dual promoter fusion (pCG742, see Fig. 5B) in Newman wildtype. Bacteria cells were grown to defined growth phase T_0 - T_4. Representative pictures from at least three independent cultures are shown. (B) Bacterial cells were harvested at different growth phases (T_0-T_2) and total RNA was isolated. *capA* transcripts in Newman wild-type and a P_{cap} upstream truncated strain with strong SigB -10 consensus sequence and additional constitutive *sigB* expression (Newman *ΔP_{cap} upstream*, *strong SigB*, const. *sigB*) were measured by qRT-PCR and normalized to *gyr*. The genomic P_{cap} variant is described in Fig. 5C. Experiments were performed in biological triplicates, error bars represent the standard deviation. Statistical significance was determined by ordinary one-way ANOVA followed by Tukey's multiple comparison test (ns: not significant, **: p<0.01).

cap regulation is conserved in different *S. aureus* strains

To validate the findings that we made for strain Newman which is special in terms of its hyperactive Sae system [84] in a different *S. aureus* background, we chose the widely studied CA-MRSA strain USA300. Due to three crucial mutations, one in the SigB -35 consensus sequence in P_{cap} and two in the coding regions of *cap5D* and *cap5E* [52] this strain has an acapsular phenotype. In order to analyze CP production in a first step we either only repaired the mutation in P_{cap} or all three mutations. In line with previous studies the USA300 wildtype is acapsular and the repair of the mutation in P_{cap} is not sufficient to allow CP production *in vitro* [52]. Only upon repair of all three mutations USA300 was capable of producing CP. Of note, the repaired strain shows the same peculiar CP expression pattern as strain Newman with CP-positive cells only being observed towards stationary growth phase and CP expression being strongly

heterogeneous. With deletion of the upstream promoter region and a strong SigB -10 consensus sequence, the onset of CP production could be shifted towards an earlier time point and CP was uniformly expressed. Thus, CP expression and its regulation in USA300 and Newman is highly conserved.

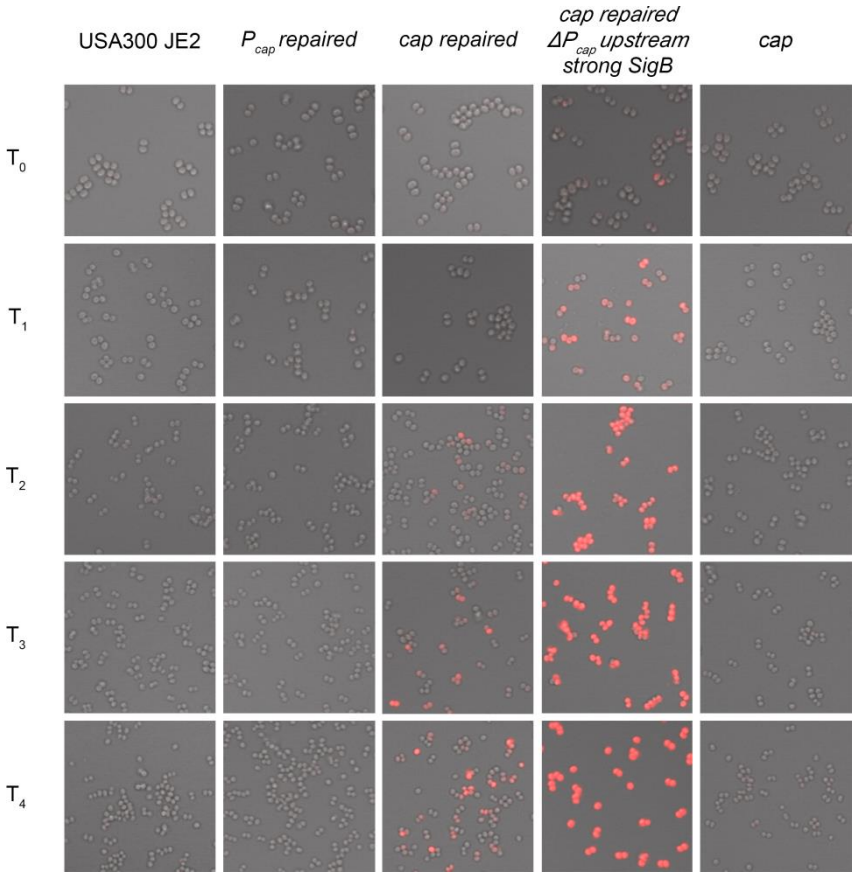

Fig. 12 CP production in strain USA300 JE2 (Figure and Figure legend modified from Figure 8, Keinhörster et al., 2019, Molecular Microbiology). Detection of CP in bacteria from different growth phases. USA300 JE2 wildtype and mutants in which either the mutation in P_{cap} alone (*P_{cap} repaired*) or in the whole *cap* locus (*P_{cap}, capD, capE*; *cap repaired*) are repaired were grown to defined growth phase T_0 - T_4 and CP was detected by immunofluorescence. In addition, the effect of P_{cap} upstream truncation and a strong SigB -10 consensus sequence (*cap repaired, ΔP_{cap} upstream, strong SigB*) was analyzed. This genomic P_{cap} variant is described in Fig. 5C. Representative pictures of at least three independent cultures are shown.

Discussion

Regulation of WTA biosynthesis

We identified the increased expression of the WTA biosynthesis gene *tarH* in late growth phase as molecular mechanism behind the WTA^{high} phenotype of CA-MRSA strains. *tarH* expression is connected to the activity of the Agr quorum sensing system via Rot-dependent repression. Rot is an important repressor of several Agr targets [15,16] and increased *tarH* expression is mediated by high levels of the Agr effector molecule RNAIII, which efficiently reduces Rot-mediated repression [17]. To date there is no defined consensus sequence for Rot but it seems to preferentially bind to AT-rich promoters [85]. With the *tarH* promoter region being AT-rich this argues for Rot-dependent control of the *tarH* promoter and we were indeed able to show that Rot directly represses *tarH* by binding to its promoter region.

Our results support previous findings in which the Agr system was demonstrated to be highly active in CA-MRSA strains [30,31,74]. All WTA^{high} strains analysed showed a high activity of Agr, whereas in WTA^{low} strains Agr activity was weak or even inactive due to a non-functional Agr regulon. High Agr levels subsequently result in Agr-dependent overexpression of *tarH* which as part of the TarGH transporter constitutes the possible bottleneck in WTA production. That its indeed translocation which is the rate limiting factor of WTA biosynthesis is in line with the fact that several identified WTA biosynthesis inhibitors function by only targeting TarG [41,86,87].

In addition to leading to a higher WTA content of CA-MRSA strains, the Agr system was previously shown to be involved in regulation of WTA polymer length. Meredith et al reported, that in NCTC8325 background high Agr activity leads to the dominant formation of longer WTA [32]. In our experiments we could not detect differences in polymer length of WTA of WTA^{high} and WTA^{low} strains. However, it is possible that in NCTC8325 as a methicillin-sensitive *S. aureus* strain WTA biosynthesis might be regulated differently and that Agr activity might also differ in these strains.

Interestingly, our results indicate that Agr does not impact WTA modification as there was no difference in D-alanine and GlcNAc content of WTA isolated from WTA^{high} and WTA^{low} strains or in the expression of modification enzymes. Only strain USA300 showed a slight increase in GlcNAc content, which indicates strain specific differences in the regulation of WTA GlcNAc modification via so far elusive mechanisms.

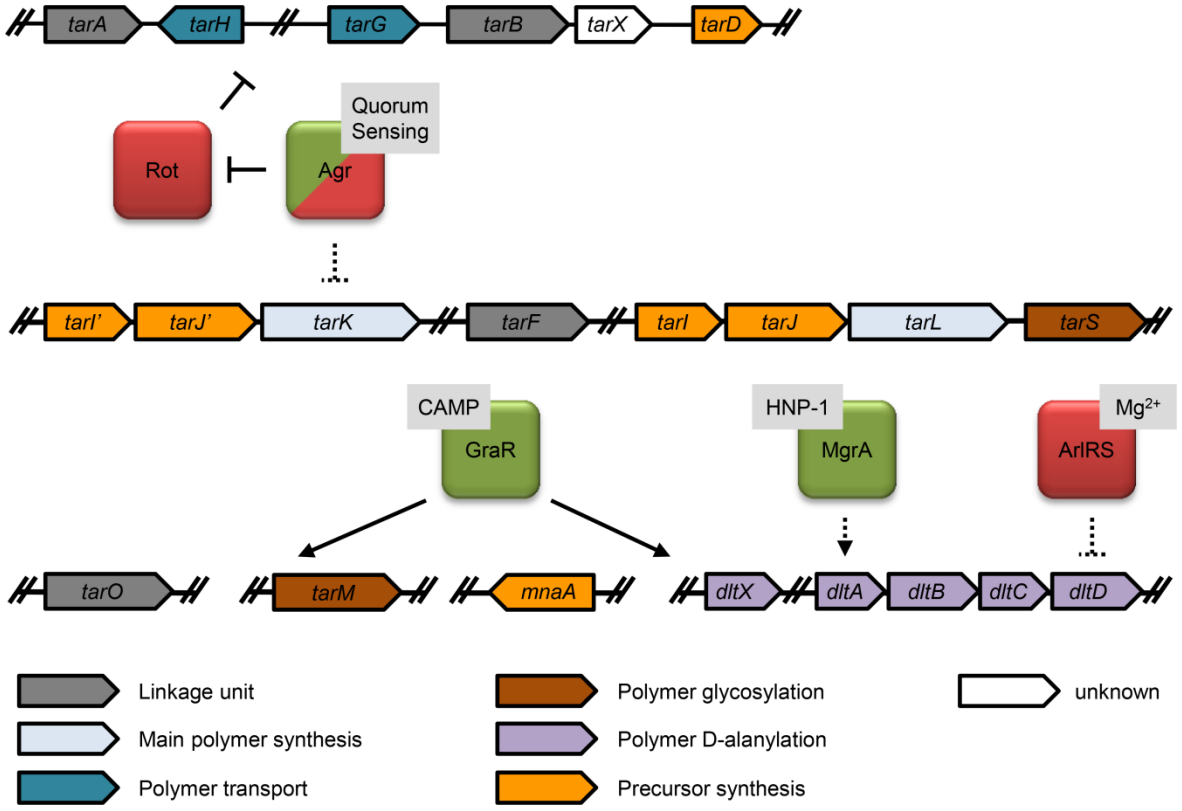

Fig. 13 Genetic organisation, function and regulation of genes involved in WTA biosynthesis and modification (Figure and Figure legend modified from Figure 1, Keinhörster et al., 2019, International Journal of Medical Microbiology). Regulators in green indicate upregulation, in red downregulation. Solid lines show direct interaction of the regulators with target genes, dashed lines mark unknown mechanisms of regulation. Signals controlling the activity of the regulators are shown in boxes. CAMP: cationic antimicrobial peptides, HNP: human neutrophil peptide.

With our work we shed some new light on the poorly investigated regulatory mechanisms involved in WTA biosynthesis and modification. The current understanding of WTA regulation is summarized in Fig. 13. By elucidating the molecular basis for enhanced WTA content we have potentially identified a new target for the development of novel anti-staphylococcal strategies that might help to combat highly virulent CA-MRSA strains.

Regulation of CP biosynthesis

We could show that on the transcriptional level the peculiar *cap* expression pattern is the consequence of direct SigB-dependent regulation and interference of regulators targeting the P_{cap} upstream region with SigB-dependent promoter activity.

Remarkably, the identified SigB-35 region is directly located within the IR which was shown to be crucial for *cap* expression [70]. Hence, any mutations in this region led to abolished *cap* expression due to its function as a SigB binding site. Next to direct activation of *cap* expression, SigB is also known to activate other *cap* activators like SpoVG, ArlRS-MgrA and RsbR [21,22,60,71,88]. While direct SigB-dependent regulation seems to be the main driver of *cap* expression, other SigB-dependent *cap* regulators likely contribute to its finetuning and amplify SigB dependency.

The two putative *cap* activators RbsR and MsaB were previously shown to bind to the SigB -35 region [71,72]. However, we could not observe an effect of RbsR on P_{cap} activity. As RbsR likely functions as metabolic sensor the discrepancy with the previous results of Lei and Lee [71] could be due to different growth conditions. For MsaB/CspA we could observe an activating effect on *cap* expression. However, we found that this was mediated by modulation of SigB activity instead of directly binding to P_{cap}. Thus, a role of MsaB as classical transcription factor needs to be questioned. In fact, it was shown that MsaB/CspA binds *rsbVWsigB* mRNA and increases transcript stability [26]. Our findings that MsaB/CspA increases the expression of *sigB* and SigB-dependent genes is in line with previous observations [27-29]. Together, our data indicate that under the conditions employed, the only function of the previously described IR is to contain the binding site for the SigB holoenzyme.

In addition to the SigB-dependent promoter we identified an additional SigA-dependent promoter further upstream. However, due to its weak promoter activity this promoter only seems to play a minor role in *cap* expression. An explanation for such a low promoter activiy could be the sub-optimal structure and spacing of the SigA consensus sequence in P_{cap} [89,90] and the in general lower activity of SigA promoters compared to SigB promoters [78]. Nevertheless, changes in temperature, salt and solute concentrations, as well as protein factors and ligands can affect promoter kinetics by 10 - 1000 fold or more [90]. Thus, under certain conditions the SigA-dependent promoter can get activated, which might be the case during infections with strains from

the USA300 lineage. These strains have a non-functional SigB promoter due to point mutations in the SigB consensus motif. However, recently these strains were shown to produce CP during infection [53], which could be the consequence of activation of the weak SigA-dependent promoter.

Despite containing a second promoter, the main function of the P_{cap} upstream region seems to be repressive. Repression is mediated by several transcription factors and TCS such as CodY, Rot and Sae that directly target the upstream region. While CodY and Rot only interfered with SigB-dependent promoter activity, Sae was capable to additionally repress SigA-dependent promoter activity. In line with a predicted SaeR binding site located between both promoters and in close proximity to the SigB consensus sequence [12], SaeR likely represses SigB via sterical hindrance and the SigA-dependent promoter via a roadblock mechanism. In contrast, how Rot and CodY affect SigB-dependent promoter activity remains unclear but one might speculate that their repression is mediated by secondary promoter structures that bring them into close proximity to the SigB consensus and allow them to interfere with SigB binding. It has been shown that DNA structures like supercoiling are involved in the regulation of bacterial gene expression [91] and for *cap* expression it was shown that its supercoiling sensitive [92]. Regarding the two CodY binding sites in P_{cap} we were able to show that the binding site in the upstream region alone is sufficient for *cap* repression.

While the regulators targeting the upstream region of P_{cap} were identified to be mainly responsible for heterogeneous CP production, the residual heterogeneity resulted from variable SigB activity within cells. These findings are in line with a prediction stating that more transcription factor binding sites result in noisier promoters [93]. Of note, CP production always remained growth phase-dependent even though *cap* expression was rendered constitutive. This indicates that there are further post-transcriptional levels of regulation involved. In fact, these might be required with CP synthesis being linked to the metabolic status of the cell. As such the precursor for CP biosynthesis UDP N-acetylglucosamine is mainly derived from gluconeogenesis which mainly takes place when glucose becomes limited towards later growth phases [94]. Furthermore, peptidoglycan, WTA and CP biosynthesis all make use of the universal bactoprenol carrier lipid, which could become limited in earlier growth phases [86]. The coordination of cell wall polymer synthesis was recently reported to involve reversible protein phosphorylation of CapM and CapE [95].

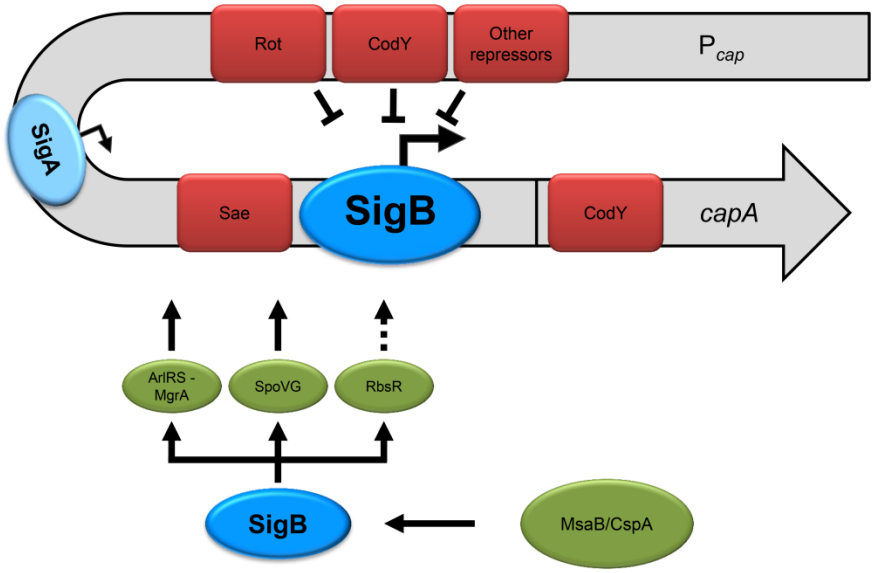

Fig. 14 Transcriptional regulation of *cap* expression (Figure and Figure legend modified from Figure 9, Keinhörster et al., 2019, Molecular Microbiology). *cap* expression is mainly driven from a SigB-dependent promoter. However, there is a second weak SigA-dependent promoter further upstream. In addition, the P_{cap} upstream region is targeted by the *cap* repressors SaeR, CodY, Rot and others. Of note, Rot and CodY only interfere with SigB-dependent promoter activity, whereas Sae is able to repress both. A predicted SaeR binding motif is located between the SigA- and SigB-dependent promoters. P_{cap} contains a second CodY binding site reaching into the coding region of *capA*. The depicted binding sites for the upstream regulators (relative to each other and the SigA promoter) are arbitrary and further studies are needed to localize these site(s) and their mechanisms of action. SigB activity is modulated by MsaB/CspA, promoting *sigB* transcript stability. Consequently, MsaB/CspA likely also affects indirect SigB-dependent P_{cap} activation through ArlRS-MgrA, SpoVG and RbsR. However, for RbsR we were unable to prove an activating effect on *cap* expression.

All together, we could elucidate the transcriptional regulation of CP synthesis and identify the determinants of the peculiar earlyOff/lateHeterogeneous *cap* expression pattern (Fig. 14). These include the alternative sigma factor SigB as well as several repressors targeting the P_{cap} upstream region. In addition, with the identification of an additional SigA-dependent promoter we provide the molecular basis for the unusual finding that some strains of the USA300 lineage which were thought to be CP-negative are capable of producing a capsule *in vivo*. Thus, CP production during infection might be of greater importance than currently anticipated. With CP5 and CP8 conjugate vaccines still believed to be important components for multivalent staphylococcal vaccines (Weidenmaier and Lee, 2017), knowledge on how and when CP is expressed might provide a rationale for its use as vaccine component and to predict a patient cohort which likely benefits from such a vaccine.

Cell wall glycopolymers in CA-MRSA

We identified WTA as an important virulence factor which is directly involved in strain-specific virulence of *S. aureus*. CA-MRSA exploit overexpression of WTA biosynthesis as a mechanism to gain virulence. In contrast, the majority strains of the USA300 lineage were shown to be acapsular [52]. With peptidoglycan, WTA and CP biosynthesis all depending on the universal bactoprenol carrier lipid [86] abolished CP production can be one strategy of CA-MRSA to ensure the high precursor amounts needed for enhanced WTA biosynthesis. In addition, CA-MRSA cells avoid spending energy on the synthesis of two structures with likely opposing functions in regard of adhesion. However, other CA-MRSA strains like MW2 which express high levels of WTA and are capable of producing CP [51] indicate that in general WTA and CP production are not exclusive. Interestingly, both structures are preferentially expressed towards later growth phases. In the first place this is likely to ensure an essential amount of precursors for peptidoglycan biosynthesis. However, how coordination between WTA and CP biosynthesis is regulated, especially with both pathways involving the same regulator Agr remains to be investigated. Further studies are required to investigate whether WTA biosynthesis and modification also shows such a high degree of heterogeneity as CP does. If so, with respect to the function of these molecules and the available precursor levels one would expect that WTA producing cells are CP-negative and vice versa. Consequently, a combination of both structures as antigens for vaccine development should then be discussed to combat *S. aureus* infections.

References

1. DeLeo FR, Otto M, Kreiswirth BN, Chambers HF. Community-associated meticillin-resistant *Staphylococcus aureus*. Lancet. 2010;375(9725):1557-68.
2. Stryjewski ME, Chambers HF. Skin and soft-tissue infections caused by community-acquired methicillin-resistant *Staphylococcus aureus*. Clin Infect Dis. 2008;46 Suppl 5:S368-S77.
3. Otto M. MRSA virulence and spread. Cell Microbiol. 2012;14(10):1513-21.
4. Otto M. Basis of virulence in community-associated methicillin-resistant *Staphylococcus aureus*. Annu Rev Microbiol. 2010;64:143-62.
5. Gordon RJ, Lowy FD. Pathogenesis of methicillin-resistant *Staphylococcus aureus* infection. Clin Infect Dis. 2008;46 (Supplement 5):350-9.
6. de Jong NWM, van Kessel KPM, van Strijp JAG. Immune Evasion by *Staphylococcus aureus*. Microbiol Spectr. 2019;7(2).
7. Weidenmaier C, Lee JC. Structure and function of surface polysaccharides of *Staphylococcus aureus*. Curr Top Microbiol Immunol. 2017;409:57-93.
8. Novick RP. Autoinduction and signal transduction in the regulation of staphylococcal virulence. Mol Microbiol. 2003;48(6):1429-49.
9. Hoch JA. Two-component and phosphorelay signal transduction. Curr Opin Microbiol. 2000;3(2):165-70.
10. Geiger T, Goerke C, Mainiero M, Kraus D, Wolz C. The virulence regulator Sae of *Staphylococcus aureus*: promoter activities and response to phagocytosis-related signals. J Bacteriol. 2008;190(10):3419-28.
11. Sun F, Li C, Jeong D, Sohn C, He C, Bae T. In the *Staphylococcus aureus* two-component system *sae*, the response regulator SaeR binds to a direct repeat sequence and DNA binding requires phosphorylation by the sensor kinase SaeS. J Bacteriol. 2010;192(8):2111-27.
12. Liu Q, Yeo WS, Bae T. The SaeRS two-component system of *Staphylococcus aureus*. Genes (Basel). 2016;7(10):81.
13. Luong TT, Sau K, Roux C, Sau S, Dunman PM, Lee CY. *Staphylococcus aureus* ClpC divergently regulates capsule via *sae* and *codY* in strain Newman but activates capsule via *codY* in strain UAMS-1 and in strain Newman with repaired *saeS*. J Bacteriol. 2011;193(3):686-94.
14. Novick RP, Geisinger E. Quorum sensing in staphylococci. Annu Rev Genet. 2008;42:541-64.

15. Said-Salim B, Dunman PM, McAleese FM, Macapagal D, Murphy E, McNamara PJ, et al. Global Regulation of Staphylococcus aureus Genes by Rot. Journal of Bacteriology. 2003;185(2):610-9.
16. Geisinger E, Adhikari RP, Jin R, Ross HF, Novick RP. Inhibition of rot translation by RNAIII, a key feature of agr function. Mol Microbiol. 2006;61(4):1038-48.
17. Boisset S, Geissmann T, Huntzinger E, Fechter P, Bendridi N, Possedko M, et al. *Staphylococcus aureus* RNAIII coordinately represses the synthesis of virulence factors and the transcription regulator Rot by an antisense mechanism. Genes Dev. 2007;21(11):1353-66.
18. Thoendel M, Kavanaugh JS, Flack CE, Horswill AR. Peptide signaling in the staphylococci. Chem Rev. 2011;111(1):117-51.
19. Majerczyk CD, Dunman PM, Luong TT, Lee CY, Sadykov MR, Somerville GA, et al. Direct targets of CodY in *Staphylococcus aureus*. J Bacteriol. 2010;192(11):2861-77.
20. Senn MM, Giachino P, Homerova D, Steinhuber A, Strassner J, Kormanec J, et al. Molecular analysis and organization of the sigmaB operon in Staphylococcus aureus. J Bacteriol. 2005;187(23):8006-19.
21. Bischoff M, Dunman P, Kormanec J, Macapagal D, Murphy E, Mounts W, et al. Microarray-based analysis of the *Staphylococcus aureus* sigmaB regulon. J Bacteriol. 2004;186(13):4085-99.
22. Bischoff M, Entenza JM, Giachino P. Influence of a functional sigB operon on the global regulators *sar* and *agr* in *Staphylococcus aureus*. J Bacteriol. 2001;183(17):5171-9.
23. Palma M, Cheung AL. sigma(B) activity in Staphylococcus aureus is controlled by RsbU and an additional factor(s) during bacterial growth. Infect Immun. 2001;69(12):7858-65.
24. Pane-Farre J, Jonas B, Förstner K, Engelmann S, Hecker M. The sigmaB regulon in *Staphylococcus aureus* and its regulation. Int J Med Microbiol. 2006;296(4-5):237-58.
25. Donegan NP, Cheung AL. Regulation of the mazEF toxin-antitoxin module in Staphylococcus aureus and its impact on sigB expression. J Bacteriol. 2009;191(8):2795-805.
26. Caballero CJ, Menendez-Gil P, Catalan-Moreno A, Vergara-Irigaray M, Garcia B, Segura V, et al. The regulon of the RNA chaperone CspA and its auto-regulation in *Staphylococcus aureus*. Nucleic Acids Res. 2018;46(3):1345-61.

27. Sahukhal GS, Elasri MO. Identification and characterization of an operon, *msaABCR*, that controls virulence and biofilm development in *Staphylococcus aureus*. BMC Microbiol. 2014;14:154.
28. Katzif S, Lee EH, Law AB, Tzeng YL, Shafer WM. CspA regulates pigment production in *Staphylococcus aureus* through a SigB-dependent mechanism. J Bacteriol. 2005;187(23):8181-4.
29. Donegan NP, Manna AC, Tseng CW, Liu GY, Cheung AL. CspA regulation of *Staphylococcus aureus* carotenoid levels and sigma(B) activity is controlled by YjbH and Spx. Molecular Microbiology. 2019.
30. Otto M. Community-associated MRSA: what makes them special? Int J Med Microbiol. 2013;303(6-7):324-30.
31. Cheung GY, Wang R, Khan BA, Sturdevant DE, Otto M. Role of the accessory gene regulator *agr* in community-associated methicillin-resistant *Staphylococcus aureus* pathogenesis. Infect Immun. 2011;79(5):1927-35.
32. Meredith TC, Swoboda JG, Walker S. Late-stage polyribitol phosphate wall teichoic acid biosynthesis in *Staphylococcus aureus*. J Bacteriol. 2008;190(8):3046-56.
33. Pohlmann-Dietze P, Ulrich M, Kiser KB, Döring G, Lee JC, Fournier JM, et al. Adherence of *Staphylococcus aureus* to endothelial cells: influence of capsular polysaccharide, global regulator *agr*, and bacterial growth phase. Infect Immun. 2000;68(9):4865-71.
34. George SE, Nguyen T, Geiger T, Weidenmaier C, Lee JC, Liese J, et al. Phenotypic heterogeneity and temporal expression of the capsular polysaccharide in *Staphylococcus aureus*. Mol Microbiol. 2015;98(6):1073-88.
35. Dassy B, Hogan T, Foster TJ, Fournier JM. Involvement of the accessory gene regulator (*agr*) in expression of type 5 capsular polysaccharide by *Staphylococcus aureus*. J Gen Microbiol. 1993;139 (Pt 6):1301-6.
36. Luong T, Sau S, Gomez M, Lee JC, Lee CY. Regulation of *Staphylococcus aureus* capsular polysaccharide expression by *agr* and *sarA*. Infect Immun. 2002;70(2):444-50.
37. van Wamel W, Xiong YQ, Bayer AS, Yeaman MR, Nast CC, Cheung AL. Regulation of *Staphylococcus aureus* type 5 capsular polysaccharides by *agr* and *sarA in vitro* and in an experimental endocarditis model. Microb Pathog. 2002;33(2):73-9.

38. Ansari S, Jha RK, Mishra SK, Tiwari BR, Asaad AM. Recent advances in *Staphylococcus aureus* infection: focus on vaccine development. Infect Drug Resist. 2019;12:1243-55.
39. van Dalen R, De La Cruz Diaz JS, Rumpret M, Fuchsberger FF, van Teijlingen NH, Hanske J, et al. Langerhans cells sense *Staphylococcus aureus* wall teichoic acid through langerin to induce inflammatory responses. MBio. 2019;10(3):e00330-19.
40. Weidenmaier C, Peschel A. Teichoic acids and related cell-wall glycopolymers in gram-positive physiology and host interactions. Nat Rev Microbiol. 2008;6(4):276-87.
41. Brown S, Santa Maria JP, Jr., Walker S. Wall teichoic acids of gram-positive bacteria. Annu Rev Microbiol. 2013;67:313-36.
42. Neuhaus FC, Baddiley J. A continuum of anionic charge: structures and functions of D-alanyl-teichoic acids in gram-positive bacteria. Microbiol Mol Biol Rev. 2003;67(4):686-723.
43. Koprivnjak T, Mlakar V, Swanson L, Fournier B, Peschel A, Weiss JP. Cation-induced transcriptional regulation of the *dlt* operon of *Staphylococcus aureus*. J Bacteriol. 2006;188(10):3622-30.
44. Mistretta N, Brossaud M, Telles F, Sanchez V, Talaga P, Rokbi B. Glycosylation of *Staphylococcus aureus* cell wall teichoic acid is influenced by environmental conditions. Sci Rep. 2019;9(1):3212.
45. Falord M, Mäder U, Hiron A, Debarbouille M, Msadek T. Investigation of the *Staphylococcus aureus* GraSR regulon reveals novel links to virulence, stress response and cell wall signal transduction pathways. PLoS One. 2011;6(7):e21323.
46. Li L, Wang G, Cheung A, Abdelhady W, Seidl K, Xiong YQ. MgrA governs adherence, host cell interaction, and virulence in a murine model of bacteremia due to *Staphylococcus aureus*. J Infect Dis. 2019: jiz219.
47. Thakker M, Park JS, Carey V, Lee JC. *Staphylococcus aureus* serotype 5 capsular polysaccharide is antiphagocytic and enhances bacterial virulence in a murine bacteremia model. Infect Immun. 1998;66(11):5183-9.
48. Nanra JS, Buitrago SM, Crawford S, Ng J, Fink PS, Hawkins J, et al. Capsular polysaccharides are an important immune evasion mechanism for *Staphylococcus aureus*. Hum Vaccin Immunother. 2013;9(3):480-7.

49. Tuchscherr L, Löffler B, Buzzola FR, Sordelli DO. *Staphylococcus aureus* adaptation to the host and persistence: role of loss of capsular polysaccharide expression. Future Microbiol. 2010;5(12):1823-32.
50. O'Riordan K, Lee JC. *Staphylococcus aureus* capsular polysaccharides. Clinical Microbiology Reviews. 2004;17(1):218-34.
51. Cocchiaro JL, Gomez MI, Risley A, Solinga R, Sordelli DO, Lee JC. Molecular characterization of the capsule locus from non-typeable *Staphylococcus aureus*. Mol Microbiol. 2006;59(3):948-60.
52. Boyle-Vavra S, Li X, Alam MT, Read TD, Sieth J, Cywes-Bentley C, et al. USA300 and USA500 clonal lineages of *Staphylococcus aureus* do not produce a capsular polysaccharide due to conserved mutations in the *cap5* locus. MBio. 2015;6(2):e02585-14.
53. Mohamed N, Timofeyeva Y, Jamrozy D, Rojas E, Hao L, Silmon de Monerri NC, et al. Molecular epidemiology and expression of capsular polysaccharides in *Staphylococcus aureus* clinical isolates in the United States. PLoS One. 2019;14(1):e0208356.
54. Cunnion KM, Lee JC, Frank MM. Capsule production and growth phase influence binding of complement to *Staphylococcus aureus*. Infect Immun. 2001;69(11):6796-803.
55. Dassy B, Fournier JM. Respiratory activity is essential for post-exponential-phase production of type 5 capsular polysaccharide by *Staphylococcus aureus*. Infect Immun. 1996;64(7):2408-14.
56. Poutrel B, Gilbert FB, Lebrun M. Effects of culture conditions on production of type 5 capsular polysaccharide by human and bovine *Staphylococcus aureus* strains. Clin Diagn Lab Immunol. 1995;2(2):166-71.
57. Conlon BP, Rowe SE, Gandt AB, Nuxoll AS, Donegan NP, Zalis EA, et al. Persister formation in *Staphylococcus aureus* is associated with ATP depletion. Nature Microbiology. 2016;1(5):16051.
58. Poutrel B, Rainard P, Sarradin P. Heterogeneity of cell-associated CP5 expression on *Staphylococcus aureus* strains demonstrated by flow cytometry. Clin Diagn Lab Immunol. 1997;4(3):275-8.
59. Hartmann T, Baronian G, Nippe N, Voss M, Schulthess B, Wolz C, et al. The catabolite control protein E (CcpE) affects virulence determinant production and pathogenesis of *Staphylococcus aureus*. J Biol Chem. 2014;289(43):29701-11.

60. Meier S, Goerke C, Wolz C, Seidl K, Homerova D, Schulthess B, et al. sigmaB and the sigmaB-dependent *arlRS* and *yabJ-spoVG* loci affect capsule formation in *Staphylococcus aureus*. Infect Immun. 2007;75(9):4562-71.
61. Seidl K, Stucki M, Ruegg M, Goerke C, Wolz C, Harris L, et al. *Staphylococcus aureus* CcpA affects virulence determinant production and antibiotic resistance. Antimicrob Agents Chemother. 2006;50(4):1183-94.
62. Jansen A, Szekat C, Schröder W, Wolz C, Goerke C, Lee JC, et al. Production of capsular polysaccharide does not influence *Staphylococcus aureus* vancomycin susceptibility. BMC Microbiol. 2013;13:65.
63. Fournier JM, Vann WF, Karakawa WW. Purification and characterization of *Staphylococcus aureus* type 8 capsular polysaccharide. Infect Immun. 1984;45(1):87-93.
64. Fournier JM, Hannon K, Moreau M, Karakawa WW, Vann WF. Isolation of type 5 capsular polysaccharide from *Staphylococcus aureus*. Ann Inst Pasteur Microbiol. 1987;138(5):561-7.
65. Moreau M, Richards JC, Fournier JM, Byrd RA, Karakawa WW, Vann WF. Structure of the type 5 capsular polysaccharide of *Staphylococcus aureus*. Carbohydr Res. 1990;201(2):285-97.
66. Jones C. Revised structures for the capsular polysaccharides from *Staphylococcus aureus* Types 5 and 8, components of novel glycoconjugate vaccines. Carbohydr Res. 2005;340(6):1097-106.
67. Goerke C, Esser S, Kümmel M, Wolz C. *Staphylococcus aureus* strain designation by *agr* and *cap* polymorphism typing and delineation of *agr* diversification by sequence analysis. Int J Med Microbiol. 2005;295(2):67-75.
68. Herbert S, Newell SW, Lee C, Wieland KP, Dassy B, Fournier JM, et al. Regulation of *Staphylococcus aureus* type 5 and type 8 capsular polysaccharides by CO2. J Bacteriol. 2001;183(15):4609-13.
69. Sau S, Sun J, Lee CY. Molecular characterization and transcriptional analysis of type 8 capsule genes in *Staphylococcus aureus*. J Bacteriol. 1997;179(5):1614-21.
70. Ouyang S, Sau S, Lee CY. Promoter analysis of the *cap8* operon, involved in type 8 capsular polysaccharide production in *Staphylococcus aureus*. J Bacteriol. 1999;181(8):2492-500.
71. Lei MG, Lee CY. RbsR activates capsule but represses the *rbsUDK* operon in *Staphylococcus aureus*. J Bacteriol. 2015;197(23):3666-75.

72. Batte JL, Samanta D, Elasri MO. MsaB activates capsule production at the transcription level in *Staphylococcus aureus*. Microbiology. 2016;162(3):575-89.
73. Schirner K, Stone LK, Walker S. ABC transporters required for export of wall teichoic acids do not discriminate between different main chain polymers. ACS Chem Biol. 2011;6(5):407-12.
74. Montgomery CP, Boyle-Vavra S, Daum RS. Importance of the global regulators Agr and SaeRS in the pathogenesis of CA-MRSA USA300 infection. PLoS One. 2010;5(12):e15177.
75. McNamara PJ, Milligan-Monroe KC, Khalili S, Proctor RA. Identification, cloning, and initial characterization of *rot*, a locus encoding a regulator of virulence factor expression in *Staphylococcus aureus*. J Bacteriol. 2000;182(11):3197-203.
76. Oscarsson J, Kanth A, Tegmark-Wisell K, Arvidson S. SarA is a repressor of *hla* (alpha-hemolysin) transcription in *Staphylococcus aureus*: its apparent role as an activator of *hla* in the prototype strain NCTC 8325 depends on reduced expression of *sarS*. J Bacteriol. 2006;188(24):8526-33.
77. Homerova D, Bischoff M, Dumolin A, Kormanec J. Optimization of a two-plasmid system for the identification of promoters recognized by RNA polymerase containing *Staphylococcus aureus* alternative sigma factor B. FEMS Microbiology Letters. 2004;232(2):173-9.
78. Mäder U, Nicolas P, Depke M, Pane-Farre J, Debarbouille M, van der Kooi-Pol MM, et al. *Staphylococcus aureus* transcriptome architecture: from laboratory to infection-mimicking conditions. PLoS Genet. 2016;12(4):e1005962.
79. Prados J, Linder P, Redder P. TSS-EMOTE, a refined protocol for a more complete and less biased global mapping of transcription start sites in bacterial pathogens. BMC Genomics. 2016;17(1):849.

80. Liese J, Rooijakkers SH, van Strijp JA, Novick RP, Dustin ML. Intravital two-photon microscopy of host-pathogen interactions in a mouse model of *Staphylococcus aureus* skin abscess formation. Cell Microbiol. 2013;15(6):891-909.
81. Giachino P, Engelmann S, Bischoff M. Sigma(B) activity depends on RsbU in *Staphylococcus aureus*. J Bacteriol. 2001;183(6):1843-52.

82. Gertz S, Engelmann S, Schmid R, Ohlsen K, Hacker J, Hecker M. Regulation of sigmaB-dependent transcription of *sigB* and *asp23* in two different *Staphylococcus aureus* strains. Mol Gen Genet. 1999;261(3):558-66.
83. Lei MG, Lee CY. Repression of capsule production by XdrA and CodY in *Staphylococcus aureus*. J Bacteriol. 2018;200(18):e00203-18.
84. Mainiero M, Goerke C, Geiger T, Gonser C, Herbert S, Wolz C. Differential target gene activation by the *Staphylococcus aureus* two-component system *saeRS*. J Bacteriol. 2010;192(3):613-23.
85. Killikelly A, Benson MA, Ohneck EA, Sampson JM, Jakoncic J, Spurrier B, et al. Structure-based functional characterization of repressor of toxin (Rot), a central regulator of *Staphylococcus aureus* virulence. J Bacteriol. 2015;197(1):188-200.
86. Campbell J, Singh AK, Swoboda JG, Gilmore MS, Wilkinson BJ, Walker S. An antibiotic that inhibits a late step in wall teichoic acid biosynthesis induces the cell wall stress stimulon in *Staphylococcus aureus*. Antimicrob Agents Chemother. 2012;56(4):1810-20.
87. Swoboda JG, Meredith TC, Campbell J, Brown S, Suzuki T, Bollenbach T, et al. Discovery of a small molecule that blocks wall teichoic acid biosynthesis in *Staphylococcus aureus*. ACS Chem Biol. 2009;4(10):875-83.
88. Schulthess B, Meier S, Homerova D, Goerke C, Wolz C, Kormanec J, et al. Functional characterization of the sigmaB-dependent *yabJ-spoVG* operon in *Staphylococcus aureus*: role in methicillin and glycopeptide resistance. Antimicrob Agents Chemother. 2009;53(5):1832-9.
89. Browning DF, Busby SJ. Local and global regulation of transcription initiation in bacteria. Nat Rev Microbiol. 2016;14(10):638-50.
90. Ruff EF, Record MT, Jr., Artsimovitch I. Initial events in bacterial transcription initiation. Biomolecules. 2015;5(2):1035-62.
91. Dorman CJ, Dorman MJ. DNA supercoiling is a fundamental regulatory principle in the control of bacterial gene expression. Biophys Rev. 2016;8(3):209-20.
92. Schröder W, Bernhardt J, Marincola G, Klein-Hitpass L, Herbig A, Krupp G, et al. Altering gene expression by aminocoumarins: the role of DNA supercoiling in *Staphylococcus aureus*. BMC Genomics. 2014;15:291.
93. Sharon E, van Dijk D, Kalma Y, Keren L, Manor O, Yakhini Z, et al. Probing the effect of promoters on noise in gene expression using thousands of designed sequences. Genome Res. 2014;24(10):1698-706.

94. Sadykov MR, Mattes TA, Luong TT, Zhu Y, Day SR, Sifri CD, et al. Tricarboxylic acid cycle-dependent synthesis of *Staphylococcus aureus* Type 5 and 8 capsular polysaccharides. J Bacteriol. 2010;192(5):1459-62.

95. Rausch M, Deisinger JP, Ulm H, Müller A, Li W, Hardt P, et al. Coordination of capsule assembly and cell wall biosynthesis in *Staphylococcus aureus*. Nature Communications. 2019;10(1):1404.

Appendix

Accepted manuscripts

1. **Wall teichoic acids mediate increased virulence in *Staphylococcus aureus***
   Stefanie Wanner, Jessica Schade, Daniela Keinhörster, Nicola Weller, Shilpa E. George, Larissa Kull, Jochen Bauer, Timo Grau, Volker Winstel, Henriette Stoy, Dorothee Kretschmer, Julia Kolata, Christiane Wolz, Barbara M. Bröker and Christopher Weidenmaier
   Nature Microbiology (2017) Volume 2, Article number: 16257

2. **Revisiting the regulation of the capsular polysaccharide biosynthesis gene cluster in *Staphylococcus aureus***

   Daniela Keinhörster, Andrea Salzer, Alejandra Duque-Jaramillo, Shilpa E. George, Gabriella Marincola, Jean C. Lee, Christopher Weidenmaier and Christiane Wolz
   Molecular Microbiology (2019) in press

3. **Function and regulation of *Staphylococcus aureus* wall teichoic acids and capsular polysaccharides**

   Daniela Keinhörster, Shilpa E. George, Christopher Weidenmaier and Christiane Wolz
   International Journal of Medical Microbiology (2019) in press

nature microbiology

ARTICLES

PUBLISHED: 23 JANUARY 2017 | VOLUME: 2 | ARTICLE NUMBER: 16257

Wall teichoic acids mediate increased virulence in *Staphylococcus aureus*

Stefanie Wanner[1†], Jessica Schade[1†], Daniela Keinhörster[1], Nicola Weller[1], Shilpa E. George[1], Larissa Kull[1], Jochen Bauer[1], Timo Grau[1], Volker Winstel[2], Henriette Stoy[1], Dorothee Kretschmer[1], Julia Kolata[3], Christiane Wolz[1], Barbara M. Bröker[4] and Christopher Weidenmaier[1,5*]

Community-associated methicillin-resistant *Staphylococcus aureus* (CA-MRSA) are the cause of a severe pandemic consisting primarily of skin and soft tissue infections. The underlying pathomechanisms have not been fully understood and we report here a mechanism that plays an important role for the elevated virulence of CA-MRSA. Surprisingly, skin abscess induction in an animal model was correlated with the amount of a major cell wall component of *S. aureus*, termed wall teichoic acid (WTA). CA-MRSA exhibited increased cell-wall-associated WTA content (WTA^{high}) and thus were more active in inducing abscess formation via a WTA-dependent and T-cell-mediated mechanism than *S. aureus* strains with a WTA^{low} phenotype. We show here that WTA is directly involved in *S. aureus* strain-specific virulence and provide insight into the underlying molecular mechanisms that could guide the development of novel anti-infective strategies.

Community-associated methicillin-resistant *Staphylococcus aureus* (CA-MRSA) strains pose a serious threat due to their rapid epidemic spread and their enormous virulence potential, which exceeds that of traditional hospital-associated strains (HA-MRSA)[1]. Skin and soft tissue infections (SSTIs) are the most common CA-MRSA infections, and 50–75% of patients present with abscesses[2]. Less frequent are lethal infections such as sepsis or necrotizing pneumonia[3–7]. In the USA, USA300 isolates are primarily responsible for the ongoing CA-MRSA epidemics[8–10], having replaced earlier USA400 isolates[11]. The success of CA-MRSA strains appears to be due to a unique combination of genetic factors that enable the bacteria to evade the human host defence systems[12–18]. However, the relative role of virulence factors in CA-MRSA virulence is still under debate[19–22]. More recent findings suggest that the cytolytic phenol-soluble modulin PSMα peptides[23–25], which are responsible for increased neutrophil killing capacity, the cytolysin α-toxin[20,24,26,27], as well as the global virulence regulator (termed accessory gene regulator (Agr)[28]) play key roles in CA-MRSA virulence in different experimental skin infection models. It has been demonstrated that the global virulence gene regulator Agr exerts strict control over PSM expression[29] and that the cytolytic PSMα peptides are produced in large amounts by CA-MRSA strains[23,30] as a consequence of high Agr activity[30]. The *agr* four-gene operon encodes a typical autoactivation circuit[31] and makes use of a regulatory RNA, RNAIII, as its effector[32,33]. In this study, we present evidence for a novel important factor in CA-MRSA virulence. Until now the focus has largely been on toxins and a putative pathogenicity island termed the 'arginine catabolic mobile element' (ACME)[34–36]. However, the impact of cell wall components has not been studied so far. Here, we introduce a novel concept of staphylococcal strain-specific virulence that includes a major cell wall glycopolymer. Cell wall teichoic acid (WTA) is a zwitterionic, secondary cell wall polymer of *S. aureus* that has important functions in bacterial physiology[37] as well as in *S. aureus* colonization and infection[38–41]. WTA is one of the most abundant surface determinants of *S. aureus* and has recently attracted major attention as a target structure for novel anti-infective strategies[42] and antibiotics[43–48]. The WTA of *S. aureus* is composed of ~40 ribitol phosphate repeating units modified with *N*-acetylglucosamine and D-alanine[49,50] (Supplementary Fig. 1). Negatively charged phosphate groups in the repeating unit and ester-linked D-alanine residues are responsible for the zwitterionic charge of WTA. We have demonstrated previously that the zwitterionic WTA of *S. aureus* activates CD4$^+$ T cells via a major histocompatibility complex (MHC) II-dependent mechanism, which modulates the development of skin abscesses in a mouse model[51] at the early stages of abscess formation. Given that CA-MRSA is the predominant cause of SSTIs, we focus here on the role of WTA in CA-MRSA skin infections and demonstrate that the WTA content in cell wall fractions from highly pathogenic CA-MRSA strains such as USA300 (LAC) and MW2 (USA400) is significantly elevated compared to less virulent patient isolates (103), HA-MRSA (USA500) or laboratory strains (SA113). We termed these phenotypes WTA^{high} and WTA^{low}, respectively, and describe here the underlying regulatory mechanisms and the impact on skin-infection-related virulence in a mouse model.

Results

Highly pathogenic CA-MRSA strains exhibit elevated WTA content in their cell walls compared to less pathogenic strains. We analysed the cell wall composition of several *S. aureus* strains that share the same ribitol–WTA structure and biosynthetic pathways (Supplementary Figs 1–3) with respect to amounts of WTA. When we determined the WTA content of the cell wall fractions, we found that the highly pathogenic CA-MRSA strains MW2 and USA300, as well as clinical isolate 103 (superantigen-free,

[1]Department of Medicine, Interfacultary Institute for Microbiology and Infection Medicine (IMIT), University of Tübingen, Elfriede-Aulhorn Straße 6, 72076 Tübingen, Germany. [2]Department of Microbiology, University of Chicago, Chicago, Illinois 60637, USA. [3]Medical Microbiology, UMC Utrecht, Heidelberglaan 100, 3584CX Utrecht, The Netherlands. [4]Department of Immunology, University Medicine Greifswald, Ferdinand-Sauerbruch-Straße DZ7, 17475 Greifswald, Germany. [5]German Center for Infection Research (DZIF), Partner Site Tübingen, 72076 Tübingen, Germany. †These authors contributed equally to this work. *e-mail: christopher.weidenmaier@med.uni-tuebingen.de

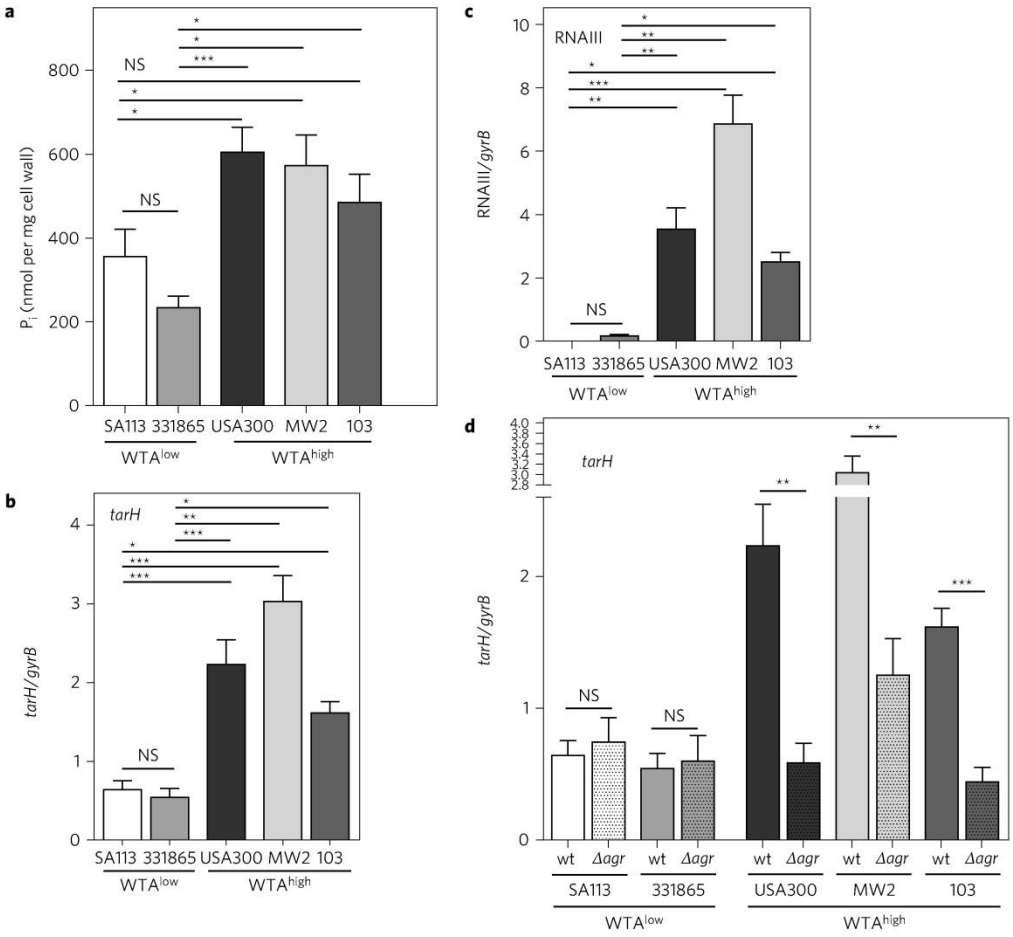

Figure 1 | Amounts of WTA in the cell wall fractions of *S. aureus* strains and transcriptional analysis by qRT–PCR. a, The amount of WTA per mg of cell wall preparation was determined with a colorimetric assay and is depicted as nmol inorganic phosphorus (P_i) per mg cell wall dry weight. CA-MRSA strains USA300 and MW2 (as well as clinical, superantigen-free isolate 103) were compared to non-CA-MRSA strains (SA113, and clinical, superantigen-free isolate 331865). Shown are means ± s.e.m. for $n = 8$–11 independent WTA isolations. *P* values for multiple comparisons were determined by one-way ANOVA with Tukey's post-test. $^*P < 0.05$, $^{**}P < 0.01$, $^{***}P < 0.0001$. NS, not significant. **b**, Transcriptional analysis of the WTA biosynthesis gene *tarH* from *in vitro* cultures grown to stationary phase in WTA^{high} strains (MW2, USA300, 103) and WTA^{low} strains (SA113, 331865). The expression of transcripts was quantified relative to the transcription of gyrase (copies of *tarH* per copy of *gyrB*). Shown are means ± s.e.m., $n = 6$ independent experiments. *P* values for multiple comparisons were determined by one-way ANOVA with Tukey's post-test. $^*P < 0.05$, $^{**}P < 0.01$, $^{***}P < 0.0001$. **c**, Transcriptional analysis of RNAIII, the downstream regulator of the global virulence Agr regulon. WTA^{high} strains (MW2, USA300, 103) and WTA^{low} strains (SA113, 331865) were grown to stationary phase. Transcripts were quantified relative to the transcription of gyrase (copies of RNAIII per copy of *gyrB*). Shown are means ± s.e.m., $n = 6$ independent experiments. *P* values for multiple comparisons were determined by one-way ANOVA with Tukey's post-test. $^*P < 0.05$, $^{**}P < 0.01$, $^{***}P < 0.0001$. **d**, Transcriptional analysis of the WTA biosynthesis gene *tarH*. *In vitro* cultures of WTA^{high}, WTA^{high} *Δagr* mutant, WTA^{low} and WTA^{low} *Δagr* mutant strains were grown to stationary phase. Transcripts were quantified relative to the transcription of gyrase (copies of *tarH* per copy of *gyrB*). Shown are means ± s.e.m., $n = 6$ independent experiments. Statistically significant differences between WTA^{high} and WTA^{low} and their respective *Δagr* mutant strains were determined by Student's *t*-test. $^*P < 0.05$, $^{**}P < 0.01$, $^{***}P < 0.001$.

included as a control for superantigen activity; see section beginning with 'Cell wall fractions'), exhibited elevated WTA content in their cell wall fractions compared to laboratory strain SA113 and clinical isolate 331865 (superantigen-free, included as a control for superantigen activity). We grouped the isolates as WTA^{high} (MW2, USA300, 103) and WTA^{low} (SA113, 331865) strains (Fig. 1a).

The WTA^{high} phenotype is mediated by overexpression of the *tarH* gene. To understand the mechanisms underlying the WTA^{high} and WTA^{low} phenotypes, we quantified the expression of genes involved in WTA biosynthesis using quantitative real-time–polymerase chain reaction (qRT–PCR) of *in vitro* cultures. The WTA biosynthesis genes *tarO*, *tarA*, *tarK*, *tarL*, *tarG* and *tarH* (Supplementary Figs 2 and 3) were analysed in the logarithmic and stationary growth phases (Fig. 1 and Supplementary Figs 4 and 5). Only *tarH* transcription was significantly increased in WTA^{high} strains (MW2, USA300, 103) compared to WTA^{low} strains (SA113, 331865). This effect was only observed in the stationary growth phase (Fig. 1b) (transcriptional analyses for *tarH* in logarithmic and *tarO*, *tarA* in stationary and logarithmic growth phases are shown in Supplementary Fig. 4, and for *tarK* and *tarL* in Supplementary Fig. 5a,b, respectively). *tarH* encodes for the energizing part of the two-component ABC transporter (*TarGH*), which facilitates WTA translocation across the membrane[52,53]. Because we detected decreased tarK expression in MW2, we also analysed a potential

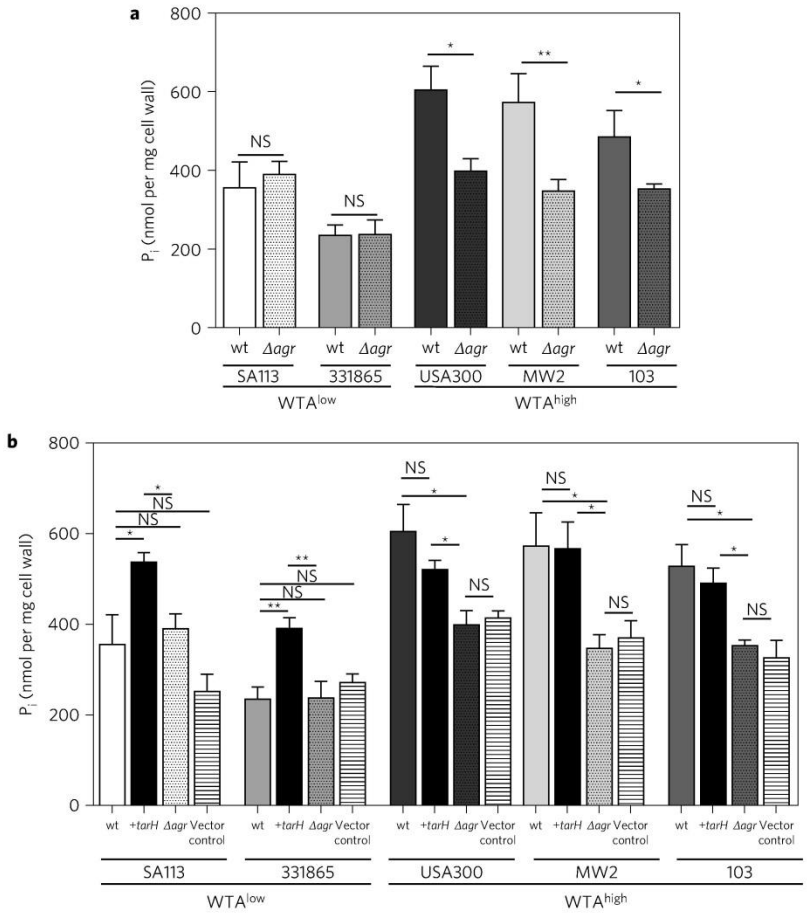

Figure 2 | Agr-dependent control of WTA content in the staphylococcal cell wall. a, Content of WTA in the cell wall of WTA^{high} (MW2, USA300, 103), WTA^{high} *Δagr* mutant (MW2*Δagr*, USA300*Δagr*, 103*Δagr*), WTA^{low} (SA113, 331865) and WTA^{low} *Δagr* mutant (SA113*Δagr*, 331865*Δagr*) strains**.** The amount of WTA per mg cell wall preparation was determined with a colorimetric assay (WTA amount is depicted as nmol inorganic phosphorus (P_i) per mg cell wall dry weight). Shown are means ± s.e.m. for $n = 8$–11 independent WTA isolations. Statistically significant differences between WTA^{high} and WTA^{low} and their respective *Δagr* mutant strains were determined by Student's *t*-test. $^{*}P < 0.05$, $^{**}P < 0.01$, $^{***}P < 0.001$. **b**, Content of WTA in the cell wall fractions of WTA^{high}, WTA^{high} *Δagr* mutant and WTA^{low} strains after *tarH* overexpression. Overexpression of *tarH* in expression vector pRB474 (under control of a constitutive promoter) was tested in WTA^{low} strains SA113 and 331865. Expression vector pRB474 alone was used as a negative (vector) control. The amount of WTA per mg cell wall preparation was determined with a colorimetric assay. Shown are means ± s.e.m. for $n = 8$–12 independent WTA isolations. *P* values for multiple comparisons were determined by one-way ANOVA with Tukey's post-test for each strain. $^{*}P < 0.05$, $^{**}P < 0.01$, $^{***}P < 0.001$.

chain length variation in the WTA polymer. However, WTA PAGE analysis (Supplementary Fig. 4a) of polymer isolated from stationary-phase cells did not reveal significant differences in polymer lengths between WTA^{high} and WTA^{low} strains.

The WTA^{high} phenotype depends on a highly active Agr regulon. The Agr system has been linked to staphylococcal pathogenesis in a subcutaneous abscess infection model[54], and is known to increase the expression of virulence factors during the transition from the late-exponential to stationary growth phase *in vitro*[55,56]. To test whether the Agr system is differentially expressed in WTA^{high} and WTA^{low} strains, we measured the expression of the primary transcript RNAIII in the stationary growth phase by qRT–PCR. All WTA^{high} strains possessed an intact Agr regulon and produced high levels of RNAIII. One of the WTA^{low} strains was a naturally occurring functional *agr*-deletion mutant (SA113), while the other produced low levels of RNAIII (Fig. 1c).

To test whether the agr system is involved in the differential regulation of the WTA biosynthesis gene *tarH*, we compared *agr*-deletion mutants (Supplementary Table 1) with their corresponding isogenic wild type (wt) by qRT–PCR. In WTA^{high} strains, *tarH* expression in *Δagr* mutants was significantly decreased compared to the WTA^{high} wt strains. In contrast, there was no difference in *tarH* expression between WTA^{low} *Δagr* mutants and their wt strains (Fig. 1d).

To validate the role of Agr in WTA biosynthesis, we quantified the WTA content of WTA^{high} and WTA^{low} strains and their *Δagr* mutants with a colorimetric assay. WTA content correlated with *tarH* expression levels and was significantly reduced in WTA^{high} *Δagr* mutants. Conversely, WTA^{low} *Δagr* mutants and WTA^{low} wt strains showed no difference in WTA content. WTA^{high} *Δagr* mutants demonstrated the same WTA content as both wt and *Δagr* mutants in the WTA^{low} strain background (Fig. 2a). This is evidence for a distinct role for the Agr system in WTA biosynthesis regulation in WTA^{high} strains. Moreover, there appears to be a correlation between loss of Agr function and the reduced expression of *tarH* in WTA^{low} strains. In line with these results, we found that an HA-MRSA strain (USA 500) that exhibited low agr-activity (Supplementary Fig. 6a) also exhibited low *tarH* expression (Supplementary Fig. 6b) and therefore a WTA^{low} phenotype (Supplementary Fig. 6c) when compared to WTA^{high} CA-MRSA strain USA300.

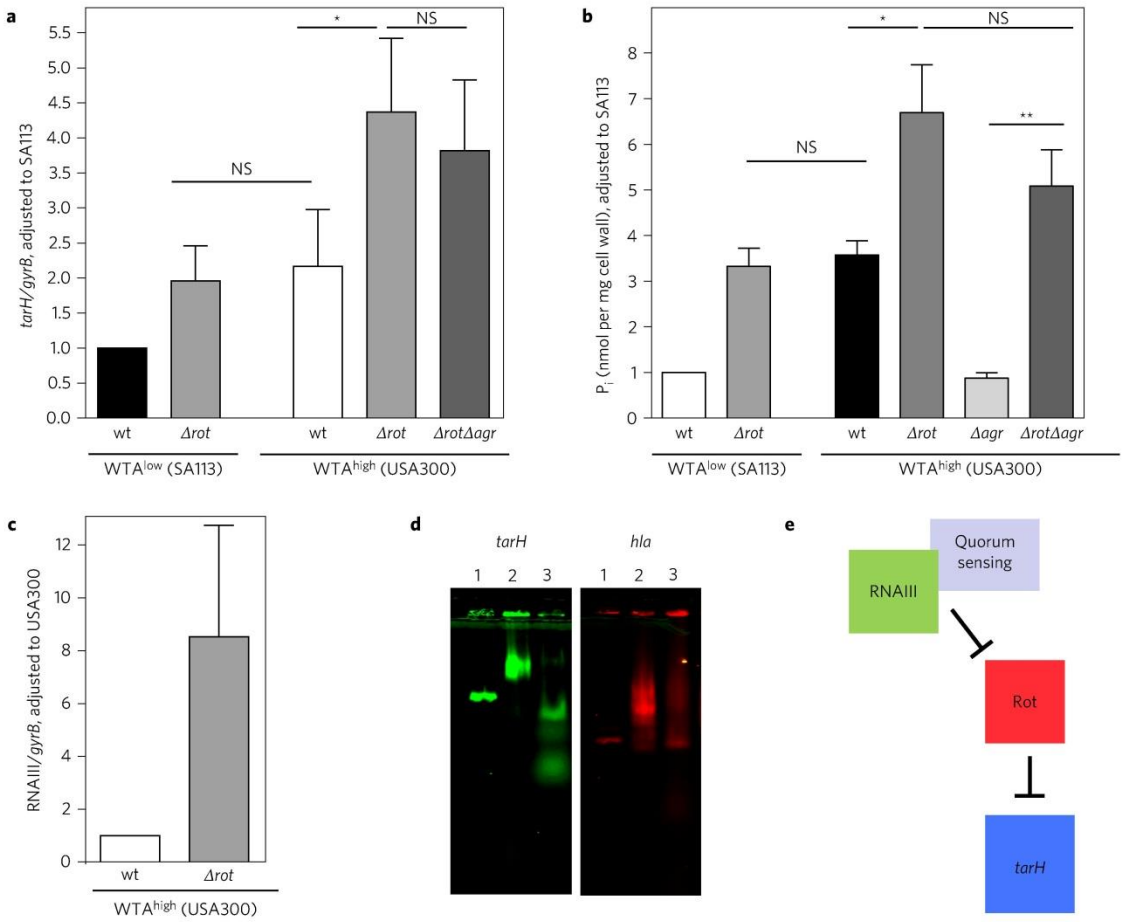

Figure 3 | Rot controls *tarH* expression and WTA biosynthesis downstream of RNAIII. a, Transcription analysis of the WTA biosynthesis gene *tarH* from *in vitro* cultures grown to stationary phase. Expression of transcripts was quantified relative to the transcription of gyrase (copies of *tarH* per copy of *gyrB*) and adjusted to SA113 (expression of SA113 in each independent experiment was set to 1). Shown are means ± s.e.m., $n = 8$ independent experiments. *P* values for multiple comparisons were determined by one-way ANOVA with Bonferroni's post-test. $^{*}P < 0.05$. **b**, Content of WTA in the cell wall of WTA^{high} (USA300), WTA^{high} *Δrot* mutant (USA300*Δrot*), WTA^{low} (SA113) and WTA^{low} *Δagr* mutant (SA113*Δagr*) strains. Amount of WTA per mg cell wall preparation was determined with a colorimetric assay (WTA amount is depicted as nmol inorganic phosphorus (P_i) per mg cell wall dry weight) and adjusted to SA113 (WTA amount of SA113 in each independent experiment was set to 1). Shown are means ± s.e.m., $n = 6$ independent experiments. *P* values for multiple comparisons were determined by one-way ANOVA with Bonferroni's post-test. $^{*}P < 0.05$, $^{**}P < 0.01$. **c**, Transcription analysis of RNAIII in WTA^{high} and WTA^{high} *Δrot S. aureus* in stationary-phase cultures. Expression of the RNAIII transcript was quantified relative to the transcription of gyrase (copies of RNAIII per copy of *gyrB*) and adjusted to wt WTA^{high}. Shown are means ± s.e.m., $n = 8$ independent experiments. **d**, LI-COR Odyssey-based gel-shift assays with cell extracts and *tarH* promoter (green). Rot binding to the promoter was visualized with cell extracts from a Rot-expressing USA300 strain lacking *agr* (lane 2) and an isogenic *rot* mutant (lane 3). Lane 1 contains the promoter fragment without cell extract as a control. The *hla* promoter (red) was used as a positive control. Rot binding to the *hla* promoter was visualized with cell extracts from a Rot-expressing USA300 strain lacking *agr* (lane 2) and an isogenic *rot* mutant (lane 3). Lane 1 contains the promoter fragment without cell extract as a control. Shown is a representative example of $n = 3$ independent experiments. **e**, The *tarH* regulatory cascade; *tarH* is under negative control of a repressor termed 'repressor of toxins' (Rot). Rot mRNA stability is controlled by RNAIII and at high RNAIII levels Rot-mediated repression is relaxed.

Transcriptional control of *tarH* by the repressor of toxins, a major downstream regulator of the Agr system. The repressor of toxins (Rot) is a major effector downstream of *agr*[56] and acts as a transcriptional regulator of an array of genes. Rot mRNA stability is negatively affected by RNAIII and therefore RNAIII mediates derepression of Rot-regulated genes[57]. When we measured *tarH* expression in WTA^{high} and WTA^{low} wt and *rot* mutants, we found a significant impact of *rot* on t*arH* expression (Fig. 3a). In fact, a WTA^{low} rot mutant exhibited the same *tarH* expression level as a WTA^{high} wt. In addition, the *rot* mutation alleviated the strong decrease of *tarH* expression found in an *agr* mutant (see Fig. 2). In fact, the *rot agr* double mutant exhibited similarly elevated levels of *tarH* expression as a *rot* mutant alone. When we measured the amounts of WTA in the cell walls of WTA^{high} and WTA^{low} wt and *rot* mutants (Fig. 3b), we found that WTA amounts correlated with a *rot*-dependent *tarH* expression pattern. A WTA^{low} *rot* mutant exhibited an elevated amount of WTA that was comparable to the WTA amount detected in a WTA^{high} wt. The *rot* mutation increased the WTA amounts in the WTA^{high} background even further, and in a *rot agr* double mutant the *agr* mutation phenotype was completely alleviated. Interestingly, when we measured RNAIII levels in the WTA^{high} background in the wt and *rot* mutant we found that the absence of *rot* severely increased the levels of RNAIII (Fig. 3c). This indicates a direct interplay between *rot* mRNA and RNAIII and an altered steady state for RNAIII when Rot is missing. To

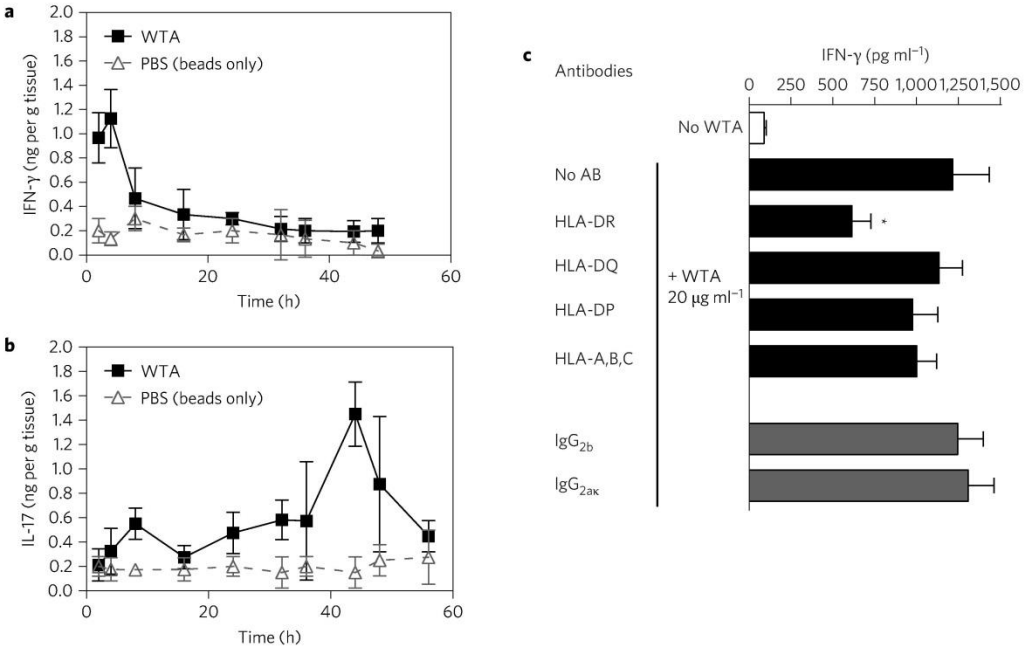

Figure 4 | MHC II-dependent cytokine secretion of WTA-stimulated T cells during skin abscess formation. a,**b**, Skin abscesses were induced by injecting 20 μg of purified wt *S. aureus* WTA mixed with cytodex beads into the flanks of mice. Abscesses were excised, and the amounts of IFN-γ per gram of abscess tissue (**a**) and IL-17 per gram of abscess tissue (**b**) were measured by ELISA; $n = 6$ (three mice per time point with two abscesses per mouse). For controls dextran beads in PBS without WTA were used. Results are expressed as means ± s.d. **c**, WTA activates human T cells to produce IFN-γ in an MHC II-dependent mechanism. Total mononuclear cells, such as APCs, were pre-incubated with blocking Abs (2 μg ml^{-1}) to the MHC II molecules HLA-DR, HLA-DP and HLA-DQ or MHC I molecules HLA-A, HLA-B and HLA-C and appropriate isotype control Abs for 1 h before the addition of CD4$^+$ T cells. Co-cultures of the APCs (1×10^5) and CD4$^+$ T cells (1×10^5) were then stimulated with 20 μg ml^{-1} WTA for 72 h. IFN-γ levels in the supernatants were then quantified by ELISA. The HLA-DR Ab significantly reduced IFN-γ production. Results are expressed as means ± s.e.m. for $n = 6$ independent experiments. *P* values for comparisons with no Ab were determined by one-way ANOVA with Dunnett's post-test. *$P < 0.05$.

demonstrate Rot binding to the *tarH* promoter region we performed gel-shift assays (Fig. 3d). Cell extracts from a Rot-expressing strain (in the USA300 *agr* mutant to ensure high Rot levels) mediated a clear shift of the promoter fragment when run in an agarose gel, while a cell extract from an isogenic strain lacking Rot was not able to mediate such a shift and the promoter fragment was partially degraded. A promoter fragment of the *hla* gene, which is Rot-repressed[59], was used and showed a similar shift.

In addition, when we measured WTA expression over time (Supplementary Fig. 7), we found that WTA amounts increased during logarithmic growth and peaked in the stationary growth phase. In line with an RNAIII and *rot*-dependent mechanism, this effect was more pronounced in a WTA^{high} wt strain when compared to a WTA^{low} strain, and the WTA^{high} phenotype only became evident at the onset of the stationary phase. Taken together, we conclude a regulatory cascade that involves high RNAIII levels, a more efficient Rot mRNA degradation and thus a more efficient Rot derepression on the *tarH* promoter level than the molecular mechanism behind the WTA^{high} phenotype (Fig. 3e).

Overexpression of *tarH* in WTA^{low} strains can restore the WTA^{high} phenotype. We hypothesized that high *tarH* expression leads to the WTA^{high} phenotype due to increased translocation of WTA molecules. We therefore tested whether the WTA^{high} phenotype could be restored in WTA^{low} strains by overexpressing the *tarH* gene in WTA^{low} strain SA113 from the plasmid vector 474 (Supplementary Fig. 8). The *tarH* gene was put under the control of a promoter encoded on plasmid pRB474 (Supplementary Table 1). Overexpression of *tarH* in the WTA^{low} (SA113 pRB474+ *tarH*) strain indeed induced the WTA^{high} phenotype (Fig. 2b). As indicated above, *tarH* gene expression in WTA^{high} *Δagr* mutants was reduced to the level of WTA^{low} strains. We therefore used the *tarH* overexpression vector in WTA^{high} *Δagr* mutants (103*Δagr* pRB474+*tarH*, MW2*Δagr* pRB474+*tarH*, USA300*Δagr* pRB474 +*tarH*) and were able to restore the WTA^{high} phenotype. In contrast, transformation with the empty plasmid pRB474 (SA113 pRB474, 331865 pRB474, 103*Δagr* pRB474, MW2*Δagr* pRB474, USA300*Δagr* pRB474) did not affect WTA levels in any *S. aureus* strain (Fig. 2b).

WTA induces interferon-γ at the onset of skin abscess formation and IL-17 at the late stages of abscess formation. We have seen before that self-clearing, non-lesion-forming subcutaneous abscesses, induced by WTA, depend on CD4$^+$ T cells[51], and we wanted to elucidate the hallmark cytokines involved in this process. Abscess formation was induced by injecting WTA mixed with cytodex beads into the flanks of mice. We measured interferon-γ (IFN-γ) and interleukin 17 (IL-17) production in the abscess by enzyme-linked immunosorbent assay (ELISA) at different time points (Fig. 4) and detected strong IFN-γ production only in the very early phases of abscess formation (Fig. 4a), while IL-17 showed only weak production at early time points (Fig. 4b) and peaked at later time points that coincided with abscess clearing.

We have seen before that mouse and human T cells are activated by WTA-presenting APCs (antigen-presenting cells) in an MHC II-dependent manner[51]. To demonstrate the MHC II dependency of the IFN-γ response after WTA-induced CD4$^+$ T cell (human T cells) activation *in vitro*, we tested whether IFN-γ production could be inhibited in the presence of blocking

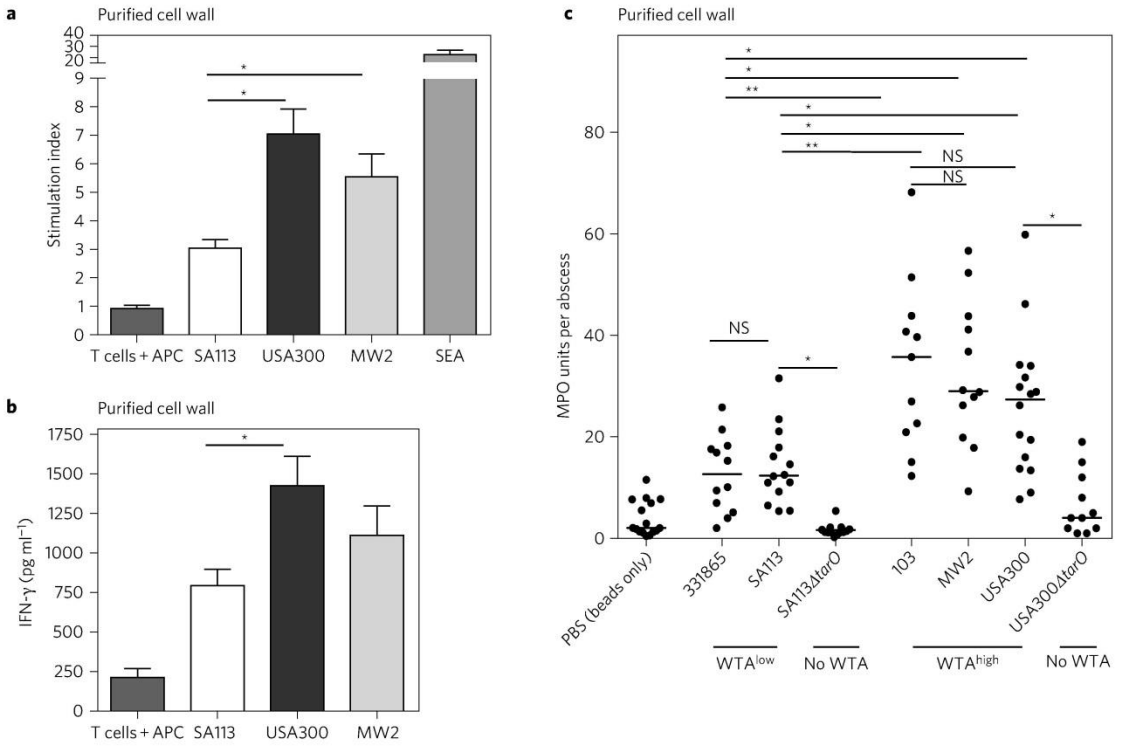

Figure 5 | Induction of T-cell-dependent IFN-γ secretion and abscess formation by cell wall fractions. a, T cell proliferation assay with highly pure, protein-free cell wall fractions. Cell wall fractions isolated from highly pathogenic CA-MRSA strains (MW2, USA300) were incubated with APCs (1×10^5) and T cells (2×10^5) for 6 days. *S. aureus* enterotoxin A (SEA) was used as a positive control (2 ng ml^{-1}). Cell wall fractions from CA-MRSA strains (MW2, USA300) induce T cell proliferation more efficiently than cell wall fractions from MSSA and the laboratory *S. aureus* strain SA113. Results are expressed as means ± s.e.m. for $n = 5$ independent experiments. *P* values for comparisons with SA113 were determined by one-way ANOVA with Dunnett's post-test. $^*P < 0.05$. **b**, Measurement of T-cell-dependent IFN-γ expression. A T cell proliferation assay with cell wall fractions was performed. Cell wall fractions isolated from MW2 and USA300 (CA-MRSA) induce T-cell-dependent IFN-γ expression more efficiently than cell wall fractions from SA113 (MSSA, laboratory strain) ($n = 5$). T cells and APCs were incubated with cell wall preparations for 72 h. IFN-γ secretion was determined by ELISA. Results are expressed as the means ± s.e.m. for $n = 5$ independent experiments. *P* values for comparisons with SA113 were determined by one-way ANOVA with Dunnett's post-test. $^*P < 0.05$. **c**, Abscess formation induced by cell wall fractions monitored via a myeloperoxidase (MPO) assay. Cell wall fractions from the CA-MRSA strains USA300, MW2 and the superantigen-free clinical isolate 103 induce abscesses more efficiently than cell wall fractions from laboratory strain SA113 and superantigen-free clinical isolate 331865. MPO is a marker of inflammation in abscess tissue. Twenty micrograms of cell wall were injected into the flanks of mice, and abscesses were extracted. MPO activity was measured in an enzymatic assay. Shown is a dot-blot with medians, with each dot representing a single abscess (two abscesses per mouse). *P* values for multiple comparisons were determined by one-way ANOVA with Bonferroni's post-test. $^*P < 0.05$, $^{**}P < 0.01$.

antibodies (Abs) against the MHC II molecules HLA-DR, HLA-DP and HLA-DQ or the MHC I molecules HLA-A, HLA-B and HLA-C and isotype control Abs. We were able to inhibit IFN-γ production significantly by adding an HLA-DR blocking Ab (Fig. 4c). Antibodies to HLA-DP, HLA-A, HLA-B or HLA-C and their respective isotype controls showed no effect. The experiment revealed that WTA activates human T cells to produce IFN-γ via an MHC II-dependent mechanism.

Cell wall fractions from highly pathogenic WTA^{high} strains induce T cell proliferation, IFN-γ secretion, and skin abscess formation more efficiently than cell wall fractions isolated from WTA^{low} strains. To compare the ability of highly pure, protein-free cell wall fractions isolated from the pathogenic CA-MRSA strains MW2 and USA300 and a less virulent methicillin-sensitive *Staphylococcus aureus* (MSSA) laboratory strain (SA113) to activate T cells and induce IFN-γ production, we cultured human CD4$^+$ T cells with irradiated APCs and cell wall fractions. Cell wall fractions from CA-MRSA strains MW2 and USA300 provoked stronger T cell proliferation (Fig. 5a) and induced stronger IFN-γ secretion than cell wall fractions from the laboratory strain SA113 (Fig. 5b).

We then tested the ability of purified cell wall fractions to induce abscess formation in mice. Protein-free, highly pure cell wall fractions were derived from the highly virulent CA-MRSA strains MW2, USA300, the superantigen-free clinical isolate 103, as well as the less virulent *S. aureus* strains SA113 and 331865 (superantigen-free clinical isolate), and were used in a skin abscess mouse model. Abscess-inducing activity was quantified by measuring neutrophil accumulation at the infection site with a myeloperoxidase (MPO) assay[51]. Cell wall fractions from highly virulent (WTA^{high}) *S. aureus* strains induced strong MPO activity, whereas cell wall fractions from the less virulent (WTA^{low}) *S. aureus* isolates were significantly less active (Fig. 5c). To test whether WTA amounts alone affect the induction of abscess formation, we injected different amounts of purified WTA and found that MPO activity indeed depends on the amount of WTA injected subcutaneous (s.c.) into the flanks of mice (Supplementary Fig. 9). To exclude the possibility that WTA tailoring modifications[58] (D-ala, GlcNAc) contribute to cell-wall-mediated abscess formation, we assessed the expression of the *dlt* operon, which is responsible for WTA D-alanylation[59], and the two *N*-acetylglucosaminyl-transferases (TarM and TarS), which are responsible for WTA modification with α- or β-GlcNAc,

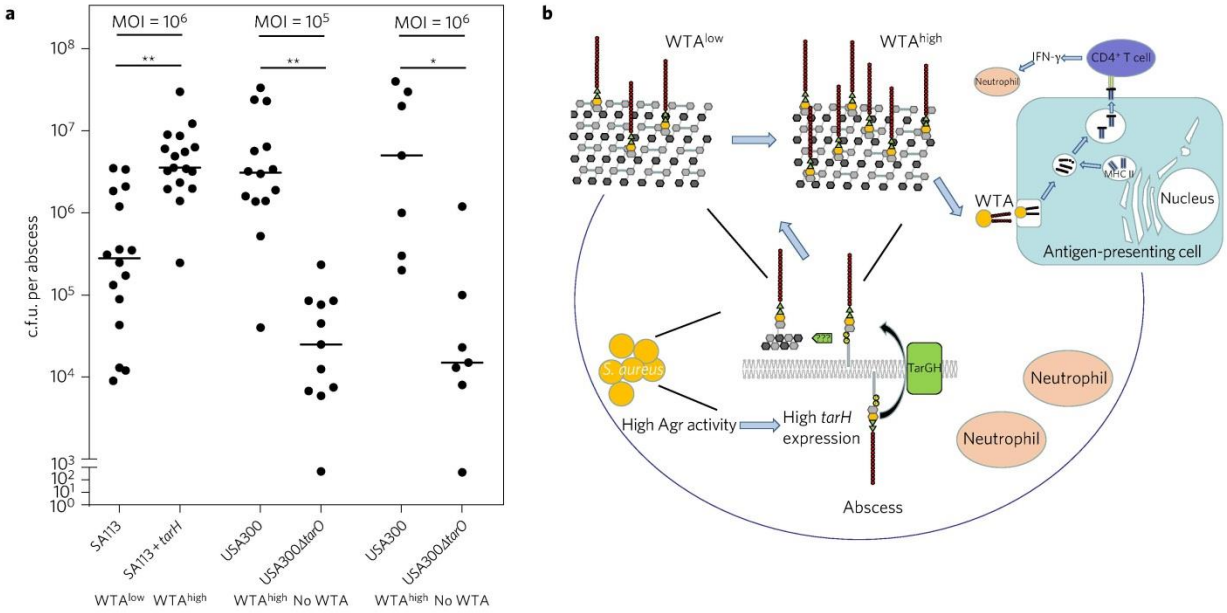

Figure 6 | Skin abscess formation with whole bacterial cells and model for WTA-mediated strain-specific virulence. a, To induce abscess formation, 10^6–10^5 colony-forming units (c.f.u.) of living bacterial cells (*S. aureus* SA113 (WTA^{low}), SA113 pRB*tarH* (*tarH* overexpression plasmid which facilitates a WTA^{high} phenotype), USA300 (WTA^{high}) and USA300Δ*tarO* (lacks all WTA)) were mixed with cytodex beads and injected s.c. into the flanks of mice. After 48 h, the mice were euthanized, and each abscess was excised, homogenized and cultured quantitatively. In the case of USA300, we found dermonecrosis at a higher multiplicity of infection (MOI of 10^6) and therefore included an MOI of 10^5 where defined abscesses can be excised. Shown is a dot-blot with medians, with each dot representing a single abscess (two abscesses per mouse). Pairwise *P* values were determined by *t*-test with Welch correction. $*P < 0.05$, $**P < 0.01$. **b**, Model for the impact of WTA on strain-specific virulence. In CA-MRSA, cell WTA incorporation into the peptidoglycan is significantly elevated. This WTA^{high} phenotype depends on the specific upregulation of *tarH* expression by the global virulence regulator Agr, which exhibits intrinsically high activity in CA-MRSA. WTA^{high} cell walls are able to stimulate T-cell-dependent IFN-γ production at the onset of abscess formation more efficiently than cell walls with lower WTA amounts. This mechanism plays an important role in modulation of early abscess development.

respectively[60] (Supplementary Figs 1 and 2). We could detect differences in the expression of the GlcNAc transferases in the tested strains (Supplementary Fig. 10). WTA^{low} strain SA113 exhibited expression of both *tarM* (Supplementary Fig. 10a) and *tarS* (Supplementary Fig. 10b) expression. Compared to SA113 and another HA-MRSA, WTA^{low} strain (USA500), the WTA^{high} strain USA300 clearly exhibited elevated levels of *tarM* mRNA (Supplementary Fig. 10a). All three strains also exhibited *tarS* expression (elevated in USA300 only). In contrast, MW2 (WTA^{high}) showed very low *tarM* mRNA levels and moderate *tarS* levels. Strains 331865 (WTA^{low}) and 103 (WTA^{high}) only expressed *tarS* in considerable amounts (Supplementary Fig. 10b), but *tarS* mRNA levels were severely decreased compared to SA113. In line with these results, USA 300 exhibited a slightly, albeit not statistically significant, increased amount of GlcNAc in its WTA when compared to SA113, while 331865 and 103 showed very low GlcNAc levels (Supplementary Fig. 11). We then assessed the impact of WTA GlcNAc modification on abscess formation. To that end, we compared cell wall fractions isolated from USA300 wt and an isogenic mutant lacking both TarM and TarS in the s.c. abscess model (Supplementary Fig 12). We could not detect a significant impact on abscess induction when both GlcNAc modifications were missing from WTA. In addition, WTA^{low} cell wall isolated from an HA-MRSA strain (USA500) exhibited a significantly lower abscess-inducing capacity when compared to USA300 cell wall. When we compared whole, live bacteria in the abscess model (Supplementary Fig. 13), we again detected no significant phenotype in the *tarM/S* mutant, while the WTA^{low} strain USA500 was clearly a less efficient abscess inducer. In addition, when we injected purified WTA together with live bacterial cells of the two WTA^{low} strains SA113 and USA500 (HA-MRSA), the colony-forming units (c.f.u.) recovered after 48 h were significantly increased and the WTA^{low} strains exhibited a phenotype that was comparable to USA300 (CA-MRSA). With respect to D-alanine modifications, we could not detect differences in the expression of the *dlt* operon (Supplementary Fig. 10c), nor in the D-alanine levels of isolated WTA (Supplementary Fig. 11), from all tested strains.

Overexpression of *tarH* in WTA^{low} strains increases the ability to induce skin abscess formation, comparable to WTA^{high} strain USA300. Finally, we compared the ability of strain SA113, with and without the *tarH* overexpression plasmid (which leads to a WTA^{high} phenotype), to induce abscess formation (Fig. 6a). When we used whole bacterial cells in the s.c. abscess model, the *tarH* plasmid-harbouring strain demonstrated an increased capacity to induce abscess formation. This was in line with the elevated abscess induction observed with USA300. To test if WTA has an impact on abscess formation in the highly pathogenic USA300 background, we used an isogenic mutant lacking all WTA molecules (USA300Δ*tarO*). This mutant exhibited a significantly reduced ability to induce abscess formation when compared to the WTA^{high} wt USA300. Furthermore, when we overexpressed *tarH* in an additional WTA^{low} strain background (HA-MRSA USA500), we could again detect an increased ability to induce s.c. abscesses in the flanks of mice (Supplementary Fig. 14).

Discussion

Here, we have demonstrated a novel role for the zwitterionic cell wall polymer WTA in *S. aureus* strain-specific virulence. Our data indicate that increased expression of the late-phase WTA biosynthesis gene *tarH* leads to a WTA^{high} phenotype in CA-MRSA,

which is characterized by significantly elevated amounts of WTA in the cell wall. Surprisingly, we found that the WTA^{high} phenotype exhibited by CA-MRSA is connected to the quorum sensing system Agr. It has been reported previously that this global virulence regulator system is highly active in CA-MRSA strains[22,28,61]. Indeed, we found highly active Agr in all WTA^{high} strains, while WTA^{low} strains showed weak Agr activity or even a functionally inactive *agr* regulon. In WTA^{high} strains an excess of WTA in the cell wall is achieved by Agr-dependent over-expression of a *tarH* that encodes a possible bottleneck enzyme in WTA biosynthesis. The mature WTA polymer is exported by the TarG/H transporter and TarH constitutes the energizing ATPase unit of the ABC transporter. The coupling of *tarH* overexpression and transporter activity is currently under investigation in our laboratory. Evidence for Agr-mediated control of WTA polymer length has been reported by Meredith and colleagues[62]. However, we could not detect differences in polymer length when we compared the WTA^{high} and WTA^{low} strains analysed here. Interestingly, screening for late-stage WTA biosynthesis inhibitors in large compound libraries[45,63,64] only identified TarG inhibitors, indicating again that WTA precursor export might be the rate-limiting step in the pathway. Furthermore, we demonstrate here for the first time that Agr control of WTA biosynthesis is mediated by Rot, an important repressor of several Agr targets[65]. The Agr effector RNAIII has been demonstrated to decrease *rot* mRNA stability and efficiently reduce Rot-mediated repression[66]. A defined consensus sequence for Rot binding in promoter regions of Rot-controlled genes has not been identified[67]. However, Rot seems to exhibit high affinity to AT-rich promoter regions[67]. In fact, the *tarH* promoter region is AT-rich, arguing for Rot-dependent control of the *tarH* promoter (Supplementary Fig. 15). In whole-cell lysates (in *agr*-negative background to ensure high Rot levels) of isogenic *rot* wt and mutant we could detect binding of Rot to the *tarH* promoter region. Our analysis clearly indicates that the WTA^{high} phenotype is mediated by high RNAIII levels, which facilitate a more efficient Rot derepression in WTA^{high} strains. In line with this explanation of strain-specific differences, we found that in a WTA^{low} strain, which is a functional *agr* mutant (SA113), mutation of *rot* leads to *tarH* expression levels and WTA amounts that are comparable to WTA^{high} strains. Measuring WTA levels over time we found that the WTA amounts for WTA^{high} and WTA^{low} strains only started to differ significantly at the onset of the stationary growth phase. We conclude that in *agr* mutants or low Agr-activity isolates, Rot activity is not decreased at the onset of the stationary phase as much as in WTA^{high} isolates. In addition, we detected a strong increase in the RNAIII level when we mutated *rot* in the WTA^{high} background, indicating an altered steady state of RNAIII amounts. These results are in line with a more efficient, RNAIII-mediated, Rot derepression in WTA^{high} strains.

We have shown before that WTA is able to activate CD4$^+$ T cells in an MHC II-dependent manner, which modulates the early development of skin abscesses in a mouse model[51]. Consequently, the increased amounts of WTA render the cell wall of CA-MRSA more immunologically active. In line with these findings, abscess induction correlated with the amount of WTA incorporated in the cell wall of *S. aureus* strains. This phenotype probably depends on the ability of WTA^{high} cell wall fractions to induce CD4$^+$ T cell proliferation and IFN-γ secretion more efficiently than WTA^{low} cell walls. This is in line with a recent study reporting that WTA-specific T cells can be detected in healthy humans[68], with a sub-fraction of these WTA-specific T cells exhibiting a robust IFN-γ response. In contrast, other reports implicate IL-17-producing γδT cells and TH17-dependent responses in controlling mouse[69] or rabbit[70] cutaneous *S. aureus* infection at the innate stage. However, the authors either studied dermonecrotic lesions and not defined skin abscesses, or monitored later time points. When we injected purified WTA mixed with cytodex beads s.c. into the flanks of mice, we detected only a weak peak of IL-17 in the early phases of abscess formation. The primary IL-17 peak occurred at later time points that coincided with abscess clearing. The earliest relevant cytokine we detected in this model was IFN-γ, which peaks early, even before IL-17 could be detected. In addition, abscess induction with WTA did not lead to severe necrotic skin lesions but to a self-clearing, defined abscess. Thus, we conclude that WTA modulates the very early phases of skin abscess formation by a CD4$^+$ T cell- and IFN-γ-dependent mechanism, while IL-17-dependent mechanisms play a host-protective role at later time points and contribute to the clearing of the abscess and wound healing. Another study provided evidence for a host protective role of IL-17/TH17 responses and an anti-protective role for IFN-γ/TH1 responses in *S. aureus* skin infections[71], arguing for an active role of *S. aureus* in early abscess formation as a mechanism supporting immune evasion. High WTA amounts might permit *S. aureus* to amplify early mechanisms of abscess formation, thereby creating a microenvironment that protects bacteria from host responses. In line with this idea, overexpression of *tar*H in a WTA^{low} strain (SA113), which turned the strain into a WTA^{high} strain, led to increased abscess-inducing activity (Fig. 6a). More strikingly, we could increase abscess formation and c.f.u.s in the abscess by injecting purified WTA together with the bacterial inoculums of WTA^{low} strains USA500 and SA113 (Supplementary Fig. 13). USA500 is a strong toxin producer, and the fact that purified WTA alone allows USA500 to reach higher c.f.u.s in the abscess clearly underlines that WTA and toxins play different roles in the process of abscess formation. We also tested the impact of important WTA tailoring modifications D-alanine and GlcNAc and could not detect differences in D-alanylation between the WTA^{high} and WTA^{low} strains. The GlcNAc tailoring modification was slightly increased in USA300; however, when we compared the wt to an isogenic *tarM/S* mutant that lacks all GlcNAc modifications, we could not detect a significant phenotype in the s.c. mouse model of abscess formation.

Taken together, we conclude that overexpression of WTA biosynthesis is a mechanism that certain CA-MRSAs exploit to gain virulence (Fig. 6b). Recent advances in the development of antimicrobial substances led to the conclusion that WTA is an ideal target for novel anti-infective strategies[42] and antibiotics[43,44], and we believe that our report will aid in the development of novel anti-staphylococcal strategies that can be especially helpful in combating highly virulent CA-MRSA.

Methods

Bacterial strains and growth conditions. The bacterial strains, plasmids and oligonucleotides used in this study are described in Supplementary Table 1. *S. aureus* strains were cultivated in B-Medium (for cell wall or WTA isolation and infection experiments) or in TSB (tryptic soy broth) medium (Difco Laboratories) and incubated at 37 °C with shaking. Resistant *S. aureus* were cultivated in media supplemented with appropriate antibiotics (tetracycline (5 μg ml^{-1}) or chloramphenicol (10 μg ml^{-1})). All strains were kept on blood agar plates to monitor toxin *agr* activity and toxin production.

Construction of *agr* deletion mutants. For deletion of *agr* (Supplementary Table 1), bacteriophage Φ11 containing *agr::tet(M)* was propagated in strain RN4220. Using standard methods, Φ11 was used to transduce *agr::tet(M)* from RN6911 (ref. 32) to different target strains. In this construct, the entire *agr* locus, including *agrDBCA* and RNAIII, has been deleted[32]. The deletion of *agr* was confirmed by PCR and transcription analysis (primer *rnaIIIfor* and *rnaIIIrev*).

Construction of a recombinant expression vector (pRB474) for *tarH* with Gibson cloning. The open reading frame of *tarH* was amplified and cloned into expression vector pRB474 using a modified Gibson cloning protocol[72]. Wild-type *tarH* gene was amplified by PCR (primers gib_pRB474_*tarH*_for and gib_pRB474_*tarH*_rev) from the genomic DNA of the corresponding strains. Oligonucleotide sequences are provided in Supplementary Table 1. Vector pRB474 was amplified by PCR with primers gib_pRB474_f and gib_pRB474_r to generate *tarH* insert overhangs. Vector and insert PCR products were digested for 1 h at 37 °C with 10 U of DpnI. Each of

the DpnI-digested DNA samples (1 µl) was added to 15 µl of the Gibson master mix and incubated for 45 min at 50 °C. Gibson reaction mix (pRB474+*tarH*, 5 µl) was used to transform 50 µl of chemo-competent *Escherichia coli* DC10B or DH5α cells.

PAGE analysis of WTA. For PAGE analysis of WTA samples, a 26% and 0.75-mm-thick resolving gel was cast, as described recently[62]. WTA samples (100 nmol of phosphate per lane) were loaded onto gels and resolved for 24 h using a constant current of 40 mA per gel. WTA bands were visualized using the Alcian blue silver staining method. Briefly, the gels were fixed and stained with 0.005% (wt/vol) Alcian blue in EAW solution (40% ethanol and 5% acetic acid in water) at room temperature for several hours until the WTA ladder became visible. To intensify the staining pattern, the Bio-Rad silver stain kit (Bio-Rad) was used according to the manufacturer's instructions after oxidation of the gels with 0.7% $NaIO_4$ for 20 min.

Cell wall and WTA isolation and polymer analysis. Cell wall and WTA were isolated as described previously[38]. The instruments and devices used in the isolation process were depyrogenated by heat inactivation for 4 h at 240 °C. Bacteria were grown overnight in B-medium, supplemented with 0.2% glucose. WTA and cell wall extraction for immunological assays and *in vivo* experiments were performed on a large scale with a Euler cell mill (Euler) and a mini scale for WTA quantification with a FastPrep-24 Instrument (MP Biomedicals). Cell lysates were incubated overnight with DNase I (40 units ml^{-1}, Roche) and RNase A (80 units ml^{-1}, Sigma) at 37 °C and 200 r.p.m. followed by a proteinaseK digest (80 units per g cell wall, Applichem). Cell wall and WTA were dialysed against pyrogen-free water (Ambion). WTA amounts were quantified by determining the inorganic phosphate (P_i) content, as described previously[38,58].

D-Alanylation and GlcNAc amounts for the WTA polymers were quantified as described previously[73,74].

Purified, pyrogen-free cell wall and WTA for immunological assays and *in vivo* experiments were analysed for endotoxin with the Limulus amoebocyte lysate test (Charles River Laboratories), for protein via ultraviolet absorbance at 280 nm, for SDS–PAGE electrophoresis with silver stain, and for nucleic acids by agarose gel electrophoresis or a PicoGreen assay.

Gel shift assays with *tarH* promoter. Whole-cell protein extracts were prepared from over night cultures in TSB. Cells were washed in tris-EDTA buffer and lysed in a buffer containing 10 mM Tris, 1 mM EDTA, 50 mM KCl, 5 mM $MgCl_2$, 10% glycerol, pH 7.4, as described in ref. 57, supplemented with dithiothreitol (1 mM) and 1× complete proteinase inhibitor cocktail (Sigma). Protein extracts from isogenic strains with and without *rot* (all in *agr*-negative background to allow high Rot protein levels; USA300*Δagr* and USA300*ΔagrΔrot*) were mixed with infrared-dye labelled promoter probes (PCR amplification with labelled primers (DY-701 for *hla* and DY-781 for *rot*) purchased from Biomers GmbH, Supplementary Table 1) for *tarH* and *hla* (positive control) and incubated for 20 min at room temperature. The probes were 355 bp (*tar*H) and 299 bp (*hla).* Samples were directly run on a 3% agarose gel and imaged on a LI-COR Odyssey system with settings for 700 nm emission (*hla* promoter) and 800 nm (*rot* promoter).

Mouse model of subcutaneous abscess formation. Male Swiss Webster ND4 mice (4–6 weeks old) were obtained from Harlan. In the subcutaneous abscess model, 20 µg/100 µl purified cell wall WTA or live whole bacterial cells (as indicated in the figure legends) were mixed with equal volumes of sterile dextran beads (Cytodex 1, Sigma), and the mixture (0.2 ml) was injected into each flank of the mouse as described previously[75]. For controls, equal volumes of PBS were mixed with dextran beads. After 48 h, mice were euthanized, and the abscesses were excised and homogenized in 1 ml PBS (Gibco by Life Technologies) for c.f.u. determination or in 500 µl extraction buffer[76] for MPO measurement or cytokine determination. MPO is present in the azurophilic granules of neutrophils and is routinely used to assess inflammatory responses in tissues[77] as well as abscess formation. Measurements of single cytokines were performed, for example with mouse IL-17 and IFN-γ Quantikine ELISA Kits (R&D Biosystems). MPO activity was determined with a colorimetric assay[76] and was used as a quantitative measure of neutrophil infiltration. For assays where we injected purified WTA we screened for the production of a number of different cytokines by ELISA (R&D Systems Quantikine) at early (2 h) and late phases (48 h) at 20 µg per abscess (Supplementary Fig. 16a). While large amounts of IFN-γ were measurable very early, IL-17 production was primarily observed at later stages of abscess formation. We then elucidated the production of IFN-γ and IL-17 over time and in more detail. For c.f.u. counts, MPO measurements und cytokine assays, each abscess was treated as an independent *n*, as described previously (two abscesses per mouse).

T cell activation and IFN-γ cytokine production assay. Mononuclear cells were purified by density gradient centrifugation in Polymorphoprep (Axis-Shield) from blood drawn from different healthy human donors. $CD4^+$ T cells were purified with $CD4^+$ MACS enrichment columns (Milteny). Then, 2×10^5 T cells per ml were co-cultured with 1×10^5 irradiated APCs per ml and purified *S. aureus* cell wall (50 µg ml^{-1}), which was the optimal amount, as determined from titration experiments (Supplementary Fig. 16b). *S. aureus* enterotoxin A (SEA) (2 ng ml^{-1}) was used as a positive control, and T cells co-cultured with APCs alone were used as negative controls. Proliferation was assayed with a carboxyfluorescein succinimidyl ester dilution assay by fluorescence-activated cell scanning. The T cell stimulation index was calculated by normalizing to wells with APCs and T cells but no stimulating antigen. After stimulation, supernatants were collected by centrifugation (300*g*, 10 min, 4 °C) and stored at −80 °C until IFN-γ was assayed by ELISA (R&D Biosystems) according to the manufacturer`s instructions. Blocking antibodies were used in some experiments to evaluate the impact of HLA on WTA-dependent IFN-γ production. The antibodies used were HLA-DR clone L243 (Abcam), HLA-DQ clone SPV-L3 (Abcam), HLA-DP clone 1E3 Abnova, HLA-A,B,C clone W6/32 (Biolegend) and the isotype controls IgG2b clone 20116 (R&D Systems) and IgG2a clone ICIGG2A (Abcam).

RNA isolation *in vitro* and qRT–PCR. For RNA isolation, bacteria were grown overnight in TSB medium to the stationary growth phase (optical density at 600 nm (OD_{600}) of 10–14), and 1 ml was collected by centrifugation for 3 min at 10,000 r.p.m. and 4 °C. Bacteria were mechanically disrupted in 1 ml TRIzol reagent (Invitrogen/Life Technologies) with 0.5 ml zirconia-silica beads (diameter of 0.1 mm, Carl-Roth) in a high-speed homogenizer (FastPrep-24 Instrument, MP Biomedicals). RNA was further isolated as described in the manual provided by the manufacturer. Primers (obtained from Metabion) used for qRT–PCR are shown in Supplementary Table 1 and were designed using Primer3web (http://bioinfo.ut.ee/primer3). qRT–PCR was carried out using Brilliant II SYBR Green 1-Step Master Mix (Agilent). Relative quantifications were performed with a LightCycler480II instrument (Roche).

The transcriptional levels of target genes (*tarO/A/K/L/G/H/M/S*, *dlt operon*, *rot*, RNAIII) were normalized against the expression of *gyr*B as an internal control and in some assays normalized to expression in WTA^{low} strain SA113.

Ethics statement. Animal experiments were performed in strict accordance with the German regulations of the Society for Laboratory Animal Science (GV-SOLAS) and the European Health Law of the Federation of Laboratory Animal Science Associations (FELASA). The protocol was approved by the Regierungspräsidium Tübingen (permit no. H2/10). Human blood was collected from healthy volunteers who gave written informed consent for venipuncture in accordance with protocols approved by the University of Tübingen, Germany.

Statistical analysis. Statistical analyses were performed with Graphpad Prism (GraphPad Software, version 5.04) using appropriate statistical methods as indicated in the figure legends. *P* values ≤0.05 were considered significant. For all experiments *n* refers to the number of independent experiments (except for animal studies, where *n* refers to a single abscess, as described previously[51]). In all experiments, two technical replicates were used unless noted otherwise. For animal studies we used SPSS Sample Power V.3 or G-Power 3.1 to estimate the group size required for statistical significance. Power calculations were performed without assumption of a normal distribution and we used Wilcoxon–Mann–Whitney to evaluate the sample size for a first-degree error of 0.05 and a second degree error of 0.2. We did not fully blind or randomize animal experiments.

Data availability. The data that support the findings are available from the corresponding author upon request.

Received 25 April 2016; accepted 28 November 2016; published 23 January 2017; corrected 13 March 2017

References

1. DeLeo, F. R., Otto, M., Kreiswirth, B. N. & Chambers, H. F. Community-associated meticillin-resistant *Staphylococcus aureus*. *Lancet* **375,** 1557–1568 (2010).
2. Stryjewski, M. E. & Chambers, H. F. Skin and soft-tissue infections caused by community-acquired methicillin-resistant *Staphylococcus aureus*. *Clin. Infect. Dis.* **46(Suppl. 5),** S368–S377 (2008).
3. Fridkin, S. K. *et al.* Methicillin-resistant *Staphylococcus aureus* disease in three communities. *N. Engl. J. Med.* **352,** 1436–1444 (2005).
4. Purcell, K. & Fergie, J. Epidemic of community-acquired methicillin-resistant *Staphylococcus aureus* infections: a 14-year study at Driscoll Children's Hospital. *Arch. Pediatr. Adolesc. Med.* **159,** 980–985 (2005).
5. Hulten, K. G. *et al.* Three-year surveillance of community onset health care-associated *Staphylococcus aureus* infections in children. *Pediatr. Infect. Dis. J.* **25,** 349–353 (2006).
6. Liu, C. *et al.* A population-based study of the incidence and molecular epidemiology of methicillin-resistant *Staphylococcus aureus* disease in San Francisco, 2004–2005. *Clin. Infect. Dis.* **46,** 1637–1646 (2008).
7. Mediavilla, J. R., Chen, L., Mathema, B. & Kreiswirth, B. N. Global epidemiology of community-associated methicillin resistant *Staphylococcus aureus* (CA-MRSA). *Curr. Opin. Microbiol.* **15,** 588–595 (2012).
8. Macal, C. M. *et al.* Modeling the transmission of community-associated methicillin-resistant *Staphylococcus aureus*: a dynamic agent-based simulation. *J. Transl. Med.* **12,** 124 (2014).

9. Moran, G. J. *et al.* Methicillin-resistant *S. aureus* infections among patients in the emergency department. *N. Engl. J. Med.* **355,** 666–674 (2006).
10. Baker, P., Cohen, B., Liu, J. & Larson, E. Incidence and risk factors for community-associated methicillin-resistant *Staphylococcus aureus* in New York City, 2006–2012. *Epidemiol. Infect.* **144,** 1014–1017 (2016).
11. Como-Sabetti, K. *et al.* Community-associated methicillin-resistant *Staphylococcus aureus*: trends in case and isolate characteristics from six years of prospective surveillance. *Public Health Rep.* **124,** 427–435 (2009).
12. Foster, T. J. Immune evasion by staphylococci. *Nat. Rev. Microbiol.* **3,** 948–958 (2005).
13. Rooijakkers, S. H., van Kessel, K. P. & van Strijp, J. A. Staphylococcal innate immune evasion. *Trends Microbiol.* **13,** 596–601 (2005).
14. Otto, M. Basis of virulence in community-associated methicillin-resistant *Staphylococcus aureus*. *Annu. Rev. Microbiol.* **64,** 143–162 (2010).
15. Voyich, J. M. *et al.* Insights into mechanisms used by *Staphylococcus aureus* to avoid destruction by human neutrophils. *J. Immunol.* **175,** 3907–3919 (2005).
16. Moran, G. J., Amii, R. N., Abrahamian, F. M. & Talan, D. A. Methicillin-resistant *Staphylococcus aureus* in community-acquired skin infections. *Emerg. Infect. Dis.* **11,** 928–930 (2005).
17. King, M. D. *et al.* Emergence of community-acquired methicillin-resistant *Staphylococcus aureus* USA 300 clone as the predominant cause of skin and soft-tissue infections. *Ann. Intern. Med.* **144,** 309–317 (2006).
18. Melles, D. C. *et al.* Panton–Valentine leukocidin genes in *Staphylococcus aureus*. *Emerg. Infect. Dis.* **12,** 1174–1175 (2006).
19. Voyich, J. M. *et al.* Is Panton–Valentine leukocidin the major virulence determinant in community-associated methicillin-resistant *Staphylococcus aureus* disease? *J. Infect. Dis.* **194,** 1761–1770 (2006).
20. Bubeck Wardenburg, J., Bae, T., Otto, M., Deleo, F. R. & Schneewind, O. Poring over pores: α-hemolysin and Panton–Valentine leukocidin in *Staphylococcus aureus* pneumonia. *Nat. Med.* **13,** 1405–1406 (2007).
21. Bubeck Wardenburg, J., Palazzolo-Ballance, A. M., Otto, M., Schneewind, O. & DeLeo, F. R. Panton–Valentine leukocidin is not a virulence determinant in murine models of community-associated methicillin-resistant *Staphylococcus aureus* disease. *J. Infect. Dis.* **198,** 1166–1170 (2008).
22. Otto, M. Community-associated MRSA: what makes them special? *Int. J. Med. Microbiol.* **303,** 324–330 (2013).
23. Wang, R. *et al.* Identification of novel cytolytic peptides as key virulence determinants for community-associated MRSA. *Nat. Med.* **13,** 1510–1514 (2007).
24. Kobayashi, S. D. *et al.* Comparative analysis of USA300 virulence determinants in a rabbit model of skin and soft tissue infection. *J. Infect. Dis.* **204,** 937–941 (2011).
25. Berube, B. J., Sampedro, G. R., Otto, M. & Bubeck Wardenburg, J. The *psmα* locus regulates production of *Staphylococcus aureus* alpha-toxin during infection. *Infect Immun.* **82,** 3350–3358 (2014).
26. Hanberger, H. *et al.* Increased mortality associated with methicillin-resistant *Staphylococcus aureus* (MRSA) infection in the intensive care unit: results from the EPIC II study. *Int. J. Antimicrob. Agents* **38,** 331–335 (2011).
27. Inoshima, I. *et al.* A *Staphylococcus aureus* pore-forming toxin subverts the activity of ADAM10 to cause lethal infection in mice. *Nat. Med.* **17,** 1310–1314 (2011).
28. Cheung, G. Y., Wang, R., Khan, B. A., Sturdevant, D. E. & Otto, M. Role of the accessory gene regulator agr in community-associated methicillin-resistant *Staphylococcus aureus* pathogenesis. *Infect. Immun.* **79,** 1927–1935 (2011).
29. Queck, S. Y. *et al.* RNAIII-independent target gene control by the *agr* quorum-sensing system: insight into the evolution of virulence regulation in *Staphylococcus aureus*. *Mol. Cell* **32,** 150–158 (2008).
30. Li, M. *et al.* Evolution of virulence in epidemic community-associated methicillin-resistant *Staphylococcus aureus*. *Proc. Natl Acad. Sci. USA* **106,** 5883–5888 (2009).
31. Novick, R. P. & Geisinger, E. Quorum sensing in staphylococci. *Annu. Rev. Genet.* **42,** 541–564 (2008).
32. Novick, R. P. *et al.* Synthesis of staphylococcal virulence factors is controlled by a regulatory RNA molecule. *EMBO J.* **12,** 3967–3975 (1993).
33. Bronesky, D. *et al. Staphylococcus aureus* RNAIII and its regulon link quorum sensing, stress responses, metabolic adaptation, and regulation of virulence gene expression. *Annu. Rev. Microbiol.* **70,** 299–316 (2016).
34. Miller, L. G. *et al.* Clinical and epidemiologic characteristics cannot distinguish community-associated methicillin-resistant *Staphylococcus aureus* infection from methicillin-susceptible *S. aureus* infection: a prospective investigation. *Clin. Infect. Dis.* **44,** 471–482 (2007).
35. Diep, B. A. *et al.* Complete genome sequence of USA300, an epidemic clone of community-acquired meticillin-resistant *Staphylococcus aureus*. *Lancet* **367,** 731–739 (2006).
36. Thurlow, L. R. *et al.* Functional modularity of the arginine catabolic mobile element contributes to the success of USA300 methicillin-resistant *Staphylococcus aureus*. *Cell Host Microbe* **13,** 100–107 (2013).
37. Weidenmaier, C. & Peschel, A. Teichoic acids and related cell-wall glycopolymers in Gram-positive physiology and host interactions. *Nat. Rev. Microbiol.* **6,** 276–287 (2008).
38. Weidenmaier, C. *et al.* Role of teichoic acids in *Staphylococcus aureus* nasal colonization, a major risk factor in nosocomial infections. *Nat. Med.* **10,** 243–245 (2004).
39. Baur, S. *et al.* A nasal epithelial receptor for *Staphylococcus aureus* WTA governs adhesion to epithelial cells and modulates nasal colonization. *PLoS Pathog.* **10,** e1004089 (2014).
40. Weidenmaier, C. *et al.* DltABCD- and MprF-mediated cell envelope modifications of *Staphylococcus aureus* confer resistance to platelet microbicidal proteins and contribute to virulence in a rabbit endocarditis model. *Infect. Immun.* **73,** 8033–8038 (2005).
41. Weidenmaier, C. *et al.* Lack of wall teichoic acids in *Staphylococcus aureus* leads to reduced interactions with endothelial cells and to attenuated virulence in a rabbit model of endocarditis. *J. Infect. Dis.* **191,** 1771–1777 (2005).
42. Lehar, S. M. *et al.* Novel antibody–antibiotic conjugate eliminates intracellular *S. aureus*. *Nature* **527,** 323–328 (2015).
43. Ling, L. L. *et al.* A new antibiotic kills pathogens without detectable resistance. *Nature* **517,** 455–459 (2015).
44. Santa Maria, J. P. Jr *et al.* Compound–gene interaction mapping reveals distinct roles for *Staphylococcus aureus* teichoic acids. *Proc. Natl Acad. Sci. USA* **111,** 12510–12515 (2014).
45. Wang, H. *et al.* Discovery of wall teichoic acid inhibitors as potential anti-MRSA β-lactam combination agents. *Chem. Biol.* **20,** 272–284 (2013).
46. Pasquina, L. W., Santa Maria, J. P. & Walker, S. Teichoic acid biosynthesis as an antibiotic target. *Curr. Opin. Microbiol.* **16,** 531–537 (2013).
47. Lee, S. H. *et al.* TarO-specific inhibitors of wall teichoic acid biosynthesis restore β-lactam efficacy against methicillin-resistant staphylococci. *Sci. Transl. Med.* **8,** 329ra332 (2016).
48. Mann, P. A. *et al.* Chemical genetic analysis and functional characterization of staphylococcal wall teichoic acid 2-epimerases reveals unconventional antibiotic drug targets. *PLoS Pathog.* **12,** e1005585 (2016).
49. Neuhaus, F. C. & Baddiley, J. A continuum of anionic charge: structures and functions of D-alanyl-teichoic acids in Gram-positive bacteria. *Microbiol. Mol. Biol. Rev.* **67,** 686–723 (2003).
50. Brown, S., Santa Maria, J. P. Jr & Walker, S. Wall teichoic acids of Gram-positive bacteria. *Annu. Rev. Microbiol.* **67,** 313–336 (2013).
51. Weidenmaier, C., McLoughlin, R. M. & Lee, J. C. The zwitterionic cell wall teichoic acid of *Staphylococcus aureus* provokes skin abscesses in mice by a novel CD4+ T-cell-dependent mechanism. *PLoS One* **5,** e13227 (2010).
52. Lazarevic, V. & Karamata, D. The *tagGH* operon of *Bacillus subtilis* 168 encodes a two-component ABC transporter involved in the metabolism of two wall teichoic acids. *Mol. Microbiol.* **16,** 345–355 (1995).
53. Schirner, K., Stone, L. K. & Walker, S. ABC transporters required for export of wall teichoic acids do not discriminate between different main chain polymers. *ACS Chem. Biol.* **6,** 407–412 (2011).
54. Bunce, C., Wheeler, L., Reed, G., Musser, J. & Barg, N. Murine model of cutaneous infection with Gram-positive cocci. *Infect. Immun.* **60,** 2636–2640 (1992).
55. Vuong, C., Gotz, F. & Otto, M. Construction and characterization of an agr deletion mutant of *Staphylococcus epidermidis*. *Infect. Immun.* **68,** 1048–1053 (2000).
56. Novick, R. P. Autoinduction and signal transduction in the regulation of staphylococcal virulence. *Mol. Microbiol.* **48,** 1429–1449 (2003).
57. Killikelly, A. *et al.* Structure-based functional characterization of repressor of toxin (Rot). A central regulator of *Staphylococcus aureus* virulence. *J. Bacteriol.* **197,** 188–200 (2015).
58. Rajagopal, M. & Walker, S. Envelope structures of Gram-positive bacteria. *Curr. Top. Microbiol. Immunol.* http://dx.doi.org.10.1007/82_2015_5021 (2016).
59. Peschel, A. *et al.* Inactivation of the *dlt* operon in *Staphylococcus aureus* confers sensitivity to defensins, protegrins, and other antimicrobial peptides. *J. Biol. Chem.* **274,** 8405–8410 (1999).
60. Winstel, V. *et al.* Wall teichoic acid glycosylation governs *Staphylococcus aureus* nasal colonization. *mBio* **6,** e00632-15 (2015).
61. Montgomery, C. P., Boyle-Vavra, S. & Daum, R. S. Importance of the global regulators *Agr* and *SaeRS* in the pathogenesis of CA-MRSA USA300 infection. *PLoS One* **5,** e15177 (2010).
62. Meredith, T. C., Swoboda, J. G. & Walker, S. Late-stage polyribitol phosphate wall teichoic acid biosynthesis in *Staphylococcus aureus*. *J. Bacteriol.* **190,** 3046–3056 (2008).
63. Lee, K., Campbell, J., Swoboda, J. G., Cuny, G. D. & Walker, S. Development of improved inhibitors of wall teichoic acid biosynthesis with potent activity against *Staphylococcus aureus*. *Bioorg. Med. Chem. Lett.* **20,** 1767–1770 (2010).
64. Swoboda, J. G. *et al.* Discovery of a small molecule that blocks wall teichoic acid biosynthesis in *Staphylococcus aureus*. *ACS Chem. Biol.* **4,** 875–883 (2009).
65. Geisinger, E., Adhikari, R. P., Jin, R., Ross, H. F. & Novick, R. P. Inhibition of *rot* translation by RNAIII, a key feature of *agr* function. *Mol. Microbiol.* **61,** 1038–1048 (2006).

66. Boisset, S. *et al. Staphylococcus aureus* RNAIII coordinately represses the synthesis of virulence factors and the transcription regulator Rot by an antisense mechanism. *Genes Dev.* **21,** 1353–1366 (2007).
67. Zhu, Y. *et al.* Structure of *Rot*, a global regulator of virulence genes in *Staphylococcus aureus*. *Acta Crystallogr. D* **70,** 2467–2476 (2014).
68. Kolata, J. *et al.* The fall of a dogma? Unexpected high T cell memory response to *S. aureus* in humans. *J. Infect. Dis.* **212,** 830–838 (2015).
69. Cho, J. S. *et al.* IL-17 is essential for host defense against cutaneous *Staphylococcus aureus* infection in mice. *J. Clin. Invest.* **120,** 1762–1773 (2010).
70. Malachowa, N., Kobayashi, S. D., Sturdevant, D. E., Scott, D. P. & DeLeo, F. R. Insights into the *Staphylococcus aureus*–host interface: global changes in host and pathogen gene expression in a rabbit skin infection model. *PLoS One* **10,** e0117713 (2015).
71. Montgomery, C. P. *et al.* Protective immunity against recurrent *Staphylococcus aureus* skin infection requires antibody and interleukin-17A. *Infect. Immun.* **82,** 2125–2134 (2014).
72. Gibson, D. G. *et al.* Enzymatic assembly of DNA molecules up to several hundred kilobases. *Nat. Methods* **6,** 343–345 (2009).
73. Bertsche, U. *et al.* Increased cell wall teichoic acid production and D-alanylation are common phenotypes among daptomycin-resistant methicillin-resistant *Staphylococcus aureus* (MRSA) clinical isolates. *PLoS One* **8,** e67398 (2013).
74. Smith, R. L. & Gilkerson, E. Quantitation of glycosaminoglycan hexosamine using 3-methyl-2-benzothiazolone hydrazone hydrochloride. *Anal. Biochem.* **98,** 478–480 (1979).
75. Portoles, M., Kiser, K. B., Bhasin, N., Chan, K. H. & Lee, J. C. *Staphylococcus aureus* Cap5O has UDP-ManNAc dehydrogenase activity and is essential for capsule expression. *Infect. Immun.* **69,** 917–923 (2001).
76. Mullane, K. M., Kraemer, R. & Smith, B. Myeloperoxidase activity as a quantitative assessment of neutrophil infiltration into ischemic myocardium. *J. Pharmacol. Methods* **14,** 157–167 (1985).
77. van der Veen, B. S., de Winther, M. P. & Heeringa, P. Myeloperoxidase: molecular mechanisms of action and their relevance to human health and disease. *Antioxid. Redox Signal.* **11,** 2899–2937 (2009).

Acknowledgements

The authors thank I. Autenrieth and A. Peschel for discussions and critical reading of the manuscript. This research was supported by grants from the German Research Foundation (SFB) to C.We. (SFB766 and TR34), C.Wo. (SFB766 and TR34) and B.M.B. (TR34). The funders had no role in the design of the experiments, in the collection, analysis and interpretation of the data, in writing the manuscript, or in the decision to submit the manuscript for publication.

Author contributions

S.W., C.Wo., J.K., B.M.B., J.S. and C.We. planned the experiments. S.W., J.S., N.W., D.Ke., L.K., J.B., T.G., V.W. and C.We. performed the experiments. C.Wo., J.K., B.M.B., V.W. and D.Kr. supplied materials and strains. S.W., J.S. and C.We. wrote the manuscript. All authors read and approved the final manuscript.

Additional information

Supplementary information is available for this paper.

Reprints and permissions information is available at www.nature.com/reprints.

Correspondence and requests for materials should be addressed to C.We.

How to cite this article: Wanner, S. *et al.* Wall teichoic acids mediate increased virulence in *Staphylococcus aureus*. *Nat. Microbiol.* **2,** 16257 (2017).

Competing interests

The authors declare no competing financial interests.

ARTICLES NATURE MICROBIOLOGY

Corrigendum: Wall teichoic acids mediate increased virulence in *Staphylococcus aureus*

Stefanie Wanner, Jessica Schade, Daniela Keinhörster, Nicola Weller, Shilpa E. George, Larissa Kull, Jochen Bauer, Timo Grau, Volker Winstel, Henriette Stoy, Dorothee Kretschmer, Julia Kolata, Christiane Wolz, Barbara M. Bröker and Christopher Weidenmaier

Nature Microbiology **2,** 16257 (2017); published online 23 January 2017; corrected 13 March 2017

In the version of this Article originally published, the horizontal bars in Fig. 1a that indicate statistical differences were incorrectly placed. This has now been corrected in all versions of the Article, so that the horizontal bars indicate the statistical differences between strain 331865 and strains USA300, MW2 and 103.

Molecular Microbiology (2019) 0(0), 1–17 doi:10.1111/mmi.14347

Revisiting the regulation of the capsular polysaccharide biosynthesis gene cluster in *Staphylococcus aureus*

Daniela Keinhörster,[1] Andrea Salzer,[1] Alejandra Duque-Jaramillo,[1] Shilpa E. George,[1] Gabriella Marincola,[1†] Jean C. Lee,[2] Christopher Weidenmaier[1] and Christiane Wolz [1*]

[1] *Interfaculty Institute of Microbiology and Infection Medicine, University of Tübingen, Tübingen, Germany.*

[2] *Department of Medicine (Infectious Diseases), Brigham and Women's Hospital, Harvard Medical School, Boston, MA 02115, USA.*

Summary

Capsular polysaccharide (CP) biosynthesis in *Staphylococcus aureus* is tightly controlled resulting in a heterogeneous phenotype within a population and CP being mainly detectable in nongrowing cells. Expression of the corresponding biosynthesis gene cluster is driven by one promoter element (P_{cap}). Here, we demonstrate that P_{cap} contains a main SigB-dependent promoter. The SigB consensus motif overlaps with a previously described inverted repeat (IR) that is crucial for *cap* expression. The essentiality of the IR is derived from this region acting as a SigB binding site rather than as an operator site for the proposed *cap* activators RbsR and MsaB. Furthermore, P_{cap} contains an extensive upstream region harboring a weak SigA-dependent promoter and binding sites for *cap* repressors such as SaeR, CodY and Rot. Heterogeneous CP synthesis is determined by SigB activity and repressor binding to the upstream region. SigB dependency and regulation by the upstream repressors are also sufficient to explain the temporal gene expression pattern at the transcriptional level. However, CP synthesis remains growth phase-dependent even when transcription is rendered constitutive, suggesting additional post-transcriptional regulatory circuits. Thus, the interference of multiple repressors with SigB-dependent promoter activity as well as post-transcriptional mechanisms ensure the appropriate regulation of CP synthesis.

Accepted 3 July, 2019. *For correspondence. E-mail christiane.wolz@uni-tuebingen.de; Tel. +49 7071 2974648; Fax 00497071295937. Present address: †Institute for Molecular Infection Biology, University of Würzburg, Würzburg, Germany.

Introduction

Staphylococcus aureus is an opportunistic pathogen that asymptomatically colonizes parts of the human population, thereby increasing the risk of subsequent infections. Its capacity to cause a wide variety of diseases depends on secreted virulence factors as well as cell surface-attached proteins and polysaccharides (Gordon and Lowy, 2008; Weidenmaier and Lee, 2017; de Jong *et al.*, 2019). The capsular polysaccharide (CP) is one of these cell surface structures playing an important role in *S. aureus* pathogenesis and bacterial evasion of the host immune defenses (O'Riordan and Lee, 2004; Weidenmaier and Lee, 2017). Therefore, it is being discussed as a target for immunotherapy and as a vaccine candidate (Missiakas and Schneewind, 2016; Weidenmaier and Lee, 2017; Ansari *et al.*, 2019).

CP serotypes 5 and 8 are the two main CP serotypes produced by *S. aureus* strains (Arbeit *et al.*, 1984; Hochkeppel *et al.*, 1987; Roghmann *et al.*, 2005; Verdier *et al.*, 2007). Their structure is highly similar due to the closely related *cap5* and *cap8* gene clusters. These allelic operons consist of 16 genes, *cap5/8A* to *cap5/8P*, whose gene products are involved in CP biosynthesis, O-acetylation, transport and regulation (O'Riordan and Lee, 2004; Weidenmaier and Lee, 2017; Rausch *et al.*, 2019). The *cap* operon is thought to be mainly transcribed as a single large 17 kb transcript driven by one principal promoter element (P_{cap}), located upstream of *capA* (Sau *et al.*, 1997; Ouyang *et al.*, 1999). While *cap* gene clusters are extremely conserved across *S. aureus* genomes, not all clinically relevant isolates produce CP and acapsular variants may emerge during chronic infections. The loss of CP expression can typically be explained by mutations in any of the *cap* genes essential for CP synthesis or in the promoter region (Cocchiaro *et al.*, 2006; Tuchscherr *et al.*, 2010). For instance, the acapsular phenotype of strains from the USA300 lineage was attributed to conserved mutations in the *cap5* locus (Boyle-Vavra *et al.*, 2015). However, this assumption has been recently challenged

by the finding that USA300 strains might indeed produce CP during infection (Mohamed *et al.*, 2019). In addition to mutations that abolish its production, CP synthesis can also be switched off in response to environmental conditions via a complex regulatory network. Extensive *in vitro* and *in vivo* analyses have shown that *cap* expression is highly sensitive to changes in nutrients, pH, CO_2 and oxygen availability (Sutra *et al.*, 1990; Dassy *et al.*, 1991; Stringfellow *et al.*, 1991; Lee *et al.*, 1993; Poutrel *et al.*, 1995; Herbert *et al.*, 1997; Pohlmann-Dietze *et al.*, 2000; George *et al.*, 2015). Interestingly, CP synthesis was commonly found to be strictly growth phase-dependent and detectable only after post-exponential growth phase (Poutrel *et al.*, 1995; Dassy and Fournier, 1996; Pohlmann-Dietze *et al.*, 2000; Cunnion *et al.*, 2001; George *et al.*, 2015). In addition, not all bacteria in a population are CP-positive as revealed by flow cytometry and immunofluorescence (IF) of *in vitro*- and *in vivo*-grown bacteria (Poutrel *et al.*, 1997; Pohlmann-Dietze *et al.*, 2000; George *et al.*, 2015; Conlon *et al.*, 2016). As only nonencapsulated cells are able to adhere to endothelial cells (Pohlmann-Dietze *et al.*, 2000), while CP protects bacterial cells from phagocytosis (Karakawa *et al.*, 1988; Thakker *et al.*, 1998; Portoles *et al.*, 2001), it is likely that CP heterogeneity provides better adaptability of the population as a whole. So far, the underlying regulatory mechanisms of this particular expression pattern (early-Off/late-Heterogeneous) are only partially understood.

In general, P_{cap} activity correlates with CP synthesis, indicating that regulation occurs predominantly at the transcriptional level (Ouyang *et al.*, 1999; Meier *et al.*, 2007; Jansen *et al.*, 2013; Hartmann *et al.*, 2014; George *et al.*, 2015). Yet, the data to explain the molecular mechanisms of *cap* regulation are puzzling. The identified transcriptional start site (TSS) is not preceded by a classical sigma factor consensus sequence (Ouyang *et al.*, 1999); instead, several inverted and direct repeats were identified further upstream, among which a 10 bp inverted repeat (IR) was shown to be crucial for promoter activity (Ouyang *et al.*, 1999). It has been proposed that this IR functions as an operator site for the *cap* activators RbsR and MsaB (Lei and Lee, 2015; Batte *et al.*, 2016). RbsR also functions as a repressor of the *rbsUDK* operon involved in ribose uptake. While the presence of ribose relieves repression of the *rbsUDK* operon by RbsR, the presence and absence of ribose had no effect on *cap* expression (Lei and Lee, 2015). MsaB is described as a transcriptional factor with DNA binding capacity (Batte *et al.*, 2016) but is also annotated as cold-shock protein CspA, which exerts regulatory effects via RNA binding (Caballero *et al.*, 2018). In addition to RbsR and MsaB/CspA, there are several other transcription factors (MgrA, CcpA, RpiR, SpoVG, CcpE, XdrA, CodY, Rot), two-component regulatory systems (Agr, ArlRS, KdpDE, AirRS, SaeRS) and the alternative sigma factor B (SigB) known to be involved in the regulation of *cap* expression (O'Riordan and Lee, 2004; Weidenmaier and Lee, 2017). The role of these regulators was mainly deduced from the characterization of single regulatory mutants and, in most cases, it remains unclear how they affect *cap* expression. In particular, SigB and Agr are believed to act indirectly via other regulatory systems. For instance, the absence of a SigB consensus motif in front of the proposed TSS led to the hypothesis that SigB acts through the SigB-dependent *cap* regulators SpoVG, ArlRS and RbsR (Bischoff *et al.*, 2001; 2004; Meier *et al.*, 2007; Schulthess *et al.*, 2009; Lei and Lee, 2015). SigB is a central part of the general stress response, and is activated upon environmental stresses and toward stationary growth phase (Pane-Farre *et al.*, 2006). Its activity is regulated mainly at the post-translational level by a complex regulatory cascade involving RsbW, RsbV and RsbU, encoded within the *rsbUVWsigB* operon (Senn *et al.*, 2005).

For the quorum sensing system Agr, it was shown that Agr-mediated *cap* activation occurs via inactivation of the repressor Rot (George *et al.*, 2015). Rot is known to bind to several target genes; however, its binding motif is ill-defined (Killikelly *et al.*, 2015). Nevertheless, Rot as well as the DNA binding proteins CodY and SaeR are likely candidates for direct interference with the P_{cap} promoter element. CodY represses many metabolic and virulence genes, including the *cap* operon (Pohl *et al.*, 2009; Majerczyk *et al.*, 2010), and binding of CodY to the P_{cap} region has been demonstrated (Majerczyk *et al.*, 2010; Batte *et al.*, 2018; Lei and Lee, 2018). The two-component system (TCS) SaeRS regulates a number of virulence factors, with *cap* being one of the few genes repressed (Steinhuber *et al.*, 2003; Luong *et al.*, 2011; George *et al.*, 2015). With only a poorly conserved SaeR consensus sequence in P_{cap}, it remains unclear whether SaeR exerts its effect on *cap* expression indirectly or via direct promoter interaction.

All in all, despite a plethora of work published on *cap* regulation, results are yet inconclusive regarding P_{cap} architecture and the molecular interference of the different regulatory elements. Here, we redefined the P_{cap} promoter structure and reinvestigated the main players of *cap* expression. We identified a SigB consensus motif overlapping with the IR structure. In addition, we found a second weak SigA-dependent promoter in the P_{cap} upstream region, as well as binding sites for three *cap* repressors, CodY, Rot and SaeR, which interfere with SigB-dependent promoter activity. Thus, the early-Off/late-Heterogeneous *cap* expression pattern is a consequence of SigB activity together with repression mediated through the P_{cap} upstream region. However, negative regulation of CP synthesis in early growth phase is maintained through additional post-transcriptional mechanisms.

Results

P_{cap} contains SigA- and SigB-dependent promoters

Previous primer extension analysis of the 344 bp comprising P_{cap} revealed a TSS –17 bp upstream of the ATG start codon of *capA* (Ouyang *et al.*, 1999). However, RNA-Seq data indicate an alternative TSS further upstream, at position –41 from the *capA*-coding region (data not shown), consistent with recent whole genome analyses of TSSs in *S. aureus* (Mäder *et al.*, 2016; Prados *et al.*, 2016). To resolve this ambiguity, we employed 5′ rapid amplification of cDNA endings (5′ RACE) (Fig. 1A). Most of the clones (6/10) revealed a TSS at position –41 bp from the *capA* start codon, which is preceded by a putative SigB consensus sequence. This SigB promoter consists of a conserved SigB –35 motif (GTTTAA) and a –10 region harboring three mismatches (ATGTAA versus GGGTAT) (Homerova *et al.*, 2004). Remarkably,

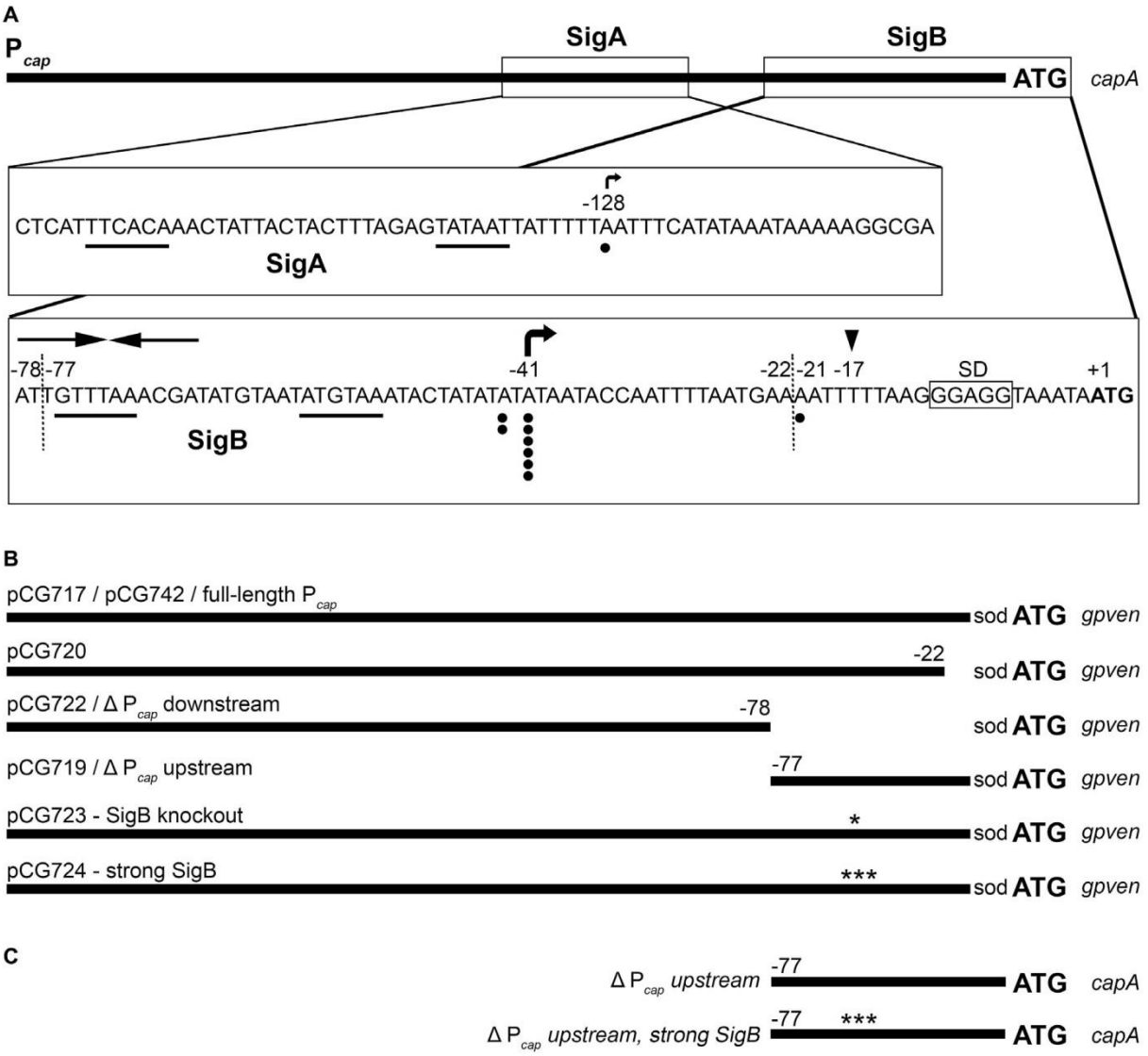

Fig. 1. P_{cap} promoter architecture and P_{cap} variants employed in this study.
A. P_{cap} (344 bp) in front of *capA* with magnified SigA and SigB promoters. Black dots represent the putative TSSs suggested by 10 analyzed 5′ RACE clones. Sigma factor –35 and –10 motifs are underlined, bent arrows indicate the corresponding TSSs. The TSS and inverted repeat (IR) structure proposed by Ouyang *et al.* (1999) are marked as black triangle and opposing arrows, respectively. Vertical dashed lines indicate sites of promoter truncation. Numbers mark positions with reference to the ATG of *capA*. The native Shine Dalgano (SD) sequence is labeled and indicated by a box.
B. P_{cap} promoter fusion variants in front of an artificial ribosomal binding site (sod) and *gpven* gene. Numbers show truncation sites and asterisks indicate point mutations (* –56:G → T; *** –58:A → G, –57:T → G, –52:A → T).
C. Genomic P_{cap} variants in front of *capA*. Numbers show truncation sites and asterisks indicate point mutations (*** –58:A → G, –57:T → G, –52:A → T).

the SigB –35 consensus sequence is located within the IR that is crucial for P_{cap} activity (Ouyang *et al.*, 1999). The identified TSS confirmed our RNA-Seq data and the TSS prediction of Prados *et al.* (2016). In addition, 5′ RACE revealed one clone with a putative TSS at position –128 bp upstream of the *capA* start codon, which was also predicted by Prados *et al.* (2016). A conserved SigA consensus sequence was identified in front of this TSS containing canonical –35 and –10 regions. Interestingly, the TSS –17 bp upstream of the *capA* start codon proposed by Ouyang *et al.* (1999) was not detected. Though one 5′ RACE clone suggested a potential TSS in close proximity, at position –21, this was not preceded by a sigma factor consensus sequence, challenging the presence of a functional promoter. Using 5′ RACE and sequence analysis, we provide evidence for a dominant SigB-dependent promoter and an additional SigA-dependent promoter further upstream in the P_{cap} promoter element.

cap expression is mainly driven by direct SigB regulation

To analyze promoter activities, we constructed various P_{cap}-*gpven* promoter fusions (Fig. 1B), including deletions and variations of the putative SigA- and SigB-dependent promoters. Cloning the full-length P_{cap} in front of *gpven* and an artificial ribosomal binding site (Liese *et al.*, 2013) (pCG717) resulted in detectable *gpven* expression and was used as reference for all further experiments (Fig. 2A). Deletion of the downstream element containing the putative TSSs at position –17 (Ouyang *et al.*, 1999) and –21 in pCG720 did not influence *gpven* expression. This supports that there is no active promoter located in this region and that these putative TSSs may have been derived from RNA processing. A construct containing only the SigA-dependent promoter (pCG722) resulted in a low but detectable fluorescence signal, suggesting weak promoter activity. In contrast, a construct containing only the SigB-dependent promoter (pCG719) resulted in a strong promoter activity. This indicates dual promoter activity driving P_{cap} expression: a weak SigA-dependent promoter located in the upstream region plus a main SigB-dependent promoter further downstream. The deletion of the upstream region containing the SigA consensus sequence (pCG719) resulted in promoter activity higher than that of the full-length construct (pCG717). Taken together, these results suggest that despite containing a functional SigA-dependent promoter, the upstream region mainly functions as a repressive element.

To further prove that SigB is directly involved in *cap* activation, the expression of the full-length P_{cap} promoter fusion was measured in wild-type and a *sigB* mutant over time. In addition, constructs where the SigB –10 consensus sequence was mutated to either abolish (pCG723) or

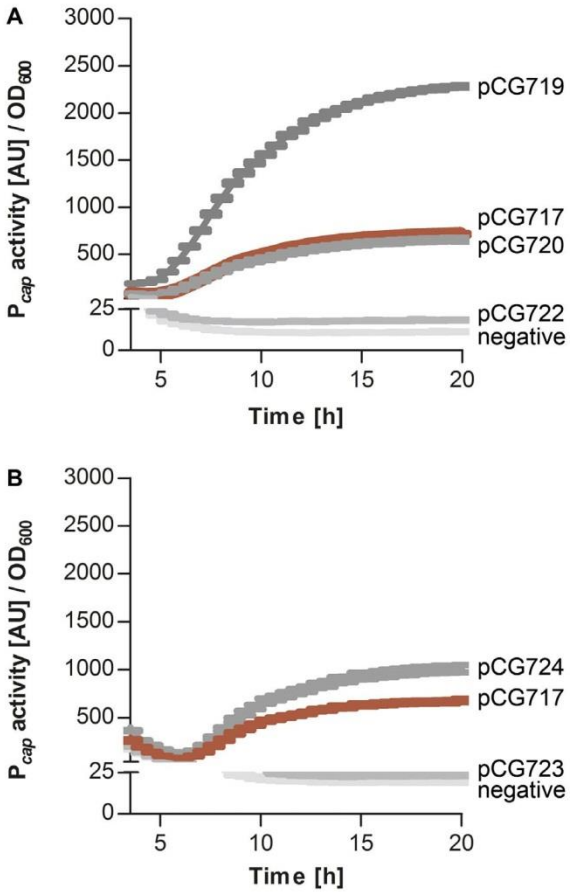

Fig. 2. SigB is the main driver of P_{cap} activity. Promoter activities of different truncated (A) or mutated (B) P_{cap} fusions in Newman wild-type. The different promoter fusion constructs are described in Fig. 1B. The promoter activity of the full-length P_{cap} promoter fusion (pCG717) serves as reference and is marked in red. Mean gpVenus intensity per OD_{600} plus standard deviation of biological triplicates is shown over time.

enhance (pCG724) SigB affinity were included (Fig. 2B). Deletion of *sigB* (data not shown) or a loss-of-function mutation in the SigB consensus sequence eliminated P_{cap} activity. In contrast, the strong SigB consensus motif further enhanced promoter activity in comparison to the native promoter. These results reveal that *cap* expression is mainly and directly driven by SigB activity.

MsaB/CspA activates cap expression by modulating SigB activity

Interestingly, the crucial IR structure that in fact constitutes the SigB –35 motif was shown to be the binding site for two *cap* activators, RbsR and MsaB (Lei and Lee, 2015; Batte *et al.*, 2016). To elucidate whether and how these regulators interfere with SigB-dependent promoter activity, full-length P_{cap} promoter fusions were introduced

into *msa* and *rbsR* knockout mutants. Under our growth conditions, deletion of *rbsR* showed no effect on P_{cap} activity (Fig. S1).

In the *msa* mutant, P_{cap} promoter activity was lower than in the wild-type, supporting the finding that MsaB/CspA contributes to *cap* activation (Fig. 3A). We hypothesized that MsaB/CspA exerted its effect by modulating SigB activity. To test this hypothesis, we used the dual promoter fusion construct pCG742 to simultaneously measure P_{cap} and P_{asp23} activities. The P_{asp23} promoter is widely used as marker for SigB activity (Gertz *et al.*, 1999; Giachino *et al.*, 2001; Homerova *et al.*, 2004) and was cloned in front of *gpcer* (Liese *et al.*, 2013). We found P_{cap} and P_{asp23} activities to be highly correlated, in line with the assumption that both are controlled directly by SigB. The activity of both promoters was lower in a *msa* mutant (Fig. 3A and B). It was previously shown that MsaB/CspA could bind to *rsbVWsigB* transcript, likely leading to its stabilization (Caballero *et al.*, 2018). In this case, expression of *sigB* alone should lead to MsaB/CspA-independent regulation. Therefore, we expressed *sigB* from a constitutive promoter in a *rsbUVWsigB* mutant (const. *sigB*). By this means, we also circumvented post-transcriptional regulation of SigB by the RsbUVW phosphorelay. As expected, neither P_{cap} activity (Fig. 3A) nor P_{asp23} activity (Fig. 3B) was affected by *msa* deletion in this background. To exclude additional regulation by direct binding of MsaB/CspA to P_{cap}, we performed electrophoretic mobility shift assays (EMSAs) with purified MsaB/CspA protein. Even using high amounts of MsaB/CspA protein, no band shift was observed (Fig. S2). Thus, MsaB/CspA promotes *cap* expression via modulation of SigB activity and not by direct interaction with P_{cap}.

Upstream promoter region leads to P_{cap} repression

To follow up on the observation that the P_{cap} upstream region is of repressive function (Fig. 2A), we investigated the role of the known *cap* repressors CodY, Rot and Sae. Full-length (pCG717) and truncated (pCG719 and pCG722) P_{cap} promoter fusions were introduced in *codY*-, *rot*- or *sae*-negative background. Mutation of any of the three regulators resulted in a significant increase of full-length P_{cap} activity (Fig. 4A). The effect of the individual regulators is additive, since in the *sae codY rot* triple mutant, the promoter activity is further enhanced compared to the single mutants. If these repressors target the P_{cap} upstream region, their deletion should not affect promoter activity of a construct lacking this part of the promoter. Indeed, repressor mutations have no or only minor effects on promoter activity of construct pCG719 (Fig. 4B). Interestingly, promoter activity of the full-length construct in the triple mutant remained significantly below the level of the upstream-truncated construct (Fig. 4A and B). This indicates that, besides CodY, Sae and Rot, additional repressive factors are acting on the P_{cap} upstream region.

We further analyzed whether the repressors also affect the activity of the weak SigA-dependent promoter located in this region (Fig. 4C). Remarkably, neither Rot

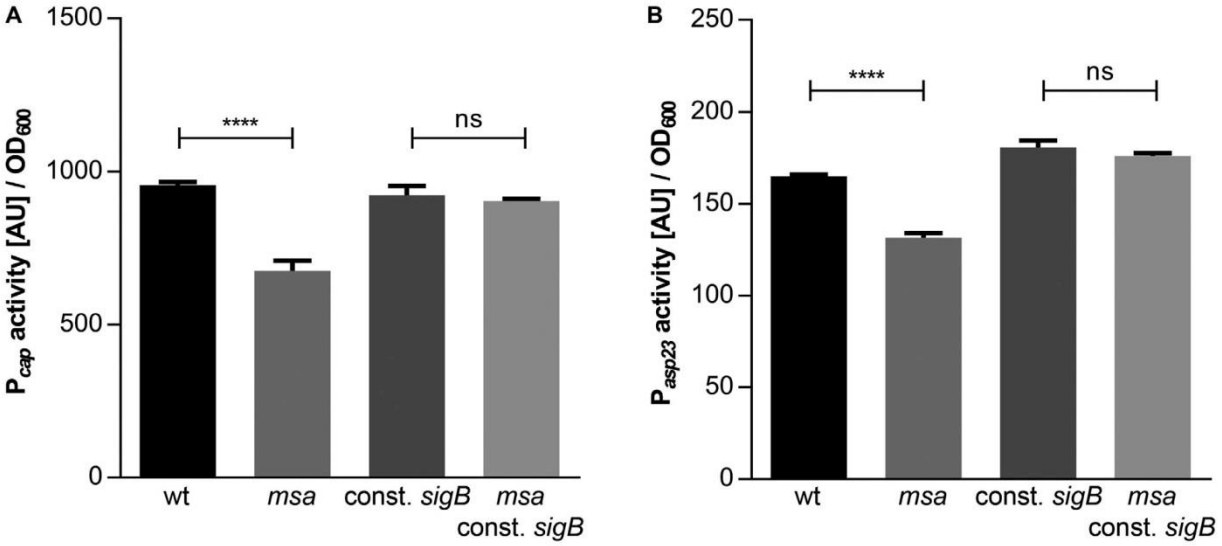

Fig. 3. MsaB/CspA activates *cap* expression by modulating SigB activity. Promoter activity of full-length P_{cap}-*gpven* (A) and P_{asp23}-*gpcer* (B) dual promoter fusion (pCG742, see Fig. 1B) in Newman wild-type and a *msa* mutant with or without constitutive *sigB* expression (const. *sigB*). gpCerulean (P_{asp23}) and gpVenus (P_{cap}) intensities are given per OD_{600} after 16 h of growth. Experiments were performed in biological triplicates, error bars represent the standard deviation. Statistical significance was obtained by ordinary one-way ANOVA followed by Tukey's multiple comparison test (ns: not significant, ****: $P < 0.0001$).

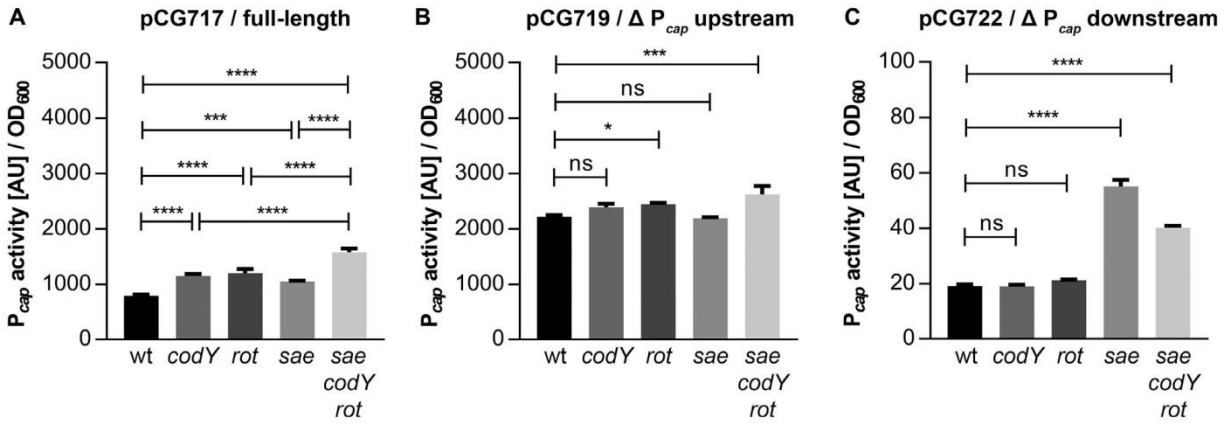

Fig. 4. CodY, Rot and Sae repress *cap* expression by interfering with the P_{cap} upstream region. Promoter activity of different P_{cap} truncations in Newman wild-type, *codY*, *rot*, *sae* single and triple mutants (A–C). The different promoter fusion constructs are described in Fig. 1B. gpVenus intensity is given per OD_{600} after 16 h of growth. Experiments were performed in biological triplicates, error bars represent the standard deviation. Statistical significance was determined by ordinary one-way ANOVA followed by Dunnett's multiple comparison test (ns: not significant, *: $P < 0.1$, ***: $P < 0.001$, ****: $P < 0.0001$).

nor CodY showed any influence on promoter activity in a construct only containing the upstream part of the promoter (pCG722). However, mutation of *sae* resulted in increased SigA-dependent promoter activity, even though it remained weak in comparison to the full-length promoter (pCG717). Hence, while all three repressors target the upstream region and affect SigB-dependent promoter activity, only Sae additionally represses the weak SigA-dependent promoter.

Sae, Rot and CodY repress P_{cap} by direct binding

We have demonstrated that Sae, Rot and CodY repress P_{cap}, but it remains unclear whether repression occurs through direct DNA–protein interaction or rather indirectly through the complex regulatory network. To elucidate the nature of the repressors, we performed EMSAs with purified SaeR, Rot and CodY proteins. As SaeR only binds DNA in its phosphorylated state (Sun *et al.*, 2010), we created a phosphomimetic SaeR with a D51E substitution. Incubation of increasing amounts of $SaeR^{D51E}$ with fluorescence-labeled P_{cap} upstream fragment (–78 to –344 from *capA*, see Fig. 1A) resulted in a retarded protein–DNA complex (Fig. 5A), which was not observed using the unphosphorylated native SaeR (Fig. 5B). Binding is consistent with a putative SaeR binding motif located between –79 bp and –94 bp upstreams of the *capA* start codon (Liu *et al.*, 2016). Specific binding to the P_{cap} upstream region was also found for Rot and CodY (Fig. 5C and D). These findings are in line with the promoter activities described above showing that Sae, Rot and CodY target the P_{cap} upstream region (Fig. 4A and B). Binding of CodY to the downstream fragment (+10 to –77 from *capA*, see Fig. 1A) is unspecific as band shifts are eliminated by specific and unspecific unlabeled competitors (Fig. S3D). However, it was previously found that CodY can interact with a region downstream (+160 to –152 from *capA*, see Fig. 1A) reaching into the *capA* coding sequence (Lei and Lee, 2018). This region was so far not included in our promoter activity assays or EMSAs. We could confirm CodY binding to this region, when using a 3′ extended downstream fragment (+160 to –77 from *capA*, see Fig. 1A) covering the *capA* coding region (Fig. S3E). Together, these results show that SaeR and Rot directly bind to the P_{cap} upstream region, whereas CodY can bind to two distinct sites, one within the P_{cap} upstream region and one further downstream reaching into the *capA*-coding region.

SigB-dependent regulation and various repressors targeting the upstream region contribute to temporal and heterogeneous CP synthesis

So far, we analyzed P_{cap} promoter activity using artificial promoter fusion constructs. To confirm that our findings translate into CP production, we used IF for CP detection. This also allows monitoring the onset of CP production and CP heterogeneity on the single cell level. Cultures were diluted thrice to ensure that all bacteria are actively dividing after inoculation and do not carry residual CP from stationary phase. Bacteria were analyzed throughout growth at different time points (T_0–T_4) (Fig. 6 and Table S1). On exponentially growing bacteria, no CP was detectable, but upon reaching stationary phase approximately 40% of the population became CP-positive, which is consistent with previous results (George *et al.*, 2015). With SigB

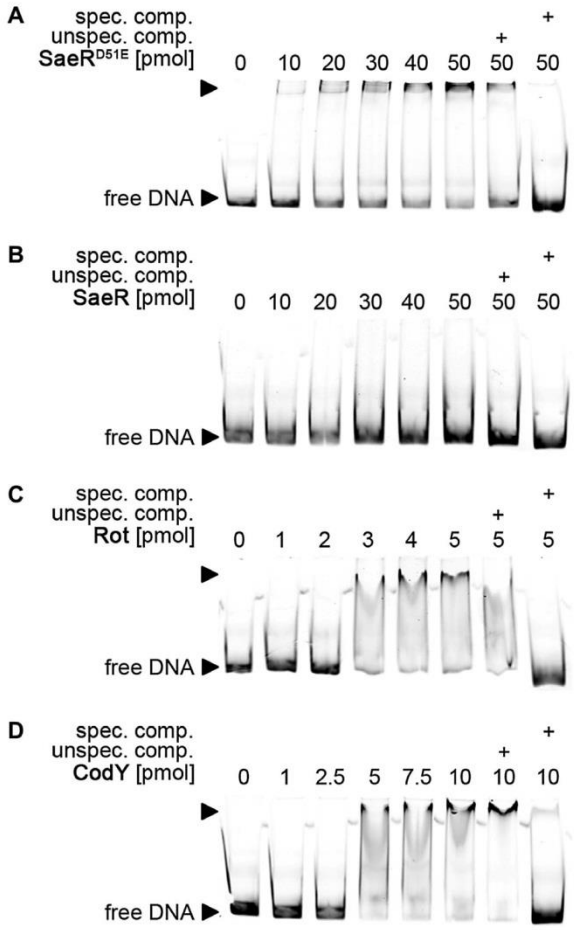

Fig. 5. CodY, Rot and SaeR bind directly to P_{cap} upstream region. Electrophoretic mobility shift assays of purified SaeR^{D51E} (A), SaeR (B), Rot (C) and CodY (D). Increasing amounts of protein were incubated with fluorescently labeled P_{cap} upstream region (–78 to –344 from *capA*, see Fig. 1A). As a control for specificity, shifts were subject to competition with the promoter of the 16 S rRNA gene (unspec. comp.) or unlabeled P_{cap} upstream region (–78 to –344 from *capA*, see Fig. 1A) (spec. comp.) in 100-fold excess. Representative pictures from at least three independently performed experiments are shown.

being a regulator of late genes, we first investigated the effect of constitutive *sigB* expression on CP synthesis during growth. Constitutive *sigB* expression in a *rsbUVWsigB*-negative background resulted in earlier onset of CP production and 50% CP-positive bacteria in stationary phase. In addition, we generated a P_{cap} mutant in which the upstream promoter region containing repressor binding sites was chromosomally deleted (ΔP_{cap} *upstream*, Fig. 1C). Also in this strain, CP production started earlier and 83% CP-positive cells could be detected in the late growth phase. Of note, the effect of the P_{cap} upstream region deletion was more profound than that of constitutive *sigB* expression. Furthermore, IF revealed that in bacteria from stationary phase, much of the heterogeneity is reduced in the ΔP_{cap} *upstream* strain and omitted in combination with constitutive *sigB* expression. Thus, it seems to be the combination of repression via transcriptional regulators and SigB-dependent promoter activity that is responsible for the heterogeneous CP expression pattern in stationary phase.

However, throughout all experiments, CP expression remained growth phase-dependent. We thought that this could be due to the weak SigB promoter of P_{cap}. Therefore, we additionally altered the SigB –10 region to the conserved SigB –10 motif on the chromosome in the P_{cap} upstream-truncated strain *(ΔP_{cap} upstream, strong SigB*, Fig. 1C*)*. Together with constitutive *sigB* expression, this shifted the onset of CP even further toward early growth phase. However, the majority of the bacterial population still remained CP-negative in early logarithmic growth phase.

The bacteria analyzed by IF also contained the dual promoter fusion construct pCG742 (P_{asp23}-*gpcer*, P_{cap}-*gpven*) which allowed us to simultaneously analyze SigB activity throughout growth on the single cell level (Fig. 7A). As expected, P_{asp23} and P_{cap} activities reached their maximum in stationary phase cells, confirming growth phase-dependent SigB activity. However, in contrast to P_{cap} activity (yellow), P_{asp23} (blue) activity was already detectable in some bacteria from the exponential growth phase. This indicates that SigB activity itself is also heterogeneous but is not sufficient to activate P_{cap} in the early growth phase.

CP synthesis is also controlled on the post-transcriptional level

To analyze whether growth phase dependency on the CP level correlates to *capA* transcript levels, *capA* mRNA was quantified by qRT-PCR at T_0–T_2 (Fig. 7B). As expected, in the wild-type strain, *capA* expression was strongly repressed in early growth phase. In contrast, constitutive *cap*A expression was achieved in a strain with upstream-deleted P_{cap} promoter, strong SigB consensus sequence and constitutive *sigB* expression (ΔP_{cap} *upstream, strong SigB*, const. *sigB)*, exceeding that of the wild-type. Of note, CP production is still growth phase-dependent under these conditions (Fig. 6), suggesting the existence of post-transcriptional mechanisms regulating CP synthesis.

P_{cap} *regulation is conserved in different* S. aureus *strains*

So far, all experiments have been performed in strain Newman which is special due to its hyperactive SaeRS system (Mainiero *et al.*, 2010). To validate our findings in a different *S. aureus* background, we chose the

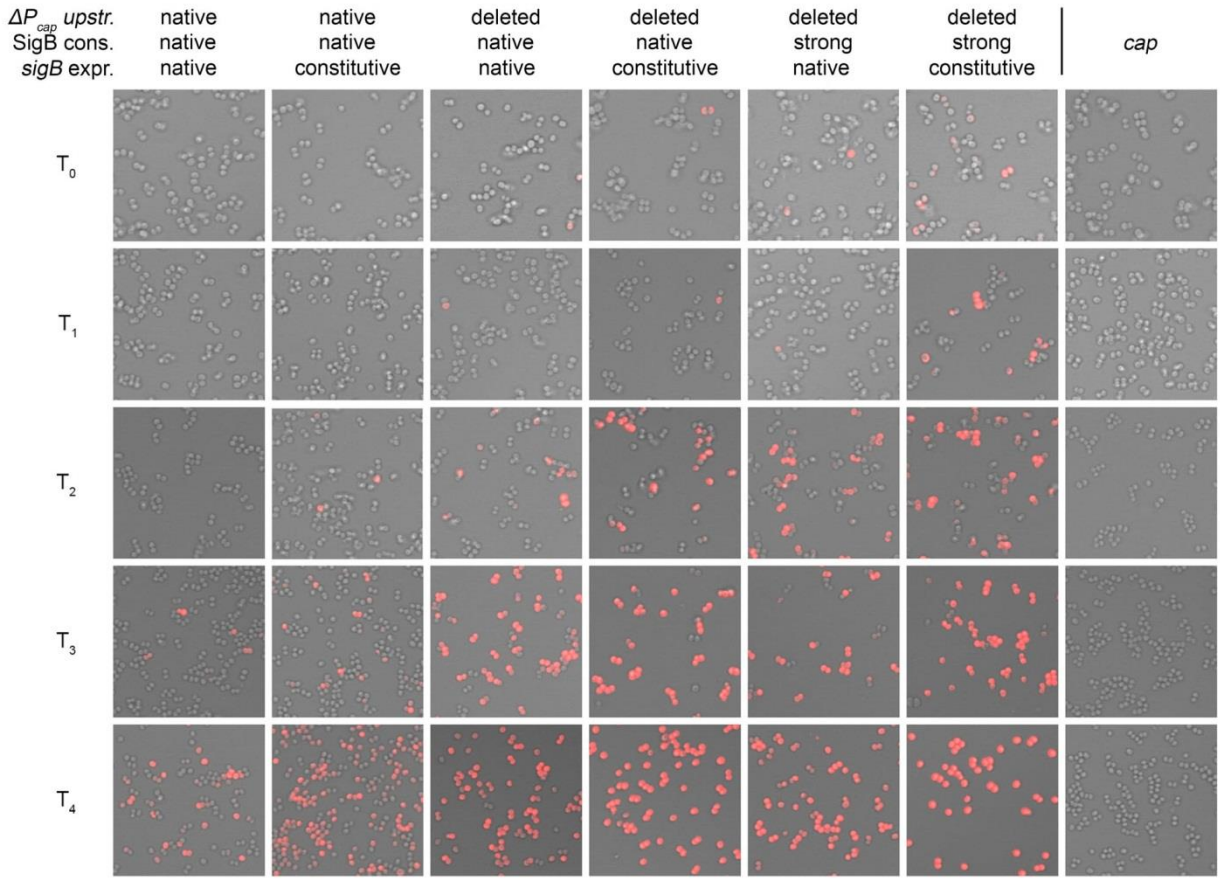

Fig. 6. SigB regulation and upstream repressors determine temporal and heterogeneous CP synthesis. Detection of CP production by bacteria from different growth phases via immunofluorescence. The wild-type strain Newman was mutated in order to delete the upstream region (ΔP_{cap} *upstr.*), to contain a strong SigB –10 consensus motif (SigB cons.) and/or constitutive *sigB* expression (*sigB* expr.) and grown to defined growth phase T_0–T_4. The different genomic P_{cap} variants are described in Fig. 1C. Representative pictures from at least three independent cultures are shown.

widely studied community-acquired methicillin-resistant *S. aureus* strain USA300 JE2. This strain has an acapsular phenotype due to three crucial mutations in the P_{cap} promoter region and in the coding regions of *cap5D* and *cap5E* (Boyle-Vavra *et al.*, 2015). Therefore, we first generated derivatives in which we either only repaired the mutation in P_{cap} (P_{cap} *repaired*) or all three mutations (*cap repaired*) (Fig. 8 and Table S2). In line with previous observations, the USA300 JE2 wild type shows an acapsular phenotype and the repair of the mutation in P_{cap} alone is not sufficient to enable CP production *in vitro* (Boyle-Vavra *et al.*, 2015). Only when all three mutations were repaired, USA300 JE2 was capable of producing CP, following the same peculiar expression pattern as strain Newman: CP-positive cells were observed toward late growth phase and CP expression was highly heterogeneous. Upon deletion of the P_{cap} upstream region and introduction of the fully conserved SigB consensus sequence (*cap repaired*, ΔP_{cap} *upstream, strong SigB*), CP-positive cells were detected earlier and, in late growth phase, all cells were CP-positive. Therefore, the CP expression pattern of USA300 *cap repair* and its regulation closely resembles that of Newman.

Discussion

CP protects *S. aureus* against phagocytosis, but also hampers adherence to endothelial cells and matrix proteins. It is believed that heterogeneity of CP expression has evolved to provide better adaptability of the bacterial population during infection and colonization (George *et al.*, 2015). Apart from this heterogeneous phenotype, CP production is strongly growth phase-dependent, with encapsulated cells found only toward stationary growth phase (George *et al.*, 2015). During the last decades, many regulatory proteins have been shown to have an impact on CP production, forming

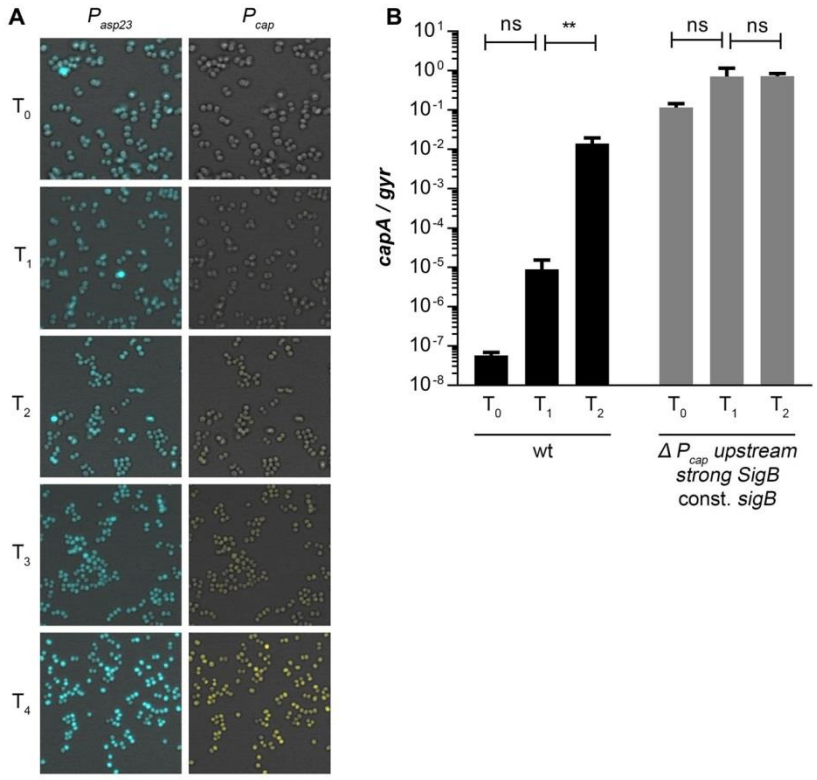

Fig. 7. *capA* transcription can be rendered constitutive.
A. Promoter activities of P_{asp23}-*gpcer* and full-length P_{cap}-*gpven* dual promoter fusion (pCG742, see Fig. 1B) in Newman wild-type. Bacteria cells were grown to defined growth phase T_0–T_4. Representative pictures from at least three independent cultures are shown.
B. Bacterial cells were harvested at different growth phases (T_0–T_2) and total RNA was isolated. *capA* transcripts in Newman wild-type and a P_{cap} upstream truncated strain with strong SigB –10 consensus sequence and additional constitutive *sigB* expression (Newman ΔP_{cap} *upstream, strong SigB*, const. *sigB*) were measured by qRT-PCR and normalized to *gyr*. The genomic P_{cap} variant is described in Fig. 1C. Experiments were performed in biological triplicates, error bars represent the standard deviation. Statistical significance was determined by ordinary one-way ANOVA followed by Tukey's multiple comparison test (ns: not significant, **: $P < 0.01$).

a complex regulatory network. However, to date, it is not known which regulator is mainly responsible for this peculiar expression pattern. Here, we revisited the role of important molecular determinants of P_{cap} activity, summarized in Fig. 9.

cap expression is mainly driven by SigB activity

We show that the main P_{cap} promoter is SigB-dependent. This is based on (i) 5′ RACE results revealing a new TSS downstream of a conserved SigB consensus sequence with minor mismatches in the –10 region; (ii) only very weak promoter activity in a *sigB* mutant or upon mutation of the –10 consensus sequence; (iii) higher P_{cap} activity when the SigB –10 region matches the proposed SigB consensus sequence; and (iv) correlation of P_{asp23} and P_{cap} promoter activity. Of note, the SigB –35 region is directly located within the IR which was shown to be crucial for *cap* expression (Ouyang *et al.*, 1999). Thus, the effects of previously reported mutations in this region can be simply explained by its function as a SigB binding site. A positive effect of SigB on *cap* expression was previously shown. However, it was believed to be mediated via the SigB-dependent c*ap* activators SpoVG, ArlRS-MgrA and RsbR (Bischoff *et al.*, 2001; 2004; Meier *et al.*, 2007; Schulthess *et al.*, 2009; Lei and Lee, 2015). Our results highlight the importance of SigB for *cap* expression and clearly demonstrate that its main impact is through direct SigB-dependent promoter activation. Nevertheless, other SigB-dependent *cap* regulators may contribute to the fine tuning of *cap* expression and amplify SigB dependency.

MsaB/CspA activates cap expression by modulating SigB activity

It was previously shown that the SigB –35 consensus sequence functions as binding site for two *cap* activators RbsR and MsaB (Lei and Lee, 2015; Batte *et al.*, 2016). We did not observe an effect of RbsR on P_{cap} activity, neither in wild-type nor in a *sae*-negative

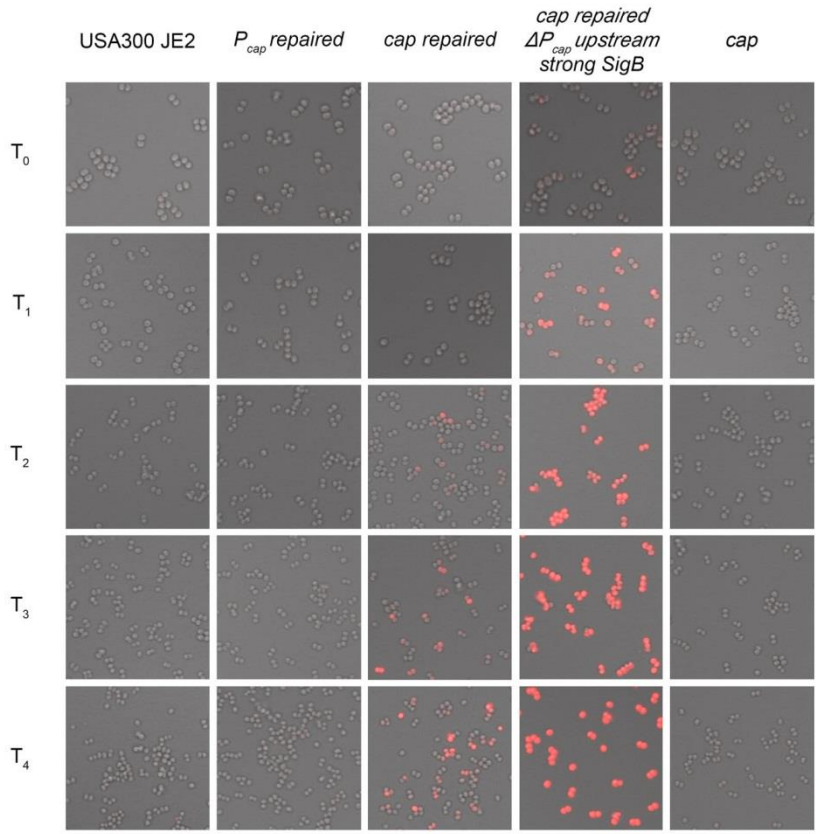

Fig. 8. CP production in strain USA300 JE2. Detection of CP in bacteria from different growth phases. USA300 JE2 wild-type and mutants in which either the mutation in P_{cap} alone (*P_{cap} repaired*) or in the whole *cap* locus (P_{cap}, *capD, capE; cap repaired*) are repaired were grown to defined growth phase T_0–T_4 and CP was detected by immunofluorescence. In addition, the effect of P_{cap} upstream truncation and a strong SigB –10 consensus sequence (*cap repaired, ΔP_{cap} upstream, strong SigB*) was analyzed. This genomic P_{cap} variant is described in Fig. 1C. Representative pictures of at least three independent cultures are shown.

background. RbsR likely functions as metabolic sensor, and thus the discrepancy with the results of Lei and Lee (Lei and Lee, 2015) could be due to differences in growth conditions.

We reproduced the activating effect of MsaB/CspA on *cap* expression, but demonstrated that it is mediated by modulation of SigB activity: *msa* deletion negatively affected P_{cap} and P_{asp23} activities and constitutive expression of *sigB* rendered both promoters insensitive to MsaB/CspA. Moreover, in contrast to Batte *et al.* (2016), no detectable MsaB/CspA binding to P_{cap} was observed, challenging the role of MsaB/CspA as a classical transcription factor. Indeed, it was recently shown that MsaB/CspA binds *rsbVWsigB* mRNA, thereby increasing transcript stability (Caballero *et al.*, 2018). Strong influence of MsaB/CspA on SigB activity is consistent with previous findings that MsaB/CspA increases expression of *sigB* and its target genes (Katzif *et al.*, 2005; Sahukhal and Elasri, 2014; Donegan *et al.*, 2019). With respect to direct P_{cap} regulation, our results indicate that under the conditions employed, the region containing the previously described IR motif functions instead as a promoter for the SigB holoenzyme.

Cap expression is modified by upstream SigA promoter and repressor binding sites

Upstream of the main SigB-dependent promoter we identified an additional weak SigA-dependent promoter with conserved SigA –35 and –10 consensus sequences. However, the SigA-dependent promoter seems to play a minor role in *cap* expression, with its activity being mainly detectable upon deletion of *sae*. The reason for such low promoter activity is unclear and might be due to suboptimal structure and spacing of the SigA consensus in P_{cap}. (Ruff *et al.*, 2015; Browning and Busby, 2016). Furthermore, the average activity of SigA promoters has been found to be generally lower than that of SigB promoters (Mäder *et al.*, 2016). However, for any given promoter sequence, changes in temperature, salt and solute

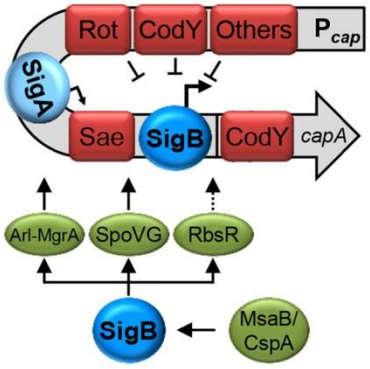

Fig. 9. Transcriptional regulation of *cap* expression. *Cap* expression is mainly driven from a SigB-dependent promoter. However, there is a second weak SigA-dependent promoter further upstream. In addition, the P_{cap} upstream region is targeted by the *cap* repressors SaeR, CodY, Rot and others. Of note, Rot and CodY only interfere with SigB-dependent promoter activity, whereas Sae is able to repress both. A predicted SaeR binding motif is located between the SigA- and SigB-dependent promoters. P_{cap} contains a second CodY binding site reaching into the coding region of *capA*. The depicted binding sites for the upstream regulators (relative to each other and the SigA promoter) are arbitrary and further studies are needed to localize these site(s) and their mechanisms of action. SigB activity is modulated by MsaB/CspA, promoting *sigB* transcript stability. Consequently, MsaB/CspA likely also affects indirect SigB-dependent P_{cap} activation through ArlRS-MgrA, SpoVG and RbsR. However, for RbsR we were unable to prove an activating effect on *cap* expression.

concentrations, as well as protein factors and ligands can affect its kinetics by 10–1000-fold or more (Ruff *et al.*, 2015). Therefore, we cannot rule out that under certain conditions the SigA-dependent promoter gets activated. This may be the case during infections with strains from the USA300 lineage. Among others, USA300 strains carry a point mutation within the SigB consensus motif of P_{cap}. Interestingly, strains harboring only this mutation seem to produce CP under infectious conditions (Mohamed *et al.*, 2019), which might be attributed to activation of the weak SigA-dependent promoter.

Besides containing a SigA-dependent promoter, we observed that the P_{cap} upstream region is of repressive function. *cap* repression was confirmed by promoter activity assays, suggesting that the main function of the upstream promoter region is to reduce SigB-dependent promoter activity. Indeed, there are many transcription factors and TCS known to repress *cap* indirectly via other regulators or directly through direct DNA binding. It is likely that the P_{cap} upstream region is targeted by many of these repressors. Here, we focused on the *cap* repressors SaeR, CodY and Rot for which a direct interaction with the P_{cap} upstream region was demonstrated by EMSAs. While Sae, CodY and Rot all interfered with SigB-dependent promoter activity, only Sae additionally repressed activity of the SigA-dependent promoter. This is in line with a predicted SaeR binding site located between the two promoters (Liu *et al.*, 2016). We hypothesize that the repression of SigB-dependent promoter activity occurs via steric interference, whereas the SigA-dependent promoter activity might be repressed via a roadblock mechanism. Nonetheless, the molecular mechanism for the long-distance effect of Rot and CodY on the SigB-dependent promoter activity remains to be elucidated. One may speculate that secondary structures of the promoter bring these two regulators in close proximity to the SigB consensus motif, allowing them to interfere with SigB binding. It is well known that DNA structural elements like supercoiling are involved in the control of bacterial gene expression (Dorman and Dorman, 2016), and *cap* expression was indeed shown to be supercoiling sensitive (Schröder *et al.*, 2014).

Of note, there are two CodY binding sites within the *cap* locus. One reaching into the coding region of *capA*, consistent with previous findings (Lei and Lee, 2018), and one in the P_{cap} upstream region. Functional assays using truncated promoter fusion constructs indicate that the upstream binding site alone is sufficient for *cap* repression.

SigB activity and upstream repressors determine temporal/heterogeneous CP synthesis

We showed that SigB-dependent regulation and the regulators targeting the upstream region contribute to the temporal pattern of CP production and to its phenotypic heterogeneity. Congruent with SigB being a known activator of late genes (Bischoff *et al.*, 2001; 2004; Pane-Farre *et al.*, 2006; Mäder *et al.*, 2016), we observed earlier onset of CP production and more CP-positive cells in stationary phase upon constitutive *sigB* expression in a *rsbUVWsigB*-negative background. However, the greater impact on temporal and heterogeneous CP production was observed upon deletion of the upstream promoter region resulting in single CP-positive cells already in early exponential growth phase and almost all cells being CP-positive in later growth. The effects of constitutive *sigB* expression and P_{cap} upstream deletion were additive, and only in combination the phenotypic heterogeneity could be completely abolished in stationary growth phase. This suggests that the regulators targeting the upstream region of P_{cap} are mainly responsible for heterogeneous CP production, with the residual heterogeneity resulting from variable SigB activity within cells. These data support the prediction by Sharon *et al.* stating that more transcription factor binding sites result in noisier promoters (Sharon *et al.*, 2014). A similar pattern of CP production was shown in the USA300 background, indicating a conserved regulatory mechanism.

Of note, even upon P_{cap} upstream deletion and constitutive *sigB* expression, CP synthesis remains growth

phase-dependent which is not reflected at the transcriptional level, indicating that further post-transcriptional levels of regulation are in place. These might be required as CP synthesis is linked to the metabolic status of the cell. For instance, UDP N-acetylglucosamine used for CP biosynthesis is mainly derived from gluconeogenesis, which naturally occurs when glucose becomes limited toward later growth phases (Sadykov *et al.*, 2010). In addition, CP, peptidoglycan and wall teichoic acids synthesis make use of the universal bactoprenol carrier lipid, which could become limited in earlier growth phases (Campbell *et al.*, 2012). This coordination of the different cell wall polymers synthesis was recently shown to involve reversible protein phosphorylation of the capsular biosynthesis gene products CapM and CapE (Rausch *et al.*, 2019).

In summary, our results show that CP synthesis is tightly controlled at the transcriptional level. However, post-transcriptional mechanisms are also in place to avoid conflict between precursor usage by the CP synthesis machinery and the synthesis machinery of other cell wall glycopolymers in growing bacterial cells. Further in-depth studies are required to fully understand this regulation and to increase the potential of CP as prospective target for novel anti-infective strategies.

Experimental procedures

Bacterial strains and growth conditions

Strains and plasmids are listed in Tables S3 and S4. For overnight culture, strains were grown in lysogeny broth (LB) medium (low salt) with appropriate antibiotics (10 μg ml^{-1} chloramphenicol (Cm10), 10 μg ml^{-1} erythromycin, 50 μg ml^{-1} kanamycin, 3 μg ml^{-1} tetracycline) at 37°C and 200 rpm. Day cultures were inoculated from overnight cultures to an OD_{600} of 0.05 and were grown without antibiotics at 37°C and 200 rpm.

Growth curves and fluorescence measurements

Overnight cultures were diluted to an OD600 of 0.05 and 200 μl were loaded onto a 96-well U-bottom plate (Greiner Bio-One). Continuous absorbance and fluorescence were monitored with a TECAN Infinite 200 microplate reader every half an hour with shaking at 37°C. Absorbance was measured at 600 ± 9 nm; gpVenus was excited at 505 ± 9 nm and emission was measured at 535 ± 20 nm, and gpCerulean was excited at 434 ± 9 nm and emission was measured at 485 ± 20 nm. Optical densities measured in microplate reader are not linear over the extended growth cycle. To address this problem, we simultaneously measured dilutions of an overnight culture in the plate reader and the Ultrospec™ 2100 pro UV/Vis spectrophotometer (Pharmacia). From the plotted values, a conversion formula was calculated and used to correct the optical densities measured in the microplate reader.

Strain construction

All plasmids and oligonucleotides are listed in Tables S4 and S5, respectively. The transposon mutants Newman *rbsR* and Newman *sae rbsR* were constructed by phage transduction of the transposon insertions from the Nebraska transposon mutant NE425 to Newman and Newman-29 and then verified by PCR.

Strains Newman *msa*, Newman ΔP_{cap} *upstream*, Newman ΔP_{cap} *upstream, strong SigB*, USA300 P_{cap} *repaired*, USA300 *cap repaired* and USA300 ΔP_{cap} *upstream, strong SigB* were created using the temperature-sensitive pIMAY plasmid for allelic exchange (Monk *et al.*, 2012). Corresponding homologous regions were PCR amplified as indicated in Table S5 and inserted into the *Eco*RI-linearized pIMAY backbone via Gibson assembly. The resulting plasmids were verified by PCR using primers piMAYcontrolfor and piMAYcontrolrev and sequencing, and then electroporated into strain RN4220 and transduced into the target strains. Allelic exchange was performed as described before (Monk *et al.*, 2012) with few alterations. Briefly, a single colony was homogenized in 200 μl of TSB and 50 μl of serial dilutions (10^{-1}–10^{-3}) were plated on TSA-Cm10 and incubated overnight at 37°C. Large colonies were picked and subcultured on TSA-Cm10 at 37°C. Integrants were confirmed via PCR using primers piMAYcontrolfor and piMAYcontrolrev as well as a primer pair flanking the individual homologous regions (Table S5). One integrant colony was used to inoculate an overnight culture in 10 ml TSB grown at 28°C without chloramphenicol, and later plated on TSA containing 0.7–1 μg ml^{-1} anhydrotetracycline. After 48 h of growth at 28°C, colonies were picked on both blood and TSA-Cm10 plates and incubated at 37°C. Cm10-sensitive colonies were screened by PCR with the oligonucleotides mentioned above and by sequencing to identify clones containing the desired mutation.

The *rsbUVWsigB* mutants were obtained using the temperature-sensitive shuttle vector pBASE6 (Geiger *et al.*, 2012). Replacement was introduced by creating PCR products using RN6390 as a template and primer pairs MazSIG-for and Hybrid-MazSIG-rev, as well as MazSIGrev and Hybrid-MazSIG-for for the homologous regions. The tetracycline resistance cassette was amplified from pCG75 using primers TetMfor and TetMrev. PCR products were linked using primers BglIIMazSIGfor and SalIMazSIGrev. The obtained amplicon was cloned into *Bgl*II and *Sal*I digested pBASE6. The resulting plasmid pCG331 was introduced into the restriction-deficient strain RN4220 and transduced into *S. aureus* target strains. Mutagenesis was performed as described elsewhere (Bae and Schneewind, 2006). The deletion was verified by PCR with oligonucleotides flanking the deleted region and within the resistance cassette.

For constitutive *sigB* expression under the control of the P_{SarA} promoter, the *sigB* gene including its native ribosomal binding site was amplified from Newman genomic DNA using primers pCG795gibfor and pCG795gibrev and inserted into *Eco*RI and *Asc*I digested pJL78. The resulting plasmid pCG795 was verified via PCR and sequencing prior to electroporation into strain RN9011 and transduction into target strains. Correct insertion into the SaPI site was verified via PCR using primers SaPIintfor and SaPIintrev.

The *sae codY rot* triple mutant was obtained by transduction of the Δ*codY::tetM* mutation from RN4220-21 (Pohl

et al., 2009) into Newman-29, followed by transduction of the *rot::bursa aurealis* transposon insertions from the Nebraska transposon mutant NE386.

For the generation of a *cap* mutant in USA300 JE2, pCG132 was transduced from RN4220 pCG132 (Jansen *et al*., 2013) into USA300 JE2 using phage Φ11.

Promoter fusion constructs

Two tandem sequences, each comprising a promoter of interest (P_{gene}) followed by a strong ribosomal binding site (RBS), genes encoding for fluorescent protein gpVenus (*gpven*) or gpCerulean (*gpcer*) (Liese *et al*., 2013) and a terminator (ter) sequence, were designed *in silico*. Restriction sites were designed to flank both promoter replacements. The entire cassette encompassing P_{cap}-RBS-*gpven*-ter–P_{tagH}-RBS-*gpcer*-ter was also flanked by restriction sites. The dual promoter–reporter protein fusion cassette was synthesized by Life Technologies GmbH and provided in a pUC18-like *E. coli* vector backbone (pMA-RQ, geneart plasmid). The dual promoter–reporter fusion cassette was subcloned into pCG246 (Helle *et al*., 2011) using restriction sites *Sph*I and *Nar*I. The resulting plasmid pCG570 was verified by restriction digestion (*Bam*HI) and using the primers pCG246for, pCG246rev, Pcap_rev and PtagHrev for sequencing. The plasmid pCG570 was introduced into RN4220 and then transduced into strain Newman.

Promoter truncations and mutations were generated with the Q5 Site-Directed Mutagenesis Kit from NEB according to the manufacturer's instructions. All primers used are enlisted in Table S5. For plasmids pCG742, pCG815 and pCG816, P_{tagH} was replaced with P_{asp23} via Gibson cloning. The *asp23* promoter region was amplified from Newman genomic DNA using primers pCG657gibfor and pCG657gibrev and inserted into *Bam*HI and *Eco*RI digested pCG717, pCG719 and pCG769.

RNA isolation

A day culture was inoculated from an overnight culture and grown to an OD_{600} of 0.3. The day culture was then used to inoculate a second day culture to an OD_{600} of 0.05, which was grown to an OD_{600} of 0.3 and used again for subculturing. When the third day culture reached an OD_{600} of 0.3, 10 ml of cell suspension was harvested (T_0). After additional 2 h (T_1) and 4 h (T_2) of growth, 5 ml of *S. aureus* cells were harvested. Cells were lysed in 1 ml TRIzol reagent (Life Technologies, Germany) with 0.5 ml of zirconia–silica beads (0.1 mm diameter) in a high-speed homogenizer. RNA was isolated as described in the instructions provided by the manufacturer of TRIzol (Life Technologies).

5′ Rapid Amplification of cDNA Endings (5′ RACE)

5′ RACE was performed as described previously (Marincola *et al*., 2012) using strain Newman pCG717. Briefly, isolated RNA from T_2 was treated with MICROBExpress (Ambion) in order to remove rRNAs. After treatment with Cap-Clip Phosphatase (Biozym) to remove pyrophosphate at the 5′ prime end of the native transcripts, a specific RNA 5′ adapter (Table S5) was ligated to the RNA. After phenol/chloroform extraction and ethanol precipitation, the RNA was subjected to reverse transcription using oligonucleotide YFPCFPpolymorrev. Nested PCR was performed using oligonucleotides Race2 and Racecapnestedrev (Table S5). The PCR amplicon was cloned into pCRII-TOPO (Invitrogen) following the manufacturer's instructions. Single clones were analyzed via PCR using primers Race2 and Racecapseqrev and the PCR products of 10 clones were sequenced with primer Racecapseqrev.

qRT-PCR

qRT-PCR to quantify *cap* and *gyr* mRNA was performed using the QuantiFast SYBR-Green RT-PCR kit (Qiagen). Standard curves were generated using 10-fold serial dilutions (10^4–10^8 copies) of specific *in vitro*-transcribed RNA standard molecules (Burian *et al*., 2010). The number of copies of each transcript was determined with the aid of the LightCycler software and *cap* mRNA was expressed in reference to copies of *gyrB*.

Protein expression

Plasmid pCWsae106 containing $SaeR^{D51E}$ was created by overlapping PCR employing the oligonucleotides saetetfor1 and 1680l29Gluok as well as 1684U31 and saetetfor1. The amplicon was inserted into pCR2.1. pCWsae106 was then transformed into RN4220 and transduced into strain Newman-29. Coagulase assays were performed to verify the function of the phosphomimetic $SaeR^{D51E}$. Strain Newman-29 pCWsae106 was used as a template to generate the insert for the $SaeR^{D51E}$ expression vector with the primers pCG791gibfor and pCG791gibrev. The amplicon was inserted into *Bam*HI-linearized pET15b via Gibson assembly. All other expression vectors were generated accordingly using primers and template DNA as indicated in Table S5. All vectors were verified via PCR and sequencing using primers pET15bfor and pET15brev.

A 10 ml LB culture containing 100 μg ml^{-1} ampicillin was inoculated with freshly transformed *E. coli* BL21 DE3 cells and incubated for 6 h at 37°C and 200 rpm. For the expression culture, 1 L LB medium supplemented with 100 μg ml^{-1} ampicillin and IPTG or D(+)-lactose monohydrate (for expression conditions see Table S6) was inoculated with 10 ml day culture and incubated at 16°C and 200 rpm overnight (16–18 h). Cells were harvested (20 min, 2000× *g*, 4°C) and resuspended in 30 ml ice-cold HisTrap binding buffer (20 mM Na_2HPO_4, 500 mM NaCl, 40 mM imidazole, pH 7.4, sterile filtered and degassed) supplemented with 10 μg ml^{-1} DNAse (Roth) and cOmplete protease inhibitor cocktail (Roche). Cells were lysed using a French press at 1000 psi. The lysate was centrifuged (236 982× *g*, 45 min, 4°C), and the clear supernatant was filtered (0.22 μm pore size) before being loaded onto a 1 ml HisTrap HP column (GE Healthcare Life Sciences) equilibrated with HisTrap binding buffer. Purification was performed with an ÄKTA purification system (GE Healthcare Life Sciences), and elution was carried out with an imidazole gradient to a final concentration of 500 mM.

For $SaeR^{D51E}$ batch purification using Ni-NTA agarose resin (Qiagen) equilibrated with HisTrap binding buffer was

performed. After incubation for 1 h at constant overhead rotation at 4°C the Ni-NTA agarose was centrifuged at 500× *g* for 2 min at 4°C and washed thrice with 37.5 ml HisTrap binding buffer. Elution was performed at increasing imidazole concentrations (250/300/350/500 mM).

Column and batch fractions were analyzed by SDS-PAGE, and the fractions containing the protein of interest were collected, concentrated and rebuffered into EMSA buffer (10 mM Tris-HCl, 50 mM KCl, 5 mM $MgCl_2$, 10% glycerol, pH 7.4) using Amicon® ultra centrifugal filters (ULTRACEL® 10K/30K) according to the instructions of the manufacturer. To determine the protein concentration of purified proteins, a Pierce™ BCA assay (Thermo Fisher) was performed following the manufacturer's protocol for a microplate procedure. The absorbance was measured with the TECAN Infinite 200 microplate reader. Purified proteins were stored in aliquots at –20°C.

Electrophoretic Mobility Shift Assay (EMSA)

The primers used for EMSAs are listed in Table S5. DNA probes were PCR amplified from strain Newman with fluorescently labeled primers (DY-781, absorption: 783 nm, emission: 800 nm) and purified with the innuPREP PCRpure Kit from Analytik Jena AG according to the manufacturer's instructions. In a volume of 20 µl, 30 fmol DNA probe were mixed with various amounts of protein. For competition experiments, unlabeled DNA fragment with a sequence identical to the labeled probe was used as a specific competitor and a 161 bp DNA fragment containing the promoter of the 16S rRNA gene was used as unspecific competitor. Competitors were obtained via ethanol precipitation after PCR and added in 100-fold excess. After incubation for 20 min at room temperature, samples were analyzed by nondenaturing native 6% TBE polyacrylamide gel electrophoresis at 75 V for 90 min in 1x TBE buffer. The fluorescently labeled DNA probes were visualized in the polyacrylamide gel with the Odyssey® infrared imaging system (LI-COR) and the Image Studio 4.0 software.

IF and promoter fusion microscopy

For synchronization, three subsequent day cultures were inoculated to an OD_{600} of 0.05, grown to an OD_{600} of 0.3 and subcultured twice. When the third subculture reached an OD_{600} of 0.3 (T_0) and after additional 2 h (T_1), 4 h (T_2), 6.5 h (T_3) and overnight growth (T_4) cells were harvested by centrifugation at 3800× *g* for 10 min at 4°C. Roughly 1.3×10^8 bacteria were suspended in 1 ml fixation solution (3.7% formaldehyde in 1x PBS) and incubated with gentle mixing for 15 min at room temperature. Wells of Ibi-treat µ-slide angiogenesis slides (ibidi®) were loaded with 32 µl of cell suspension and centrifuged at 600× *g* for 6 min. The cells were washed with 1 x PBS and protein A was blocked by incubation with pre-adsorbed human serum (diluted 1:10 in 1x PBS/0.1% Tween 20) for 1 h. After blocking, the slides were washed thrice for 5 min each with PBS/Tween 20 followed by incubation with rabbit serum raised against CP5 (1 h, diluted 1:200 in PBS/Tween 20). The slides were washed thrice with PBS/Tween 20 followed by incubation with the secondary antibody Cy3-conjugated F(ab)2 goat-anti-rabbit IgG (Dianova, Hamburg) (diluted 1:500 in PBS/Tween 20, 1 h). For generation of pre-adsorbed human serum and antibody generation, see (George *et al.*, 2015). After washing the cells thrice with PBS/Tween 20 each slide was finally mounted using ibidi® fluorescence mounting medium.

Microscopy images were acquired in the confocal mode of an inverted Zeiss LSM 710 NLO microscope equipped with a spectral detector and a Zeiss Plan-Apochromat 63x/1.40 oil DIC M27 objective and ZEN Black software. The following excitation wavelength, laser sources and detection spectra were used for IF: Cy3: Ex: 561 nm/DPSS laser/Em: 566–702 nm and for promotor activity measurement: gpVenus: Ex: 514 nm/argon laser/Em: 519–554 nm, gpCerulan: Ex: 405 nm/diode laser/Em: 454–516 nm. Additionally, a bright-field image was captured. The images were exported in the single channels or as overlays as 16-bit tagged image files after equal adjustment for gain and color intensity within one experiment. For each image about 100 bacteria as detected by bright field were randomly selected and CP-positive bacteria of the corresponding IF image enumerated. Mean percentage of CP-positive bacteria and standard deviations of three biological replicates is given in Tables S1 and S2.

Acknowledgements

The work was supported by grants from the Deutsche Forschungsgemeinschaft SFB766/A7 to CWo and CWe and GRK1708 to CWo. We thank Isabell Samp, Natalya Korn and Vittoria Bisanzio for excellent technical assistance. We thank Markus Bischoff for fruitful discussions and Jan Liese for providing plasmid pJL78. The mutants NE386 and NE425 from the Nebraska library were obtained through the Network on Antimicrobial Resistance in *Staphylococcus aureus* (NARSA) program. The authors have no conflict of interest to declare.

Author contributions

DK, SG and CWo have made major contributions to the conception and design of the study; DK, AS, ADJ, SG, GM, JL, CWe and CWo have made major contributions to the acquisition, analysis or interpretation of the data; DK and CWo have made major contributions to writing the manuscript.

References

Ansari, S., Jha, R.K., Mishra, S.K., Tiwari, B.R. and Asaad, A.M. (2019) Recent advances in *Staphylococcus aureus* infection: focus on vaccine development. *Infection and Drug Resistance*, **12**, 1243–1255.

Arbeit, R.D., Karakawa, W.W., Vann, W.F. and Robbins, J.B. (1984) Predominance of two newly described capsular polysaccharide types among clinical isolates of

Staphylococcus aureus. *Diagnostic Microbiology and Infectious Disease*, **2**(2), 85–91.

Bae, T. and Schneewind, O. (2006) Allelic replacement in *Staphylococcus aureus* with inducible counter-selection. *Plasmid*, **55**(1), 58–63.

Batte, J.L., Sahukhal, G.S. and Elasri, M.O. (2018) MsaB and CodY interact to regulate *Staphylococcus aureus* capsule in a nutrient-dependent manner. *Journal of Bacteriology*, **200**(17), e00294-00218.

Batte, J.L., Samanta, D. and Elasri, M.O. (2016) MsaB activates capsule production at the transcription level in *Staphylococcus aureus*. *Microbiology*, **162**(3), 575–589.

Bischoff, M., Dunman, P., Kormanec, J., Macapagal, D., Murphy, E., Mounts, W., *et al*. (2004) Microarray-based analysis of the *Staphylococcus aureus* sigmaB regulon. *Journal of Bacteriology*, **186**(13), 4085–4099.

Bischoff, M., Entenza, J.M. and Giachino, P. (2001) Influence of a functional sigB operon on the global regulators *sar* and *agr* in *Staphylococcus aureus*. *Journal of Bacteriology*, **183**(17), 5171–5179.

Boyle-Vavra, S., Li, X., Alam, M.T., Read, T.D., Sieth, J., Cywes-Bentley, C., *et al*. (2015) USA300 and USA500 clonal lineages of *Staphylococcus aureus* do not produce a capsular polysaccharide due to conserved mutations in the *cap5* locus. *MBio*, **6**(2), e02585-02514.

Browning, D.F. and Busby, S.J. (2016) Local and global regulation of transcription initiation in bacteria. *Nature Reviews Microbiology*, **14**(10), 638–650.

Burian, M., Wolz, C. and Goerke, C. (2010) Regulatory adaptation of *Staphylococcus aureus* during nasal colonization of humans. *PLoS ONE*, **5**(4), e10040.

Caballero, C.J., Menendez-Gil, P., Catalan-Moreno, A., Vergara-Irigaray, M., Garcia, B., Segura, V., *et al*. (2018) The regulon of the RNA chaperone CspA and its auto-regulation in *Staphylococcus aureus*. *Nucleic Acids Research*, **46**(3), 1345–1361.

Campbell, J., Singh, A.K., Swoboda, J.G., Gilmore, M.S., Wilkinson, B.J. and Walker, S. (2012) An antibiotic that inhibits a late step in wall teichoic acid biosynthesis induces the cell wall stress stimulon in *Staphylococcus aureus*. *Antimicrobial Agents and Chemotherapy*, **56**(4), 1810–1820.

Cocchiaro, J.L., Gomez, M.I., Risley, A., Solinga, R., Sordelli, D.O. and Lee, J.C. (2006) Molecular characterization of the capsule locus from non-typeable *Staphylococcus aureus*. *Molecular Microbiology*, **59**(3), 948–960.

Conlon, B.P., Rowe, S.E., Gandt, A.B., Nuxoll, A.S., Donegan, N.P., Zalis, E.A., *et al*. (2016) Persister formation in *Staphylococcus aureus* is associated with ATP depletion. *Nature Microbiology*, **1**(5), 16051.

Cunnion, K.M., Lee, J.C. and Frank, M.M. (2001) Capsule production and growth phase influence binding of complement to *Staphylococcus aureus*. *Infection and Immunity*, **69**(11), 6796–6803.

Dassy, B. and Fournier, J.M. (1996) Respiratory activity is essential for post-exponential-phase production of type 5 capsular polysaccharide by *Staphylococcus aureus*. *Infection and Immunity*, **64**(7), 2408–2414.

Dassy, B., Stringfellow, W.T., Lieb, M. and Fournier, J.M. (1991) Production of type 5 capsular polysaccharide by *Staphylococcus aureus* grown in a semi-synthetic medium. *Journal of General Microbiology*, **137**(5), 1155–1162.

Donegan, N.P., Manna, A.C., Tseng, C.W., Liu, G.Y. and Cheung, A.L. (2019) CspA regulation of *Staphylococcus aureus* carotenoid levels and sigma(B) activity is controlled by YjbH and Spx. *Molecular Microbiology*. https://doi.org/10.1111/mmi.14273.

Dorman, C.J. and Dorman, M.J. (2016) DNA supercoiling is a fundamental regulatory principle in the control of bacterial gene expression. *Biophysical Reviews*, **8**(3), 209–220.

Geiger, T., Francois, P., Liebeke, M., Fraunholz, M., Goerke, C., Krismer, B., *et al*. (2012) The stringent response of *Staphylococcus aureus* and its impact on survival after phagocytosis through the induction of intracellular PSMs expression. *PLoS Pathogens*, **8**(11), e1003016.

George, S.E., Nguyen, T., Geiger, T., Weidenmaier, C., Lee, J.C., Liese, J., *et al*. (2015) Phenotypic heterogeneity and temporal expression of the capsular polysaccharide in *Staphylococcus aureus*. *Molecular Microbiology*, **98**(6), 1073–1088.

Gertz, S., Engelmann, S., Schmid, R., Ohlsen, K., Hacker, J. and Hecker, M. (1999) Regulation of sigmaB-dependent transcription of *sigB* and *asp23* in two different *Staphylococcus aureus* strains. *Molecular and General Genetics*, **261**(3), 558–566.

Giachino, P., Engelmann, S. and Bischoff, M. (2001) Sigma(B) activity depends on RsbU in *Staphylococcus aureus*. *Journal of Bacteriology*, **183**(6), 1843–1852.

Gordon, R.J. and Lowy, F.D. (2008) Pathogenesis of methicillin-resistant *Staphylococcus aureus* infection. *Clinical Infectious Diseases*, **46**(Supplement 5), 350–359.

Hartmann, T., Baronian, G., Nippe, N., Voss, M., Schulthess, B., Wolz, C., *et al*. (2014) The catabolite control protein E (CcpE) affects virulence determinant production and pathogenesis of *Staphylococcus aureus*. *Journal of Biological Chemistry*, **289**(43), 29701–29711.

Helle, L., Kull, M., Mayer, S., Marincola, G., Zelder, M.E., Goerke, C., *et al*. (2011) Vectors for improved Tet repressor-dependent gradual gene induction or silencing in *Staphylococcus aureus*. *Microbiology*, **157**(Part 12), 3314–3323.

Herbert, S., Worlitzsch, D., Dassy, B., Boutonnier, A., Fournier, J.M., Bellon, G., *et al*. (1997) Regulation of *Staphylococcus aureus* capsular polysaccharide type 5: CO2 inhibition *in vitro* and *in vivo*. *Journal of Infectious Diseases*, **176**(2), 431–438.

Hochkeppel, H.K., Braun, D.G., Vischer, W., Imm, A., Sutter, S., Staeubli, U., *et al*. (1987) Serotyping and electron microscopy studies of *Staphylococcus aureus* clinical isolates with monoclonal antibodies to capsular polysaccharide types 5 and 8. *Journal of Clinical Microbiology*, **25**(3), 526–530.

Homerova, D., Bischoff, M., Dumolin, A. and Kormanec, J. (2004) Optimization of a two-plasmid system for the identification of promoters recognized by RNA polymerase containing *Staphylococcus aureus* alternative sigma factor B. *FEMS Microbiology Letters*, **232**(2), 173–179.

Jansen, A., Szekat, C., Schröder, W., Wolz, C., Goerke, C., Lee, J.C., *et al*. (2013) Production of capsular

polysaccharide does not influence *Staphylococcus aureus* vancomycin susceptibility. *BMC Microbiology*, **13**, 65.

de Jong, N.W.M., van Kessel, K.P.M. and van Strijp, J.A.G. (2019) Immune evasion by *Staphylococcus aureus*. *Microbiology Spectrum*, **7**(2), GPP3-0061-201.

Karakawa, W.W., Sutton, A., Schneerson, R., Karpas, A. and Vann, W.F. (1988) Capsular antibodies induce type-specific phagocytosis of capsulated *Staphylococcus aureus* by human polymorphonuclear leukocytes. *Infection and Immunity*, **56**(5), 1090–1095.

Katzif, S., Lee, E.H., Law, A.B., Tzeng, Y.L. and Shafer, W.M. (2005) CspA regulates pigment production in *Staphylococcus aureus* through a SigB-dependent mechanism. *Journal of Bacteriology*, **187**(23), 8181–8184.

Killikelly, A., Benson, M.A., Ohneck, E.A., Sampson, J.M., Jakoncic, J., Spurrier, B., *et al.* (2015) Structure-based functional characterization of repressor of toxin (Rot), a central regulator of *Staphylococcus aureus* virulence. *Journal of Bacteriology*, **197**(1), 188–200.

Lee, J.C., Takeda, S., Livolsi, P.J. and Paoletti, L.C. (1993) Effects of *in vitro* and *in vivo* growth conditions on expression of type 8 capsular polysaccharide by *Staphylococcus aureus*. *Infection and Immunity*, **61**(5), 1853–1858.

Lei, M.G. and Lee, C.Y. (2015) RbsR activates capsule but represses the *rbsUDK* operon in *Staphylococcus aureus*. *Journal of Bacteriology*, **197**(23), 3666–3675.

Lei, M.G. and Lee, C.Y. (2018) Repression of capsule production by XdrA and CodY in *Staphylococcus aureus*. *Journal of Bacteriology*, **200**(18), e00203-00218.

Liese, J., Rooijakkers, S.H., van Strijp, J.A., Novick, R.P. and Dustin, M.L. (2013) Intravital two-photon microscopy of host-pathogen interactions in a mouse model of *Staphylococcus aureus* skin abscess formation. *Cellular Microbiology*, **15**(6), 891–909.

Liu, Q., Yeo, W.S. and Bae, T. (2016) The SaeRS two-component system of *Staphylococcus aureus*. *Genes (Basel)*, **7**(10), 81.

Luong, T.T., Sau, K., Roux, C., Sau, S., Dunman, P.M. and Lee, C.Y. (2011) *Staphylococcus aureus* ClpC divergently regulates capsule via *sae* and *codY* in strain Newman but activates capsule via *codY* in strain UAMS-1 and in strain Newman with repaired *saeS*. *Journal of Bacteriology*, **193**(3), 686–694.

Mäder, U., Nicolas, P., Depke, M., Pane-Farre, J., Debarbouille, M., van der Kooi-Pol, M.M., *et al.* (2016) *Staphylococcus aureus* transcriptome architecture: from laboratory to infection-mimicking conditions. *PLoS Genetics*, **12**(4), e1005962.

Mainiero, M., Goerke, C., Geiger, T., Gonser, C., Herbert, S. and Wolz, C. (2010) Differential target gene activation by the *Staphylococcus aureus* two-component system *saeRS*. *Journal of Bacteriology*, **192**(3), 613–623.

Majerczyk, C.D., Dunman, P.M., Luong, T.T., Lee, C.Y., Sadykov, M.R., Somerville, G.A., *et al.* (2010) Direct targets of CodY in *Staphylococcus aureus*. *Journal of Bacteriology*, **192**(11), 2861–2877.

Marincola, G., Schafer, T., Behler, J., Bernhardt, J., Ohlsen, K., Goerke, C., *et al.* (2012) RNase Y of *Staphylococcus aureus* and its role in the activation of virulence genes. *Molecular Microbiology*, **85**(5), 817–832.

Meier, S., Goerke, C., Wolz, C., Seidl, K., Homerova, D., Schulthess, B., *et al.* (2007) sigmaB and the sigmaB-dependent *arlRS* and *yabJ-spoVG* loci affect capsule formation in *Staphylococcus aureus*. *Infection and Immunity*, **75**(9), 4562–4571.

Missiakas, D. and Schneewind, O. (2016) *Staphylococcus aureus* vaccines: deviating from the carol. *Journal of Experimental Medicine*, **213**(9), 1645–1653.

Mohamed, N., Timofeyeva, Y., Jamrozy, D., Rojas, E., Hao, L., Silmon de Monerri, N.C., *et al.* (2019) Molecular epidemiology and expression of capsular polysaccharides in *Staphylococcus aureus* clinical isolates in the United States. *PLoS ONE*, **14**(1), e0208356.

Monk, I.R., Shah, I.M., Xu, M., Tan, M.W. and Foster, T.J. (2012) Transforming the untransformable: application of direct transformation to manipulate genetically *Staphylococcus aureus* and *Staphylococcus epidermidis*. *mBio*, **3**(2), e00277-00211.

O'Riordan, K. and Lee, J.C. (2004) *Staphylococcus aureus* capsular polysaccharides. *Clinical Microbiology Reviews*, **17**(1), 218–234.

Ouyang, S., Sau, S. and Lee, C.Y. (1999) Promoter analysis of the *cap8* operon, involved in type 8 capsular polysaccharide production in *Staphylococcus aureus*. *Journal of Bacteriology*, **181**(8), 2492–2500.

Pane-Farre, J., Jonas, B., Förstner, K., Engelmann, S. and Hecker, M. (2006) The sigmaB regulon in *Staphylococcus aureus* and its regulation. *International Journal of Medical Microbiology*, **296**(4–5), 237–258.

Pohl, K., Francois, P., Stenz, L., Schlink, F., Geiger, T., Herbert, S., *et al.* (2009) CodY in *Staphylococcus aureus*: a regulatory link between metabolism and virulence gene expression. *Journal of Bacteriology*, **191**(9), 2953–2963.

Pohlmann-Dietze, P., Ulrich, M., Kiser, K.B., Döring, G., Lee, J.C., Fournier, J.M., *et al.* (2000) Adherence of *Staphylococcus aureus* to endothelial cells: influence of capsular polysaccharide, global regulator *agr*, and bacterial growth phase. *Infection and Immunity*, **68**(9), 4865–4871.

Portoles, M., Kiser, K.B., Bhasin, N., Chan, K.H. and Lee, J.C. (2001) *Staphylococcus aureus* Cap5O has UDP-ManNAc dehydrogenase activity and is essential for capsule expression. *Infection and Immunity*, **69**(2), 917–923.

Poutrel, B., Gilbert, F.B. and Lebrun, M. (1995) Effects of culture conditions on production of type 5 capsular polysaccharide by human and bovine *Staphylococcus aureus* strains. *Clinical and Diagnostic Laboratory Immunology*, **2**(2), 166–171.

Poutrel, B., Rainard, P. and Sarradin, P. (1997) Heterogeneity of cell-associated CP5 expression on *Staphylococcus aureus* strains demonstrated by flow cytometry. *Clinical and Diagnostic Laboratory Immunology*, **4**(3), 275–278.

Prados, J., Linder, P. and Redder, P. (2016) TSS-EMOTE, a refined protocol for a more complete and less biased global mapping of transcription start sites in bacterial pathogens. *BMC Genomics*, **17**(1), 849.

Rausch, M., Deisinger, J.P., Ulm, H., Müller, A., Li, W., Hardt, P., *et al.* (2019) Coordination of capsule assembly and

cell wall biosynthesis in *Staphylococcus aureus*. *Nature Communications*, **10**(1), 1404.
Roghmann, M., Taylor, K.L., Gupte, A., Zhan, M., Johnson, J.A., Cross, A., *et al.* (2005) Epidemiology of capsular and surface polysaccharide in *Staphylococcus aureus* infections complicated by bacteraemia. *Journal of Hospital Infection*, **59**(1), 27–32.
Ruff, E.F., Record, M.T. Jr. and Artsimovitch, I. (2015) Initial events in bacterial transcription initiation. *Biomolecules*, **5**(2), 1035–1062.
Sadykov, M.R., Mattes, T.A., Luong, T.T., Zhu, Y., Day, S.R., Sifri, C.D., *et al.* (2010) Tricarboxylic acid cycle-dependent synthesis of *Staphylococcus aureus* Type 5 and 8 capsular polysaccharides. *Journal of Bacteriology*, **192**(5), 1459–1462.
Sahukhal, G.S. and Elasri, M.O. (2014) Identification and characterization of an operon, *msaABCR*, that controls virulence and biofilm development in *Staphylococcus aureus*. *BMC Microbiology*, **14**, 154.
Sau, S., Sun, J. and Lee, C.Y. (1997) Molecular characterization and transcriptional analysis of type 8 capsule genes in *Staphylococcus aureus*. *Journal of Bacteriology*, **179**(5), 1614–1621.
Schröder, W., Bernhardt, J., Marincola, G., Klein-Hitpass, L., Herbig, A., Krupp, G., *et al.* (2014) Altering gene expression by aminocoumarins: the role of DNA supercoiling in *Staphylococcus aureus*. *BMC Genomics*, **15**, 291.
Schulthess, B., Meier, S., Homerova, D., Goerke, C., Wolz, C., Kormanec, J., *et al.* (2009) Functional characterization of the sigmaB-dependent *yabJ-spoVG* operon in *Staphylococcus aureus*: role in methicillin and glycopeptide resistance. *Antimicrobial Agents and Chemotherapy*, **53**(5), 1832–1839.
Senn, M.M., Giachino, P., Homerova, D., Steinhuber, A., Strassner, J., Kormanec, J., *et al.* (2005) Molecular analysis and organization of the sigmaB operon in *Staphylococcus aureus*. *Journal of Bacteriology*, **187**(23), 8006–8019.
Sharon, E., van Dijk, D., Kalma, Y., Keren, L., Manor, O., Yakhini, Z., *et al.* (2014) Probing the effect of promoters on noise in gene expression using thousands of designed sequences. *Genome Research*, **24**(10), 1698–1706.
Steinhuber, A., Goerke, C., Bayer, M.G., Döring, G. and Wolz, C. (2003) Molecular architecture of the regulatory locus *sae* of *Staphylococcus aureus* and its impact on expression of virulence factors. *Journal of Bacteriology*, **185**(21), 6278–6286.
Stringfellow, W.T., Dassy, B., Lieb, M. and Fournier, J.M. (1991) *Staphylococcus aureus* growth and type 5 capsular polysaccharide production in synthetic media. *Applied and Environment Microbiology*, **57**(2), 618–621.
Sun, F., Li, C., Jeong, D., Sohn, C., He, C. and Bae, T. (2010) In the *Staphylococcus aureus* two-component system *sae*, the response regulator SaeR binds to a direct repeat sequence and DNA binding requires phosphorylation by the sensor kinase SaeS. *Journal of Bacteriology*, **192**(8), 2111–2127.
Sutra, L., Rainard, P. and Poutrel, B. (1990) Phagocytosis of mastitis isolates of *Staphylococcus aureus* and expression of type 5 capsular polysaccharide are influenced by growth in the presence of milk. *Journal of Clinical Microbiology*, **28**(10), 2253–2258.
Thakker, M., Park, J.S., Carey, V. and Lee, J.C. (1998) *Staphylococcus aureus* serotype 5 capsular polysaccharide is antiphagocytic and enhances bacterial virulence in a murine bacteremia model. *Infection and Immunity*, **66**(11), 5183–5189.
Tuchscherr, L., Löffler, B., Buzzola, F.R. and Sordelli, D.O. (2010) *Staphylococcus aureus* adaptation to the host and persistence: role of loss of capsular polysaccharide expression. *Future Microbiology*, **5**(12), 1823–1832.
Verdier, I., Durand, G., Bes, M., Taylor, K.L., Lina, G., Vandenesch, F., *et al.* (2007) Identification of the capsular polysaccharides in *Staphylococcus aureus* clinical isolates by PCR and agglutination tests. *Journal of Clinical Microbiology*, **45**(3), 725–729.
Weidenmaier, C. and Lee, J.C. (2017) Structure and function of surface polysaccharides of *Staphylococcus aureus*. *Current Topics in Microbiology and Immunology*, **409**, 57–93.

Supporting Information

Additional supporting information may be found online in the Supporting Information section at the end of the article

International Journal of Medical Microbiology xxx (xxxx) xxx-xxx

Contents lists available at ScienceDirect

International Journal of Medical Microbiology

journal homepage: www.elsevier.com

Function and regulation of *Staphylococcus aureus* wall teichoic acids and capsular polysaccharides

Daniela Keinhörster , Shilpa Elizabeth George , Christopher Weidenmaier *, Christiane Wolz *

Interfaculty Institute of Microbiology and Infection Medicine, University of Tübingen, Elfriede-Aulhorn-Str. 6, 72076 Tübingen, Germany

ARTICLE INFO

Keywords:
Staphylococcus aureus
Glycopolymers
Wall teichoic acids (WTA)
Capsular polysaccharides (CP)
Regulation
Heterogeneity

ABSTRACT

Staphylococcus aureus produces different secondary cell wall glycopolymers such as wall teichoic acids (WTA) and capsular polysaccharides (CP). These structures play an important role in *S. aureus* colonization, pathogenesis and bacterial evasion of the host immune defences. To fulfil their diverse functions, biosynthesis of both glycopolymers has to be tightly controlled. Regulation of WTA biosynthesis and modification is only partially understood. The transcription factor MgrA and the two-component systems (TCS) Agr, GraRS, and ArlRS control WTA export, chain-length and modification. CP synthesis is determined by transcriptional and post-transcriptional regulatory circuits. On the transcriptional level expression of the *capA-P* operon is mainly driven by the alternative Sigma factor B and modulated by several transcriptional factors and TCS. Post-transcriptional mechanisms are in place to avoid conflict between precursor usage by the CP synthesis machinery and the synthesis machinery of other cell wall glycopolymers. The complex interplay of these regulatory systems determines the peculiar, strictly temporal expression of CP in the late growth phase and the high degree of phenotypic heterogeneity. Differential expression of CP, WTA and its modification systems during infection and colonisation are likely important for disease development, immune escape and survival within the host.

1. Introduction

The cell envelope of *S. aureus* consists of peptidoglycan, secondary cell wall glycopolymers and proteins. This multicomponent composition affords protection against cellular immunity and antibiotics and is involved in staphylococcal virulence. Two major secondary cell wall glycopolymers are wall teichoic acids (WTA) and capsular polysaccharides (CP). Their synthesis and modification is highly variable, tightly regulated and plays a key role in host-cell interactions. Thus, they are considered promising targets for anti-infective therapies and vaccines (Weidenmaier and Lee, 2017; Ansari et al., 2019). Structure and function of WTA and CP were recently reviewed (O'Riordan and Lee, 2004; Xia et al., 2010; Brown et al., 2013; Winstel et al., 2014; Schade and Weidenmaier, 2016; Weidenmaier and Lee, 2017). Here, we briefly summarize the function and molecular make-up of the glycopolymers. We will mainly focus on the regulatory system controlling WTA and CP biosynthesis and implicated functional consequences.

2. Function and regulation of WTA

2.1. Structure and function

WTA is unique with respect to its multiple functions in cell wall biosynthesis and maintenance, cellular physiology, phage interaction, host cell adhesion, antibiotic resistance as well as immune regulation (Weidenmaier and Peschel, 2008; Weidenmaier and Lee, 2017; van Dalen et al., 2019). WTA is present in all *S. aureus* strains analysed so far where it is mostly composed of 30–50 ribitol-phosphate (RboP) repeating units (Brown et al., 2013; Weidenmaier and Lee, 2017). However, certain strains produce poly-glycerol-phosphate (GroP) WTA instead (Winstel et al., 2014). The RboP backbone is connected to the peptidoglycan via a disaccharide linkage unit that contains N-acetylglucosamine (GlcNAC) linked to N-acetylmannosamine followed by two glycerol-3-phosphates (GroP) (Brown et al., 2013; Weidenmaier and Lee, 2017).

* Corresponding authors.
Email addresses: wolz@uni-tuebingen.de (C. Weidenmaier); chrisweidenmaier@googlemail.com (C. Wolz)

https://doi.org/10.1016/j.ijmm.2019.151333
Received 7 January 2019; Received in revised form 9 July 2019; Accepted 17 July 2019
Available online xxx
1438-4221/

The RboP is attached to the last GroP of the linkage unit and the RboP repeating units are connected to each other via phophodiester linkages (Weidenmaier and Lee, 2017). In addition, the repeating units are modified with D-alanine and GlcNAc.

The D-alanyl modifications are connected via an ester linkage to position C2 of RboP by the DltABCD enzymes (Peschel et al., 1999; Neuhaus and Baddiley, 2003). The repeating units exhibit a zwitterionic charge due to the presence of negatively charged phosphodiesters and positively charged D-alanine ester modifications (Weidenmaier et al., 2010). WTA D-alanylation leads to a more cationic charge of the bacterial surface which affects the interaction of cationic antimicrobial peptides (CAMP) with the bacterial surface and renders *S. aureus* non-susceptible to relatively high CAMP concentrations (Peschel et al., 1999).

Glycosylation modification occurs on position C4 of RboP via the predominant GlcNAc transferases TarM and TarS exhibiting α- and β-(1–4) glycosyltransferase activities, respectively (Brown et al., 2012; Koc et al., 2015; Sobhanifar et al., 2015, 2016). Depending on the *S. aureus* strain, the anomeric configuration of the glycosidic linkage of GlcNAc to RboP can either be α or β or a mixture of both anomers (Endl et al., 1983; Winstel et al., 2015). In addition to the C4 glycosylation, a recent study reported the presence of GlcNAc modifications on the C3 position of RboP units (Gerlach et al., 2018). This modification was detected in a number of CC5 and CC398 strains that harbour a prophage encoding an alternative WTA glycosyltransferase (TarP). Interestingly, the C3 GlcNAc modification leads to a less immunogenic WTA polymer. Strains with C3 modifications cannot be inactivated by dominant antibodies against the C4 modified WTA which allows such strains to escape the immune response of the host more efficiently (Gerlach et al., 2018).

2.2. Regulation of WTA synthesis and modification

Although WTA is a dominant surface epitope with multiple roles in host infection, regulation of WTA biosynthesis and modification remains poorly understood. This might be attributed to the fact that the genes involved in WTA biosynthesis (*tarO, tarAHGBXD, tarI'J'KFIJL, mnaA*) and modification (*dltXABCD, tarM, tarS, tarP*) are scattered throughout the genome (Fig. 1). With respect to the regulation of the WTA main chain biosynthesis, so far only a few reports shed light on possible mechanisms that affect WTA chain length and WTA amounts in the cell wall. Chain length is determined by the two RboP polymerases TarK and TarL, which produce WTA of different size with TarK producing up to 50% shorter polymers than TarL (K-WTA versus L-WTA). The Agr quorum sensing system was shown to modulate the ratios of K-WTA and L-WTA via repression of *tarK*. Thus, while under low Agr activity K-WTA and L-WTA are produced, L-WTA is the dominant form under high Agr activity (Meredith et al., 2008). Furthermore, a recent report indicated that altered Agr activity affects WTA biosynthesis and leads to strain specific changes in the amounts of WTA in the cell wall (Wanner et al., 2017). Highly virulent strains exhibit a higher Agr activity and show a consistently higher amount of WTA in their cell walls. This WTA_{high} phenotype is dependent on an increased expression of the *tarH* gene, which encodes for the energizing ATPase subunit of the TarG/H ABC transporter (Wanner et al., 2017). TarG/H is responsible for the transport of WTA over the cytoplasmic membrane. In line with prior reports (Swoboda et al., 2009; Campbell et al., 2012; Brown et al., 2013) it is postulated that the transport constitutes a rate limiting step of WTA biosynthesis. Expression of *tarH* is controlled by direct binding of the repressor Rot to the *tarH* promoter (Wanner et al., 2017). The intracellular effector of the Agr system, RNAIII anneals to target mRNAs including *rot*

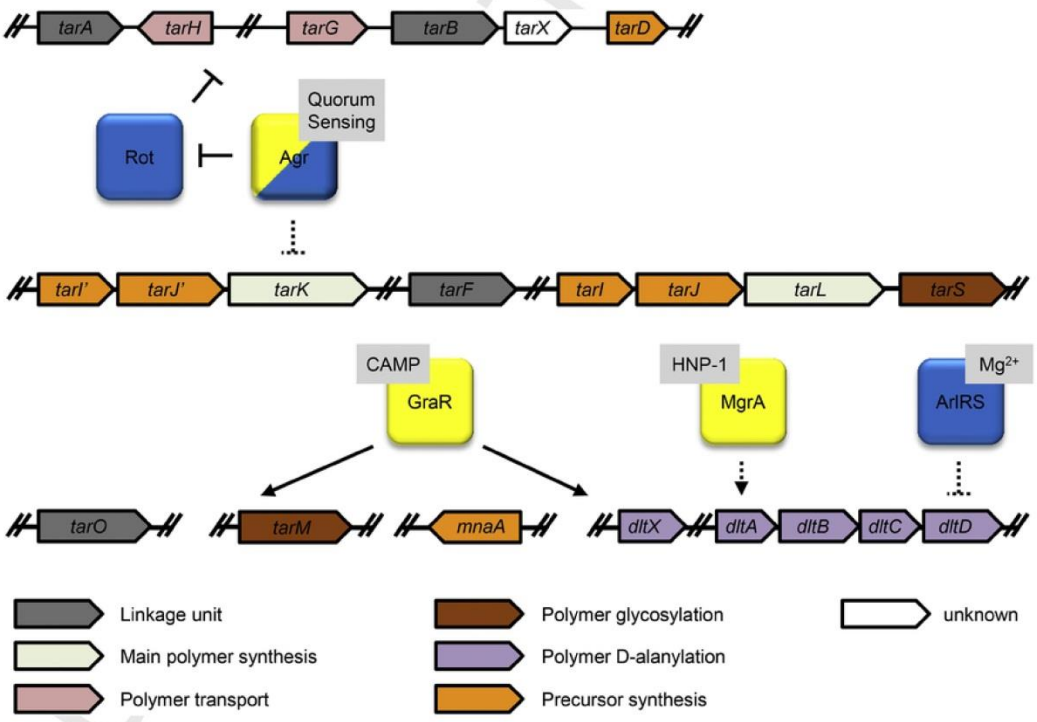

Fig. 1. Genetic organisation, function and regulation of genes involved in WTA biosynthesis and modification. Regulators in yellow indicate up-regulation, in blue down-regulation. Solid lines show direct interaction of the regulators with target genes, dashed lines mark unknown mechanisms of regulation. Signals controlling the activity of the regulators are shown in boxes. CAMP: cationic antimicrobial peptides, HNP: human neutrophil peptide.

resulting in repression of translation initiation followed by de-repression of Rot-regulated target genes (Boisset et al., 2007). Additional evidence for a differential regulation of WTA biosynthesis under certain physiological conditions came from studies that implicated WTA in antibiotic resistance (Bertsche et al., 2011, 2013). These studies reported that cell wall stress mediated by different antibiotics can lead to a phenotype that is characterized by a significant increase in WTA amounts in the cell walls of antibiotic resistant strains. The mechanism leading to altered WTA synthesis remains to be elucidated. Regulation of WTA biosynthesis gene clusters *in vivo* has been sparsely analysed. Analyses of transcription during nasal colonisation showed increased *tarO* expression at the onset of colonisation in an animal model (Burian et al., 2010).

Modification of WTA is sensitive to various environmental conditions. D-alanine ester content is regulated in response to physiological factors like salt concentration, temperature and pH (Neuhaus and Baddiley, 2003; Koprivnjak et al., 2006). For instance, Mg^{2+} induced *dlt* repression was shown to depend on the two-component system (TCS) ArlRS (Koprivnjak et al., 2006). In addition, the TCS GraRS is thought to directly up-regulate the expression of the *dlt*-operon and putative binding sites of the response regulator GraR have been identified upstream of the operon (Falord et al., 2011). GraS is involved in sensing of host-derived CAMP, but may also respond to other signals like oxidative stress (Falord et al., 2011). Recently, also the transcription factor MgrA was shown to positively regulate *dltA* expression, especially in response to human defense peptides (Li et al., 2019).

Regulation of the genes encoding for the GlcNAc glycosyltransferases TarM, TarS and TarP is only poorly studied. Recently, it was demonstrated that *S. aureus* is able to modify the phenotype of its WTA glycosylation pattern dependent on environmental conditions. The β-GlcNAc anomer was preferentially expressed at the expense of the α-GlcNAc anomer when grown on stress-inducing culture medium containing high NaCl concentration (Mistretta et al., 2019). Furthermore, while the inoculum used to infect animals produced almost exclusively α-GlcNAc WTA, bacteria recovered from infected organs produced only β-glycosylated WTA (Mistretta et al., 2019). The underlying molecular mechanisms remain elusive but may involve regulation by GraRS. A putative GraR binding site was predicted upstream of *tarM* and *tarM* expression was decreased in a *graRS* mutant (Falord et al., 2011). In another study TarS dependent GlcNAc modification of WTA was shown to play an important role in oxacillin resistance and interestingly only *tarS* but not *tarM* expression was strongly up-regulated by oxacillin (β-lactam) treatment (Brown et al., 2012). Again, the molecular mechanisms that confer this differential regulation remain unknown.

3. Function and regulation of CP

3.1. Structure and function

CP serves as essential virulence factor due to its anti-phagocytic properties which are important for immune evasion (Thakker et al., 1998; Nanra et al., 2013). However, depending on the infection setting either the presence or absence of CP has been reported to be advantageous for *S. aureus* (O'Riordan and Lee, 2004; Tuchscherr et al., 2010). CP enhances virulence in murine models of bacteraemia (Thakker et al., 1998; Watts et al., 2005), septic arthritis (Nilsson et al., 1997), abscess formation (Portoles et al., 2001), and surgical wound infection (McLoughlin et al., 2006). In contrast, in mammary gland infections (Tuchscherr et al., 2005) and in catheter-induced endocarditis (Baddour et al., 1992; Nemeth and Lee, 1995) CP mutants are more virulent. This is likely because CP also inhibits the adherence of the underlying adhesins to their specific target molecule (Pohlmann-Dietze et al., 2000; Risley et al., 2007). CP-negative *S. aureus* strains are frequently isolated from patients with osteomyelitis, mastitis or cystic fibrosis, providing evidence that the loss of CP expression may be advantageous for *S. aureus* during chronic infection (Herbert et al., 1997; Lattar et al., 2009; Tuchscherr et al., 2010). The loss of CP expression can typically be explained by mutations in any of the genes essential for CP synthesis or in the promoter region (Cocchiaro et al., 2006; Tuchscherr et al., 2010). For instance, strains from the USA300 lineage are non-encapsulated due to conserved mutations in the *cap5* locus (Boyle-Vavra et al., 2015). However, this assumption has been recently challenged by the finding that USA300 strains might indeed produce CP during infection (Mohamed et al., 2019).

Amongst clinical *S. aureus* isolates the two serotypes 5 (CP5) and 8 (CP8) are the most prevalent (O'Riordan and Lee, 2004). The structure of CP5 and CP8 is very similar as they both consist of trisaccharide repeating units of D-N-acetyl mannosaminuronic acid, L-N-acetyl fucosamine, and D-N-acetyl fucosamine. The only difference lies in the linkages between the sugars and the site of O-acetylation of the mannosaminuronic acid residues, resulting in the different serotypes (Fournier et al., 1984, 1987; Moreau et al., 1990; Jones, 2005). Polymerized CP is covalently attached to the glycan strands of the peptidoglycan (Chan et al., 2014).

3.2. Influence of environmental signals on CP synthesis in vitro and in vivo

Expression of CP5 and CP8 is strongly dependent on environmental conditions (Sutra et al., 1990; Dassy et al., 1991; Stringfellow et al., 1991; Poutrel et al., 1995). CP production *in vitro* is enhanced under high-salt conditions (Pohlmann-Dietze et al., 2000; George et al., 2015), iron limitation and on solid medium (Lee et al., 1993) but inhibited by yeast extract, alkaline growth conditions, high glucose, low oxygen conditions and high CO_2 (Fig. 2B) (Dassy et al., 1991; Stringfellow et al., 1991; Herbert et al., 1997; George et al., 2015). Most of these environmental cues can be linked to the activity of several regulatory mechanisms described below. Furthermore, *in vitro* CP expression was widely shown to be low during exponential growth phase (Fig. 2A) (Poutrel et al., 1995; Dassy and Fournier, 1996; Pohlmann-Dietze et al., 2000; Cunnion et al., 2001; George et al., 2015; Conlon et al., 2016).

During infection and colonization CP synthesis is also highly variable. CP antigens were detectable in sera and infection sites of infected animals (Arbeit and Dunn, 1987; Arbeit and Nelles, 1987; Lee et al., 1993). However, *ex vivo* analysis of bacteria from cystic fibrosis patient revealed that CP is hardly expressed and only few bacteria are CP-positive. This was linked to the high CO_2 concentrations in the lungs (Herbert et al., 1997). Similar analysis revealed that during nasal colonization only part of the *S. aureus* population is CP-positive (George et al., 2015). Thus, not all bacteria in a population seem to express CP on their surface as confirmed by flow cytometry or immunofluorescence (Poutrel et al., 1997; Pohlmann-Dietze et al., 2000; Seidl et al., 2006; Meier et al., 2007; Jansen et al., 2013; Hartmann et al., 2014; George et al., 2015).

3.3. Regulation of CP

The proteins involved in CP5 or CP8 biosynthesis, O-acetylation, transport and regulation are encoded by 16 genes, *cap5/8A* to *cap5/8P* (O'Riordan and Lee, 2004; Weidenmaier and Lee, 2017; Rausch et al., 2019). The *cap5* and *cap8* gene clusters are allelic

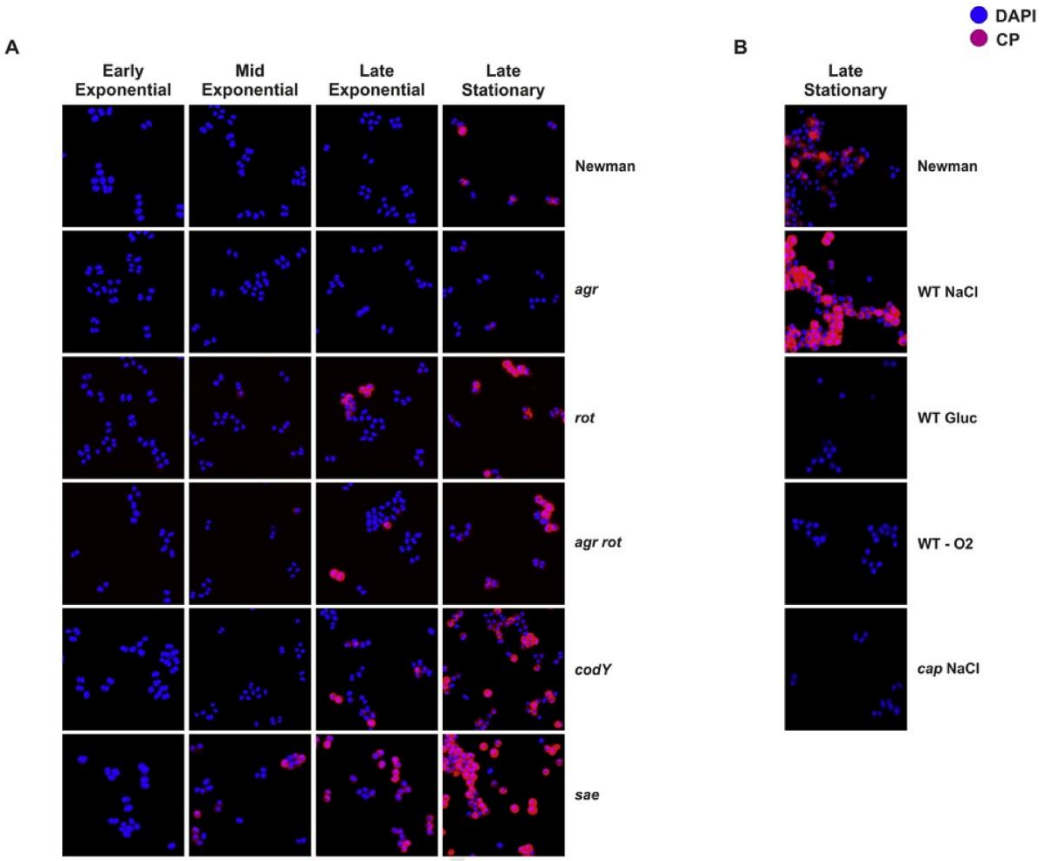

Fig. 2. Temporal and heterogeneous synthesis of CP influenced by (A) different regulators and (B) environmental conditions. CP was detected by immunofluorescence. (A) *S. aureus* strain Newman and isogenic mutants grown in LB medium to the indicated growth phase (modified from George et al., 2015). (B) *S. aureus* strain Newman grown in LB supplemented without or with 2 M NaCl, 1% glucose or grown anaerobically. A *cap* mutant strain was included as negative control (modified from George et al., 2015).

(Goerke et al., 2005) and share a highly similar promoter element (P_{cap}) upstream of *capA* (Herbert et al., 2001). From here, the operon is mainly transcribed as single large 17 kb transcript (Sau et al., 1997; Ouyang et al., 1999). P_{cap} activity generally correlates with CP synthesis indicating that regulation occurs predominantly on the transcriptional level (Ouyang et al., 1999; Meier et al., 2007; Jansen et al., 2013; Hartmann et al., 2014; George et al., 2015).

For a long time the molecular architecture of P_{cap} remained puzzling due to a determined transcriptional start site (TSS) not being preceded by a classical consensus sequence for sigma factor A (SigA) or B (SigB) binding (Ouyang et al., 1999). Instead, within the *cap* promoter region a 10 bp inverted repeat (IR) was shown to be crucial for promoter activity (Ouyang et al., 1999). Recent re-analyses of the P_{cap} promoter structure revealed a different TSS preceded by a canonical SigB consensus motif overlapping with the IR structure (Keinhörster et al., 2019; Mäder et al., 2016; Prados et al., 2016). Thus, the previously observed activating effect of SigB on *cap* expression can be explained by direct SigB-dependent regulation. Other SigB-dependent *cap* activators may contribute to the fine tuning of *cap* expression and amplify SigB-dependency (Keinhörster et al., 2019; Bischoff et al., 2001, 2004; Meier et al., 2007; Schulthess et al., 2009; Lei and Lee, 2015).

Next to the main SigB-dependent promoter a weak SigA-dependent promoter was identified further upstream (Keinhörster et al., 2019). While it seems to play only a minor role for *cap* expression it cannot be ruled out that under certain conditions the SigA-dependent promoter gets activated. This may be the case during infections with CP-positive strains from the USA300 lineage which have a common mutation in the SigB binding motif (Mohamed et al., 2019). Besides containing a SigA-dependent promoter, the extended upstream region of P_{cap} is targeted by many transcriptional factors thereby modulating *cap* expression (see below) (Keinhörster et al., 2019).

The role of regulators affecting *cap* expression was mainly deduced from the characterization of single regulatory mutants and in most cases it remains unclear how *cap* expression is modulated. In particular, the following regulators likely act indirectly via other regulatory systems: Agr (Fig. 2A) (Dassy et al., 1993; Pohlmann-Dietze et al., 2000; Luong et al., 2002; van Wamel et al., 2002; George et al., 2015), SarA (Luong et al., 2002; van Wamel et al., 2002), MgrA (Gupta et al., 2013), ArlRS (Luong and Lee, 2006), CcpA (Seidl et al., 2006, 2009), RpiR (Zhu et al., 2011; Gaupp et al., 2016), ClpC (Luong and Lee, 2006; Graham et al., 2013), RsaA (Romilly et al., 2014), SbcDC (Luong and Lee, 2006; Chen et al., 2007) and SpdC (Poupel et al., 2018). However, there are also many regulators for which a binding to P_{cap} was demonstrated, indicating direct regulation. These are the activators SpoVG, RbsR and KdpE (Fig. 3, yellow) as well as the repressors CcpE, CodY, XdrA, Rot, SaeR and AirR (Fig. 3, blue) which are discussed in the following sections.

The ribose-responsive regulator RbsR (Lei and Lee, 2015) and the putative transcription factor MsaB (Batte et al., 2016) were proposed to activate *cap* expression by directly binding to the 10

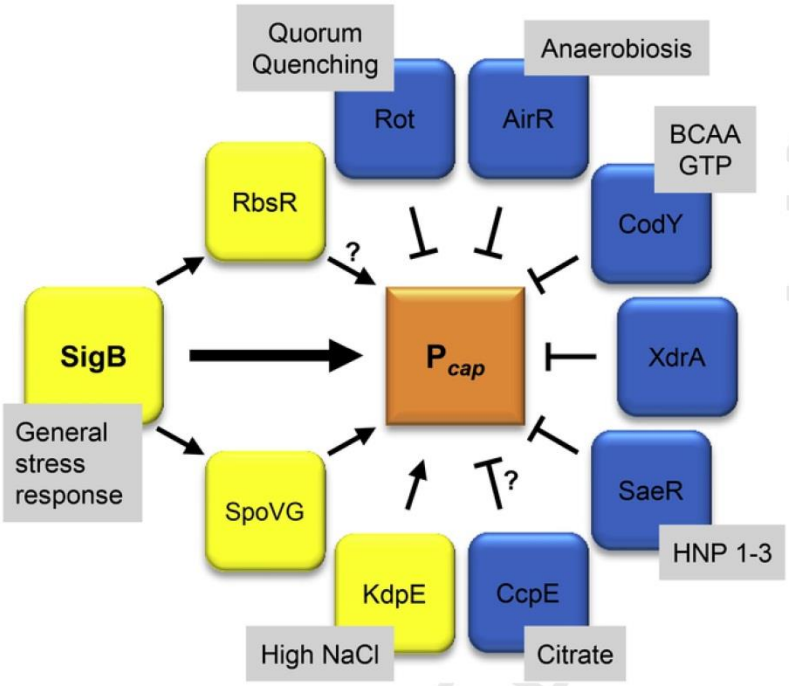

Fig. 3. Regulatory circuits known to directly impact *cap* expression. Regulators in yellow indicate up-regulation, in blue down-regulation of P_{cap} activity. Signals controlling activity of the regulators are shown in boxes. BCAA: branched-chain amino acids, HNP: human neutrophil peptides.

bp IR of P_{cap} (now identified as canonical SigB binding motif (Keinhörster et al., 2019). Interestingly, the presence or absence ribose had no effect on *cap* expression in the wild type or the *rbsR* mutant (Lei and Lee, 2015). We could not confirm the effect of RbsR on P_{cap} activity (Keinhörster et al., 2019). However, RbsR likely functions as metabolic sensor, and thus the discrepancy could be due to differences in growth conditions. *rbsR* expression itself is SigB-dependent and accordingly highest towards stationary growth phase (Lei and Lee, 2015). The *msaABCR* operon is involved in the regulation of virulence, biofilm development, antibiotic resistance and persister cell formation in *S. aureus*. Operon deletion and/or the deletion of *msaB* alone reduces *cap* transcription as well as CP production (Batte et al., 2016). However, MsaB is also annotated as cold-shock protein CspA, which exerts regulatory effects via RNA binding. It was shown that MsaB/CspA binds *rsbVWsigB* mRNA, thereby increasing transcript stability (Caballero et al., 2018). This is consistent with the observation that MsaB/CspA increases expression of *sigB* and its target genes (Katzif et al., 2005; Sahukhal and Elasri, 2014; Caballero et al., 2018; Donegan et al., 2019). We were able to reproduce the activating effect of MsaB/CspA on *cap* expression, but demonstrated that this is due to increased SigB activity. Moreover, no detectable MsaB/CspA binding to P_{cap} was observed (Keinhörster et al., 2019). Taken together, the role of the IR region as a target for other regulators besides SigB has to be questioned.

The transcription factor SpoVG regulates a number of virulence genes including *cap* via direct protein-DNA interaction (Meier et al., 2007; Schulthess et al., 2009, 2011; Jutras et al., 2013). The DNA-binding property of SpoVG is enhanced by phosphorylation via the protein kinase Stk1 (Bischoff et al., 2016). P_{cap} contains a conserved SpoVG binding motif in its extended upstream region and binding of phosphorylated SpoVG to the promoter was demonstrated (Jutras et al., 2013; Bischoff et al., 2016). *spoVG* expression itself is under the control of SigB. P_{cap} activity in a *spoVG* mutant is diminished but still growth phase-dependent (Meier et al., 2007).

KdpDE is a TCS which is inhibited by K^+, c-di-AMP and the autoinducer AI-2 but activated by high Na^+ concentration (Zhao et al., 2010; Xue et al., 2011; Freeman et al., 2013; Price-Whelan et al., 2013; Moscoso et al., 2016). The direct interaction of the response regulator KdpE and P_{cap} was shown via electrophoretic mobility shift assays (EMSA) (Zhao et al., 2010). Thus, increased *cap* expression in response to high Na^+ is likely due to KdpDE and SigB activity (Pane-Farre et al., 2006; Price-Whelan et al., 2013).

Transcription of tricaboxylic acid cycle genes are controlled by CcpE (Hartmann et al., 2013). Additionally, *capA* levels were found to be decreased in a *ccpE* mutant throughout growth and less CP-positive cells were detected. EMSA failed to show that activation of *cap* is by direct DNA binding of CcpE to P_{cap}, suggesting an indirect regulatory mechanism (Hartmann et al., 2014; Batte et al., 2018). In contrast, in another study *capA* transcription was found up-regulated in a *ccpE* mutant in a citrate-dependent manner and direct CcpE-P_{cap} interaction was shown via EMSA (Ding et al., 2014). The reason for these discrepancies remains to be elucidated.

Regarding *cap* repression many regulators seem to primarily target the extended upstream region of P_{cap} and subsequently modulate the activity of the SigB-dependent promoter (Keinhörster et al., 2019). CodY is a repressor of several metabolic and virulence genes including *cap* (Fig. 2A), where it binds to a conserved consensus sequence (AATTTTCW-GAAAATT) (Majerczyk et al., 2010). Binding and thus gene repression is enhanced in the presence of branched chain amino acids and GTP, making CodY most active under conditions of nutrient excess (e.g. early growth phase) (Pohl et al., 2009; Majerczyk et al., 2010). Protein-DNA interaction studies showed that CodY interacts with P_{cap} (Majerczyk et al., 2010; Batte et al., 2018; Lei and Lee, 2018) and footprint analysis revealed that CodY binding reaches into the *capA* coding region (Lei and Lee, 2018). We could show that CodY additionally binds to the upstream region of P_{cap} and that this region is essential and sufficient for the CodY repressive function (Keinhörster et al., 2019). In addition, CodY seems to be required for *cap* repression by XdrA. This

transcription factor was shown to bind to P_{cap} with its binding region overlapping with the downstream binding site of CodY, reaching into the *capA* coding region (McCallum et al., 2010; Lei and Lee, 2018). Thus, the two proteins likely interact functionally or physically to repress *cap*. However, the mechanism of the CodY-XdrA interaction remains to be elucidated (Lei and Lee, 2018).

The transcription factor Rot is inactivated by RNAIII of the Agr system (Boisset et al., 2007) thereby being the mediator of the well-known Agr-dependent *cap* expression (Fig. 2A) (George et al., 2015). The DNA binding motif of Rot remains unresolved but was proposed to contain an 18 bp long section of AT-rich DNA (Killikelly et al., 2015). Rot specifically binds to the upstream region of $P_{cap,}$ interfering with SigB-dependent promoter activity (Keinhörster et al., 2019).

The TCS SaeRS is activated by α-defensins and required for the expression of many virulence factors (Geiger et al., 2008). *cap* is one of the few genes which is repressed by SaeRS (Fig. 2A) (Steinhuber et al., 2003; Luong et al., 2011; George et al., 2015). Regulation occurs by binding of phosphorylated response regulator SaeR to the consensus sequence ($GTTAAN_6GTTAA$) (Sun et al., 2010). In P_{cap} the poorly conserved SaeR binding site is located within the extended upstream region. Phosphorylated SaeR specifically binds to the P_{cap} thereby repressing both SigB- and SigA-dependent promoter activity (Keinhörster et al., 2019).

The sensor kinase AirS of the TCS AirSR contains a redox active Fe-S cluster which can sense oxygen and redox signals. The oxidized AirS phosphorylates the response regulator AirR influencing the expression of many regulatory genes as well as inhibiting *cap* under anaerobic conditions. Binding of AirR to P_{cap} was shown (Sun et al., 2012, 2013) but it remains open whether the binding site is also located within the extended upstream region.

On top of all these regulators controlling *cap* expression on the transcriptional level, post-transcriptional regulation is also important for the function of the CP synthesis machinery. The CapAB tyrosine kinase complex controls multiple enzymatic checkpoints through reversible phosphorylation in order to modulate the consumption of essential precursors that are also used in peptidoglycan biosynthesis (Rausch et al., 2019). Furthermore, CP biosynthesis was linked to tyrosine phosphorylation via the Ser/Thr kinase PknB, which can sense cellular lipid II levels (Hardt et al., 2017). PknB signaling serves to reduce CapAB autokinase activity and to reduce the CapM glycosyltransferase activity thereby leading to a shutdown of CP production (Rausch et al., 2019). This likely ensures a sufficient supply of precursors for peptidoglycan synthesis and WTA formation.

3.4. Heterogeneous and temporal CP expression

The most prominent feature of *cap* expression is the strict repression in growing bacteria and the highly heterogeneous expression in bacteria from stationary growth phase (George et al., 2015). In non-growing bacteria only a subpopulation of *S. aureus* is found to express CP. Changing environments or mutations in regulatory genes can shift the ratio of CP-positive bacteria or the onset of *cap* expression during the growth cycle (Fig. 2A and 2B).

On the transcriptional level the temporal and heterogeneous *cap* expression was shown to be determined by direct SigB-dependent regulation and regulators targeting the upstream region of P_{cap} (Keinhörster et al., 2019). Earlier onset of CP production and more CP-positive cells in stationary growth phase could be observed upon constitutive *sigB* expression (Keinhörster et al., 2019), which is consistent with SigB being a known activator of late genes (Bischoff et al., 2001, 2004; Pane-Farre et al., 2006; Mäder et al., 2016). An even more pronounced effect was observed upon chromosomal deletion of the P_{cap} upstream region (Keinhörster et al., 2019). This is in line with the absence of binding sites for the transcriptional repressors Rot and CodY; these being most active during exponential growth phase. In combination, P_{cap} upstream deletion and constitutive *sigB* expression resulted in constitutive *cap* expression and abolished heterogeneity of CP production in stationary phase (Keinhörster et al., 2019). However, CP synthesis remained growth phase-dependent even when *cap* gene expression was rendered constitutive. This is most likely due to the described post-transcriptional levels of regulation (Rausch et al., 2019). Together, the different regulatory circuits ensure that CP is only produced when needed e.g. for phagosomal escape and that a certain sub-population is CP-negative to allow adherence to host cells. Furthermore they help to avoid conflict in precursor usage by machineries involved in either synthesis of CP or other glycopolymers in growing bacterial cells.

4. Conclusions

Biosynthesis of secondary cell wall glycopolymers has to be tightly controlled to ensure their diverse functions during infection. Further studies are required to unravel the regulatory network that governs WTA biosynthesis and modification. It can be anticipated that many regulatory pathways are involved, possibly resulting in a high degree of heterogeneity with regard to WTA quantity and modification at the single-cell level. So far there are limited tools available to study such variation. In contrast, regulation of CP is much more studied and several involved regulators were identified. CP synthesis is tightly controlled at the transcriptional level, and together with post-transcriptional mechanisms these regulatory circuits determine the peculiar temporal and heterogeneous CP expression. One can assume that such non-genetic variability contributes significantly to the evolutionary success of the species by increasing fitness of the bacterial population.

Acknowledgement

Our work was supported by grants from the German Research Council (DFG) SFB766/A7 to CWe and CWo. The authors have no conflict of interest to declare.

References

Ansari, S., Jha, R.K., Mishra, S.K., Tiwari, B.R., Asaad, A.M., 2019. Recent advances in Staphylococcus aureus infection: focus on vaccine development. Infect. Drug Resist. 12, 1243–1255.

Arbeit, R.D., Dunn, R.M., 1987. Expression of capsular polysaccharide during experimental focal infection with Staphylococcus aureus. J. Infect. Dis. 156 (6), 947–952.

Arbeit, R.D., Nelles, M.J., 1987. Capsular polysaccharide antigenemia in rats with experimental endocarditis due to Staphylococcus aureus. J. Infect. Dis. 155 (2), 242–246.

Baddour, L.M., Lowrance, C., Albus, A., Lowrance, J.H., Anderson, S.K., Lee, J.C., 1992. Staphylococcus aureus microcapsule expression attenuates bacterial virulence in a rat model of experimental endocarditis. J. Infect. Dis. 165 (4), 749–753.

Batte, J.L., Sahukhal, G.S., Elasri, M.O., 2018. MsaB and CodY interact to regulate Staphylococcus aureus capsule in a nutrient-dependent manner. J. Bacteriol. 200 (17), e00294–00218.

Batte, J.L., Samanta, D., Elasri, M.O., 2016. MsaB activates capsule production at the transcription level in Staphylococcus aureus. Microbiology 162 (3), 575–589.

Bertsche, U., Weidenmaier, C., Kuehner, D., Yang, S.J., Baur, S., Wanner, S., Francois, P., Schrenzel, J., Yeaman, M.R., Bayer, A.S., 2011. Correlation of daptomycin resistance in a clinical Staphylococcus aureus strain with increased cell wall teichoic acid production and D-alanylation. Antimicrob. Agents Chemother. 55 (8), 3922–3928.

Bertsche, U., Yang, S.J., Kuehner, D., Wanner, S., Mishra, N.N., Roth, T., Nega, M., Schneider, A., Mayer, C., Grau, T., Bayer, A.S., Weidenmaier,

C., 2013. Increased cell wall teichoic acid production and D-alanylation are common phenotypes among daptomycin-resistant methicillin-resistant Staphylococcus aureus (MRSA) clinical isolates. PLoS One 8 (6), e67398.

Bischoff, M., Brelle, S., Minatelli, S., Molle, V., 2016. Stk1-mediated phosphorylation stimulates the DNA-binding properties of the Staphylococcus aureus SpoVG transcriptional factor. Biochem. Biophys. Res. Commun. 473 (4), 1223–1228.

Bischoff, M., Dunman, P., Kormanec, J., Macapagal, D., Murphy, E., Mounts, W., Berger-Bächi, B., Projan, S., 2004. Microarray-based analysis of the Staphylococcus aureus sigmaB regulon. J. Bacteriol. 186 (13), 4085–4099.

Bischoff, M., Entenza, J.M., Giachino, P., 2001. Influence of a functional sigB operon on the global regulators sar and agr in Staphylococcus aureus. J. Bacteriol. 183 (17), 5171–5179.

Boisset, S., Geissmann, T., Huntzinger, E., Fechter, P., Bendridi, N., Possedko, M., Chevalier, C., Helfer, A.C., Benito, Y., Jacquier, A., Gaspin, C., Vandenesch, F., Romby, P., 2007. Staphylococcus aureus RNAIII coordinately represses the synthesis of virulence factors and the transcription regulator Rot by an antisense mechanism. Genes Dev. 21 (11), 1353–1366.

Boyle-Vavra, S., Li, X., Alam, M.T., Read, T.D., Sieth, J., Cywes-Bentley, C., Dobbins, G., David, M.Z., Kumar, N., Eells, S.J., Miller, L.G., Boxrud, D.J., Chambers, H.F., Lynfield, R., Lee, J.C., Daum, R.S., 2015. USA300 and USA500 clonal lineages of Staphylococcus aureus do not produce a capsular polysaccharide due to conserved mutations in the cap5 locus. MBio 6 (2), e02585–02514.

Brown, S., Santa Maria Jr., J.P., Walker, S., 2013. Wall teichoic acids of gram-positive bacteria. Annu. Rev. Microbiol. 67, 313–336.

Brown, S., Xia, G., Luhachack, L.G., Campbell, J., Meredith, T.C., Chen, C., Winstel, V., Gekeler, C., Irazoqui, J.E., Peschel, A., Walker, S., 2012. Methicillin resistance in Staphylococcus aureus requires glycosylated wall teichoic acids. Proc Natl Acad Sci U S A 109 (46), 18909–18914.

Burian, M., Rautenberg, M., Kohler, T., Fritz, M., Krismer, B., Unger, C., Hoffmann, W.H., Peschel, A., Wolz, C., Goerke, C., 2010. Temporal expression of adhesion factors and activity of global regulators during establishment of Staphylococcus aureus nasal colonization. J. Infect. Dis. 201 (9), 1414–1421.

Caballero, C.J., Menendez-Gil, P., Catalan-Moreno, A., Vergara-Irigaray, M., Garcia, B., Segura, V., Irurzun, N., Villanueva, M., Ruiz de Los Mozos, I., Solano, C., Lasa, I., Toledo-Arana, A., 2018. The regulon of the RNA chaperone CspA and its auto-regulation in Staphylococcus aureus. Nucleic Acids Res. 46 (3), 1345–1361.

Campbell, J., Singh, A.K., Swoboda, J.G., Gilmore, M.S., Wilkinson, B.J., Walker, S., 2012. An antibiotic that inhibits a late step in wall teichoic acid biosynthesis induces the cell wall stress stimulon in Staphylococcus aureus. Antimicrob. Agents Chemother. 56 (4), 1810–1820.

Chan, Y.G., Kim, H.K., Schneewind, O., Missiakas, D., 2014. The capsular polysaccharide of Staphylococcus aureus is attached to peptidoglycan by the LytR-CpsA-Psr (LCP) family of enzymes. J. Biol. Chem. 289 (22), 15680–15690.

Chen, Z., Luong, T.T., Lee, C.Y., 2007. The sbcDC locus mediates repression of type 5 capsule production as part of the SOS response in Staphylococcus aureus. J. Bacteriol. 189 (20), 7343–7350.

Cocchiaro, J.L., Gomez, M.I., Risley, A., Solinga, R., Sordelli, D.O., Lee, J.C., 2006. Molecular characterization of the capsule locus from non-typeable Staphylococcus aureus. Mol. Microbiol. 59 (3), 948–960.

Conlon, B.P., Rowe, S.E., Gandt, A.B., Nuxoll, A.S., Donegan, N.P., Zalis, E.A., Clair, G., Adkins, J.N., Cheung, A.L., Lewis, K., 2016. Persister formation in Staphylococcus aureus is associated with ATP depletion. Nat. Microbiol. 1 (5), 16051.

Cunnion, K.M., Lee, J.C., Frank, M.M., 2001. Capsule production and growth phase influence binding of complement to Staphylococcus aureus. Infect. Immun. 69 (11), 6796–6803.

Dassy, B., Fournier, J.M., 1996. Respiratory activity is essential for post-exponential-phase production of type 5 capsular polysaccharide by Staphylococcus aureus. Infect. Immun. 64 (7), 2408–2414.

Dassy, B., Hogan, T., Foster, T.J., Fournier, J.M., 1993. Involvement of the accessory gene regulator (agr) in expression of type 5 capsular polysaccharide by Staphylococcus aureus. J. Gen. Microbiol. 139 (Pt 6), 1301–1306.

Dassy, B., Stringfellow, W.T., Lieb, M., Fournier, J.M., 1991. Production of type 5 capsular polysaccharide by Staphylococcus aureus grown in a semi-synthetic medium. J. Gen. Microbiol. 137 (5), 1155–1162.

Ding, Y., Liu, X., Chen, F., Di, H., Xu, B., Zhou, L., Deng, X., Wu, M., Yang, C.G., Lan, L., 2014. Metabolic sensor governing bacterial virulence in Staphylococcus aureus. Proc Natl Acad Sci U S A 111 (46), E4981–4990.

Donegan, N.P., Manna, A.C., Tseng, C.W., Liu, G.Y., Cheung, A.L., 2019. CspA regulation of Staphylococcus aureus carotenoid levels and sigma(B) activity is controlled by YjbH and Spx. Mol. Microbiol. https://doi.org/10.1111/mmi.14273.

Endl, J., Seidl, H.P., Fiedler, F., Schleifer, K.H., 1983. Chemical composition and structure of cell wall teichoic acids of staphylococci. Arch. Microbiol. 135 (3), 215–223.

Falord, M., Mäder, U., Hiron, A., Debarbouille, M., Msadek, T., 2011. Investigation of the Staphylococcus aureus GraSR regulon reveals novel links to virulence, stress response and cell wall signal transduction pathways. PLoS One 6 (7), e21323.

Fournier, J.M., Hannon, K., Moreau, M., Karakawa, W.W., Vann, W.F., 1987. Isolation of type 5 capsular polysaccharide from Staphylococcus aureus. Ann. Inst. Pasteur Microbiol. 138 (5), 561–567.

Fournier, J.M., Vann, W.F., Karakawa, W.W., 1984. Purification and characterization of Staphylococcus aureus type 8 capsular polysaccharide. Infect. Immun. 45 (1), 87–93.

Freeman, Z.N., Dorus, S., Waterfield, N.R., 2013. The KdpD/KdpE two-component system: integrating K(+) homeostasis and virulence. PLoS Pathog. 9 (3), e1003201.

Gaupp, R., Wirf, J., Wonnenberg, B., Biegel, T., Eisenbeis, J., Graham, J., Herrmann, M., Lee, C.Y., Beisswenger, C., Wolz, C., Tschernig, T., Bischoff, M., Somerville, G.A., 2016. RpiRc is a pleiotropic effector of virulence determinant synthesis and attenuates pathogenicity in Staphylococcus aureus. Infect. Immun. 84 (7), 2031–2041.

Geiger, T., Goerke, C., Mainiero, M., Kraus, D., Wolz, C., 2008. The virulence regulator Sae of Staphylococcus aureus: promoter activities and response to phagocytosis-related signals. J. Bacteriol. 190 (10), 3419–3428.

George, S.E., Nguyen, T., Geiger, T., Weidenmaier, C., Lee, J.C., Liese, J., Wolz, C., 2015. Phenotypic heterogeneity and temporal expression of the capsular polysaccharide in Staphylococcus aureus. Mol. Microbiol. 98 (6), 1073–1088.

Gerlach, D., Guo, Y., De Castro, C., Kim, S.H., Schlatterer, K., Xu, F.F., Pereira, C., Seeberger, P.H., Ali, S., Codee, J., Sirisarn, W., Schulte, B., Wolz, C., Larsen, J., Molinaro, A., Lee, B.L., Xia, G., Stehle, T., Peschel, A., 2018. Methicillin-resistant Staphylococcus aureus alters cell wall glycosylation to evade immunity. Nature 563 (7733), 705–709.

Goerke, C., Esser, S., Kümmel, M., Wolz, C., 2005. Staphylococcus aureus strain designation by agr and cap polymorphism typing and delineation of agr diversification by sequence analysis. Int. J. Med. Microbiol. 295 (2), 67–75.

Graham, J.W., Lei, M.G., Lee, C.Y., 2013. Trapping and identification of cellular substrates of the Staphylococcus aureus ClpC chaperone. J. Bacteriol. 195 (19), 4506–4516.

Gupta, R.K., Alba, J., Xiong, Y.Q., Bayer, A.S., Lee, C.Y., 2013. MgrA activates expression of capsule genes, but not the alpha-toxin gene in experimental Staphylococcus aureus endocarditis. J. Infect. Dis. 208 (11), 1841–1848.

Hardt, P., Engels, I., Rausch, M., Gajdiss, M., Ulm, H., Sass, P., Ohlsen, K., Sahl, H.G., Bierbaum, G., Schneider, T., Grein, F., 2017. The cell wall precursor lipid II acts as a molecular signal for the Ser/Thr kinase PknB of Staphylococcus aureus. Int. J. Med. Microbiol. 307 (1), 1–10.

Hartmann, T., Baronian, G., Nippe, N., Voss, M., Schulthess, B., Wolz, C., Eisenbeis, J., Schmidt-Hohagen, K., Gaupp, R., Sunderkötter, C., Beisswenger, C., Bals, R., Somerville, G.A., Herrmann, M., Molle, V., Bischoff, M., 2014. The catabolite control protein E (CcpE) affects virulence determinant production and pathogenesis of Staphylococcus aureus. J. Biol. Chem. 289 (43), 29701–29711.

Hartmann, T., Zhang, B., Baronian, G., Schulthess, B., Homerova, D., Grubmüller, S., Kutzner, E., Gaupp, R., Bertram, R., Powers, R., Eisenreich, W., Kormanec, J., Herrmann, M., Molle, V., Somerville, G.A., Bischoff, M., 2013. Catabolite control protein E (CcpE) is a LysR-type transcriptional regulator of tricarboxylic acid cycle activity in Staphylococcus aureus. J. Biol. Chem. 288 (50), 36116–36128.

Herbert, S., Newell, S.W., Lee, C., Wieland, K.P., Dassy, B., Fournier, J.M., Wolz, C., Döring, G., 2001. Regulation of Staphylococcus aureus type 5 and type 8 capsular polysaccharides by CO2. J. Bacteriol. 183 (15), 4609–4613.

Herbert, S., Worlitzsch, D., Dassy, B., Boutonnier, A., Fournier, J.M., Bellon, G., Dalhoff, A., Döring, G., 1997. Regulation of Staphylococcus aureus capsular polysaccharide type 5: CO2 inhibition in vitro and in vivo. J. Infect. Dis. 176 (2), 431–438.

Jansen, A., Szekat, C., Schröder, W., Wolz, C., Goerke, C., Lee, J.C., Türck, M., Bierbaum, G., 2013. Production of capsular polysaccharide does not influence Staphylococcus aureus vancomycin susceptibility. BMC Microbiol. 13, 65.

Jones, C., 2005. Revised structures for the capsular polysaccharides from Staphylococcus aureus Types 5 and 8, components of novel glycoconjugate vaccines. Carbohydr. Res. 340 (6), 1097–1106.

Jutras, B.L., Chenail, A.M., Rowland, C.L., Carroll, D., Miller, M.C., Bykowski, T., Stevenson, B., 2013. Eubacterial SpoVG homologs constitute a new family of site-specific DNA-binding proteins. PLoS One 8 (6), e66683.

Katzif, S., Lee, E.H., Law, A.B., Tzeng, Y.L., Shafer, W.M., 2005. CspA regulates pigment production in Staphylococcus aureus through a SigB-dependent mechanism. J. Bacteriol. 187 (23), 8181–8184.

Keinhörster, D., Salzer, A., Duque-Jaramillo, A., George, S.E., Marincola, G., Lee, J.C., Weidenmaier, C., Wolz, C., 2019. Revisiting the regulation of the capsular polysaccharide biosynthesis gene cluster in Staphylococcus aureus. Mol. Microbiol.in press.

Killikelly, A., Benson, M.A., Ohneck, E.A., Sampson, J.M., Jakoncic, J., Spurrier, B., Torres, V.J., Kong, X.P., 2015. Structure-based functional characterization of repressor of toxin (Rot), a central regulator of Staphylococcus aureus virulence. J. Bacteriol. 197 (1), 188–200.

Koc, C., Gerlach, D., Beck, S., Peschel, A., Xia, G., Stehle, T., 2015. Structural and enzymatic analysis of TarM glycosyltransferase from Staphylococcus aureus reveals an oligomeric protein specific for the glycosylation of wall teichoic acid. J. Biol. Chem. 290 (15), 9874–9885.

Koprivnjak, T., Mlakar, V., Swanson, L., Fournier, B., Peschel, A., Weiss, J.P., 2006. Cation-induced transcriptional regulation of the dlt operon of Staphylococcus aureus. J. Bacteriol. 188 (10), 3622–3630.

Lattar, S.M., Tuchscherr, L.P., Caccuri, R.L., Centron, D., Becker, K., Alonso, C.A., Barberis, C., Miranda, G., Buzzola, F.R., von Eiff, C., Sordelli, D.O., 2009. Capsule expression and genotypic differences among Staphylococcus aureus isolates from patients with chronic or acute osteomyelitis. Infect. Immun. 77 (5), 1968–1975.

Lee, J.C., Takeda, S., Livolsi, P.J., Paoletti, L.C., 1993. Effects of in vitro and in vivo growth conditions on expression of type 8 capsular polysaccharide by Staphylococcus aureus. Infect. Immun. 61 (5), 1853–1858.

Lei, M.G., Lee, C.Y., 2015. RbsR activates capsule but represses the rbsUDK operon in Staphylococcus aureus. J. Bacteriol. 197 (23), 3666–3675.

Lei, M.G., Lee, C.Y., 2018. Repression of capsule production by XdrA and CodY in Staphylococcus aureus. J. Bacteriol. 200 (18), e00203–00218.

Li, L., Wang, G., Cheung, A., Abdelhady, W., Seidl, K., Xiong, Y.Q., 2019. MgrA governs adherence, host cell interaction, and virulence in a murine model of bacteremia due to Staphylococcus aureus. J. Infect. Dis. https://doi.org/10.1093/infdis/jiz219, jiz219.

Luong, T., Sau, S., Gomez, M., Lee, J.C., Lee, C.Y., 2002. Regulation of Staphylococcus aureus capsular polysaccharide expression by agr and sarA. Infect. Immun. 70 (2), 444–450.

Luong, T.T., Lee, C.Y., 2006. The arl locus positively regulates Staphylococcus aureus type 5 capsule via an mgrA-dependent pathway. Microbiology 152 (Pt 10), 3123–3131.

Luong, T.T., Sau, K., Roux, C., Sau, S., Dunman, P.M., Lee, C.Y., 2011. Staphylococcus aureus ClpC divergently regulates capsule via sae and codY in strain Newman but activates capsule via codY in strain UAMS-1 and in strain Newman with repaired saeS. J. Bacteriol. 193 (3), 686–694.

Mäder, U., Nicolas, P., Depke, M., Pane-Farre, J., Debarbouille, M., van der Kooi-Pol, M.M., Guerin, C., Derozier, S., Hiron, A., Jarmer, H., Leduc, A., Michalik, S., Reilman, E., Schaffer, M., Schmidt, F., Bessieres, P., Noirot, P., Hecker, M., Msadek, T., Völker, U., van Dijl, J.M., 2016. Staphylococcus aureus transcriptome architecture: from laboratory to infection-mimicking conditions. PLoS Genet. 12 (4), e1005962.

Majerczyk, C.D., Dunman, P.M., Luong, T.T., Lee, C.Y., Sadykov, M.R., Somerville, G.A., Bodi, K., Sonenshein, A.L., 2010. Direct targets of CodY in Staphylococcus aureus. J. Bacteriol. 192 (11), 2861–2877.

McCallum, N., Hinds, J., Ender, M., Berger-Bächi, B., Stutzmann Meier, P., 2010. Transcriptional profiling of XdrA, a new regulator of spa transcription in Staphylococcus aureus. J. Bacteriol. 192 (19), 5151–5164.

McLoughlin, R.M., Solinga, R.M., Rich, J., Zaleski, K.J., Cocchiaro, J.L., Risley, A., Tzianabos, A.O., Lee, J.C., 2006. CD4+ T cells and CXC chemokines modulate the pathogenesis of Staphylococcus aureus wound infections. Proc Natl Acad Sci U S A 103 (27), 10408–10413.

Meier, S., Goerke, C., Wolz, C., Seidl, K., Homerova, D., Schulthess, B., Kormanec, J., Berger-Bächi, B., Bischoff, M., 2007. sigmaB and the sigmaB-dependent arlRS and yabJ-spoVG loci affect capsule formation in Staphylococcus aureus. Infect. Immun. 75 (9), 4562–4571.

Meredith, T.C., Swoboda, J.G., Walker, S., 2008. Late-stage polyribitol phosphate wall teichoic acid biosynthesis in Staphylococcus aureus. J. Bacteriol. 190 (8), 3046–3056.

Mistretta, N., Brossaud, M., Telles, F., Sanchez, V., Talaga, P., Rokbi, B., 2019. Glycosylation of Staphylococcus aureus cell wall teichoic acid is influenced by environmental conditions. Sci. Rep. 9 (1), 3212.

Mohamed, N., Timofeyeva, Y., Jamrozy, D., Rojas, E., Hao, L., Silmon de Monerri, N.C., Hawkins, J., Singh, G., Cai, B., Liberator, P., Sebastian, S., Donald, R.G.K., Scully, I.L., Jones, C.H., Creech, C.B., Thomsen, I., Parkhill, J., Peacock, S.J., Jansen, K.U., Holden, M.T.G., Anderson, A.S., 2019. Molecular epidemiology and expression of capsular polysaccharides in Staphylococcus aureus clinical isolates in the United States. PLoS One 14 (1), e0208356.

Moreau, M., Richards, J.C., Fournier, J.M., Byrd, R.A., Karakawa, W.W., Vann, W.F., 1990. Structure of the type 5 capsular polysaccharide of Staphylococcus aureus. Carbohydr. Res. 201 (2), 285–297.

Moscoso, J.A., Schramke, H., Zhang, Y., Tosi, T., Dehbi, A., Jung, K., Gründling, A., 2016. Binding of cyclic di-AMP to the Staphylococcus aureus sensor kinase KdpD occurs via the universal stress protein domain and downregulates the expression of the Kdp potassium transporter. J. Bacteriol. 198 (1), 98–110.

Nanra, J.S., Buitrago, S.M., Crawford, S., Ng, J., Fink, P.S., Hawkins, J., Scully, I.L., McNeil, L.K., Aste-Amezaga, J.M., Cooper, D., Jansen, K.U., Anderson, A.S., 2013. Capsular polysaccharides are an important immune evasion mechanism for Staphylococcus aureus. Hum. Vaccin. Immunother. 9 (3), 480–487.

Nemeth, J., Lee, J.C., 1995. Antibodies to capsular polysaccharides are not protective against experimental Staphylococcus aureus endocarditis. Infect. Immun. 63 (2), 375–380.

Neuhaus, F.C., Baddiley, J., 2003. A continuum of anionic charge: structures and functions of D-alanyl-teichoic acids in gram-positive bacteria. Microbiol. Mol. Biol. Rev. 67 (4), 686–723.

Nilsson, I.M., Lee, J.C., Bremell, T., Ryden, C., Tarkowski, A., 1997. The role of staphylococcal polysaccharide microcapsule expression in septicemia and septic arthritis. Infect. Immun. 65 (10), 4216–4221.

O'Riordan, K., Lee, J.C., 2004. Staphylococcus aureus capsular polysaccharides. Clin. Microbiol. Rev. 17 (1), 218–234.

Ouyang, S., Sau, S., Lee, C.Y., 1999. Promoter analysis of the cap8 operon, involved in type 8 capsular polysaccharide production in Staphylococcus aureus. J. Bacteriol. 181 (8), 2492–2500.

Pane-Farre, J., Jonas, B., Förstner, K., Engelmann, S., Hecker, M., 2006. The sigmaB regulon in Staphylococcus aureus and its regulation. Int. J. Med. Microbiol. 296 (4-5), 237–258.

Peschel, A., Otto, M., Jack, R.W., Kalbacher, H., Jung, G., Götz, F., 1999. Inactivation of the dlt operon in Staphylococcus aureus confers sensitivity to defensins, protegrins, and other antimicrobial peptides. J. Biol. Chem. 274 (13), 8405–8410.

Pohl, K., Francois, P., Stenz, L., Schlink, F., Geiger, T., Herbert, S., Goerke, C., Schrenzel, J., Wolz, C., 2009. CodY in Staphylococcus aureus: a regulatory link between metabolism and virulence gene expression. J. Bacteriol. 191 (9), 2953–2963.

Pohlmann-Dietze, P., Ulrich, M., Kiser, K.B., Döring, G., Lee, J.C., Fournier, J.M., Botzenhart, K., Wolz, C., 2000. Adherence of Staphylococcus aureus to endothelial cells: influence of capsular polysaccharide, global regulator agr, and bacterial growth phase. Infect. Immun. 68 (9), 4865–4871.

Portoles, M., Kiser, K.B., Bhasin, N., Chan, K.H., Lee, J.C., 2001. Staphylococcus aureus Cap5O has UDP-ManNAc dehydrogenase activity and is essential for capsule expression. Infect. Immun. 69 (2), 917–923.

Poupel, O., Proux, C., Jagla, B., Msadek, T., Dubrac, S., 2018. SpdC, a novel virulence factor, controls histidine kinase activity in Staphylococcus aureus. PLoS Pathog. 14 (3), e1006917.

Poutrel, B., Gilbert, F.B., Lebrun, M., 1995. Effects of culture conditions on production of type 5 capsular polysaccharide by human and bovine Staphylococcus aureus strains. Clin. Diagn. Lab. Immunol. 2 (2), 166–171.

Poutrel, B., Rainard, P., Sarradin, P., 1997. Heterogeneity of cell-associated CP5 expression on Staphylococcus aureus strains demonstrated by flow cytometry. Clin. Diagn. Lab. Immunol. 4 (3), 275–278.

Prados, J., Linder, P., Redder, P., 2016. TSS-EMOTE, a refined protocol for a more complete and less biased global mapping of transcription start sites in bacterial pathogens. BMC Genomics 17 (1), 849.

Price-Whelan, A., Poon, C.K., Benson, M.A., Eidem, T.T., Roux, C.M., Boyd, J.M., Dunman, P.M., Torres, V.J., Krulwich, T.A., 2013. Transcriptional profiling of Staphylococcus aureus during growth in 2 M NaCl leads to clarification of physiological roles for Kdp and Ktr K+ uptake systems. MBio 4 (4), e00407–00413.

Rausch, M., Deisinger, J.P., Ulm, H., Müller, A., Li, W., Hardt, P., Wang, X., Li, X., Sylvester, M., Engeser, M., Vollmer, W., Müller, C.E., Sahl, H.G., Lee, J.C., Schneider, T., 2019. Coordination of capsule assembly and cell wall biosynthesis in Staphylococcus aureus. Nat. Commun. 10 (1), 1404.

Risley, A.L., Loughman, A., Cywes-Bentley, C., Foster, T.J., Lee, J.C., 2007. Capsular polysaccharide masks clumping factor A-mediated adherence of Staphylococcus aureus to fibrinogen and platelets. J. Infect. Dis. 196 (6), 919–927.

Romilly, C., Lays, C., Tomasini, A., Caldelari, I., Benito, Y., Hammann, P., Geissmann, T., Boisset, S., Romby, P., Vandenesch, F., 2014. A non-coding RNA promotes bacterial persistence and decreases virulence by regulating a regulator in Staphylococcus aureus. PLoS Pathog. 10 (3), e1003979.

Sahukhal, G.S., Elasri, M.O., 2014. Identification and characterization of an operon, msaABCR, that controls virulence and biofilm development in Staphylococcus aureus. BMC Microbiol. 14, 154.

Sau, S., Sun, J., Lee, C.Y., 1997. Molecular characterization and transcriptional analysis of type 8 capsule genes in Staphylococcus aureus. J. Bacteriol. 179 (5), 1614–1621.

Schade, J., Weidenmaier, C., 2016. Cell wall glycopolymers of Firmicutes and their role as nonprotein adhesins. FEBS Lett. 590 (21), 3758–3771.

Schulthess, B., Bloes, D.A., Francois, P., Girard, M., Schrenzel, J., Bischoff, M., Berger-Bächi, B., 2011. The sigmaB-dependent yabJ-spoVG operon is involved in the regulation of extracellular nuclease, lipase, and pro-

tease expression in Staphylococcus aureus. J. Bacteriol. 193 (18), 4954–4962.
Schulthess, B., Meier, S., Homerova, D., Goerke, C., Wolz, C., Kormanec, J., Berger-Bächi, B., Bischoff, M., 2009. Functional characterization of the sigmaB-dependent yabJ-spoVG operon in Staphylococcus aureus: role in methicillin and glycopeptide resistance. Antimicrob. Agents Chemother. 53 (5), 1832–1839.
Seidl, K., Müller, S., Francois, P., Kriebitzsch, C., Schrenzel, J., Engelmann, S., Bischoff, M., Berger-Bächi, B., 2009. Effect of a glucose impulse on the CcpA regulon in Staphylococcus aureus. BMC Microbiol. 9, 95.
Seidl, K., Stucki, M., Ruegg, M., Goerke, C., Wolz, C., Harris, L., Berger-Bächi, B., Bischoff, M., 2006. Staphylococcus aureus CcpA affects virulence determinant production and antibiotic resistance. Antimicrob. Agents Chemother. 50 (4), 1183–1194.
Sobhanifar, S., Worrall, L.J., Gruninger, R.J., Wasney, G.A., Blaukopf, M., Baumann, L., Lameignere, E., Solomonson, M., Brown, E.D., Withers, S.G., Strynadka, N.C., 2015. Structure and mechanism of Staphylococcus aureus TarM, the wall teichoic acid alpha-glycosyltransferase. Proc Natl Acad Sci U S A 112 (6), E576–585.
Sobhanifar, S., Worrall, L.J., King, D.T., Wasney, G.A., Baumann, L., Gale, R.T., Nosella, M., Brown, E.D., Withers, S.G., Strynadka, N.C., 2016. Structure and mechanism of Staphylococcus aureus TarS, the wall teichoic acid beta-glycosyltransferase involved in methicillin resistance. PLoS Pathog. 12 (12), e1006067.
Steinhuber, A., Goerke, C., Bayer, M.G., Döring, G., Wolz, C., 2003. Molecular architecture of the regulatory locus sae of Staphylococcus aureus and its impact on expression of virulence factors. J. Bacteriol. 185 (21), 6278–6286.
Stringfellow, W.T., Dassy, B., Lieb, M., Fournier, J.M., 1991. Staphylococcus aureus growth and type 5 capsular polysaccharide production in synthetic media. Appl. Environ. Microbiol. 57 (2), 618–621.
Sun, F., Ji, Q., Jones, M.B., Deng, X., Liang, H., Frank, B., Telser, J., Peterson, S.N., Bae, T., He, C., 2012. AirSR, a [2Fe-2S] cluster-containing two-component system, mediates global oxygen sensing and redox signaling in Staphylococcus aureus. J. Am. Chem. Soc. 134 (1), 305–314.
Sun, F., Li, C., Jeong, D., Sohn, C., He, C., Bae, T., 2010. In the Staphylococcus aureus two-component system sae, the response regulator SaeR binds to a direct repeat sequence and DNA binding requires phosphorylation by the sensor kinase SaeS. J. Bacteriol. 192 (8), 2111–2127.
Sun, H., Yang, Y., Xue, T., Sun, B., 2013. Modulation of cell wall synthesis and susceptibility to vancomycin by the two-component system AirSR in Staphylococcus aureus NCTC8325. BMC Microbiol. 13, 286.
Sutra, L., Rainard, P., Poutrel, B., 1990. Phagocytosis of mastitis isolates of Staphylococcus aureus and expression of type 5 capsular polysaccharide are influenced by growth in the presence of milk. J. Clin. Microbiol. 28 (10), 2253–2258.
Swoboda, J.G., Meredith, T.C., Campbell, J., Brown, S., Suzuki, T., Bollenbach, T., Malhowski, A.J., Kishony, R., Gilmore, M.S., Walker, S., 2009. Discovery of a small molecule that blocks wall teichoic acid biosynthesis in Staphylococcus aureus. ACS Chem. Biol. 4 (10), 875–883.
Thakker, M., Park, J.S., Carey, V., Lee, J.C., 1998. Staphylococcus aureus serotype 5 capsular polysaccharide is antiphagocytic and enhances bacterial virulence in a murine bacteremia model. Infect. Immun. 66 (11), 5183–5189.
Tuchscherr, L., Löffler, B., Buzzola, F.R., Sordelli, D.O., 2010. Staphylococcus aureus adaptation to the host and persistence: role of loss of capsular polysaccharide expression. Future Microbiol. 5 (12), 1823–1832.
Tuchscherr, L.P., Buzzola, F.R., Alvarez, L.P., Caccuri, R.L., Lee, J.C., Sordelli, D.O., 2005. Capsule-negative Staphylococcus aureus induces chronic experimental mastitis in mice. Infect. Immun. 73 (12), 7932–7937.
van Dalen, R., De La, Cruz, Diaz, J.S., Rumpret, M., Fuchsberger, F.F., van Teijlingen, N.H., Hanske, J., Rademacher, C., Geijtenbeek, T.B.H., van Strijp, J.A.G., Weidenmaier, C., Peschel, A., Kaplan, D.H., van Sorge, N.M., 2019. Langerhans cells sense Staphylococcus aureus wall teichoic acid through langerin to induce inflammatory responses. MBio 10 (3), e00330–00319.
van Wamel, W., Xiong, Y.Q., Bayer, A.S., Yeaman, M.R., Nast, C.C., Cheung, A.L., 2002. Regulation of Staphylococcus aureus type 5 capsular polysaccharides by agr and sarA in vitro and in an experimental endocarditis model. Microb. Pathog. 33 (2), 73–79.
Wanner, S., Schade, J., Keinhörster, D., Weller, N., George, S.E., Kull, L., Bauer, J., Grau, T., Winstel, V., Stoy, H., Kretschmer, D., Kolata, J., Wolz, C., Bröker, B.M., Weidenmaier, C., 2017. Wall teichoic acids mediate increased virulence in Staphylococcus aureus. Nat. Microbiol. 2, 16257.
Watts, A., Ke, D., Wang, Q., Pillay, A., Nicholson-Weller, A., Lee, J.C., 2005. Staphylococcus aureus strains that express serotype 5 or serotype 8 capsular polysaccharides differ in virulence. Infect. Immun. 73 (6), 3502–3511.
Weidenmaier, C., Lee, J.C., 2017. Structure and function of surface polysaccharides of Staphylococcus aureus. Curr. Top. Microbiol. Immunol. 409, 57–93.
Weidenmaier, C., McLoughlin, R.M., Lee, J.C., 2010. The zwitterionic cell wall teichoic acid of Staphylococcus aureus provokes skin abscesses in mice by a novel CD4+ T-cell-dependent mechanism. PLoS One 5 (10), e13227.
Weidenmaier, C., Peschel, A., 2008. Teichoic acids and related cell-wall glycopolymers in gram-positive physiology and host interactions. Nat. Rev. Microbiol. 6 (4), 276–287.
Winstel, V., Kühner, P., Salomon, F., Larsen, J., Skov, R., Hoffmann, W., Peschel, A., Weidenmaier, C., 2015. Wall teichoic acid glycosylation governs Staphylococcus aureus nasal colonization. MBio 6 (4), e00632.
Winstel, V., Xia, G., Peschel, A., 2014. Pathways and roles of wall teichoic acid glycosylation in Staphylococcus aureus. Int. J. Med. Microbiol. 304 (3-4), 215–221.
Xia, G., Kohler, T., Peschel, A., 2010. The wall teichoic acid and lipoteichoic acid polymers of Staphylococcus aureus. Int. J. Med. Microbiol. 300 (2-3), 148–154.
Xue, T., You, Y., Hong, D., Sun, H., Sun, B., 2011. The Staphylococcus aureus KdpDE two-component system couples extracellular K+ sensing and Agr signaling to infection programming. Infect. Immun. 79 (6), 2154–2167.
Zhao, L., Xue, T., Shang, F., Sun, H., Sun, B., 2010. Staphylococcus aureus AI-2 quorum sensing associates with the KdpDE two-component system to regulate capsular polysaccharide synthesis and virulence. Infect. Immun. 78 (8), 3506–3515.
Zhu, Y., Nandakumar, R., Sadykov, M.R., Madayiputhiya, N., Luong, T.T., Gaupp, R., Lee, C.Y., Somerville, G.A., 2011. RpiR homologues may link Staphylococcus aureus RNAIII synthesis and pentose phosphate pathway regulation. J. Bacteriol. 193 (22), 6187–6196.

Danksagung

An erster Stelle möchte ich mich bei Christiane Wolz für ihre großartige Betreuung bedanken. Du bist eine tolle Arbeitsgruppenleiterin und ich weiß es sehr zu schätzen, dass uns deine Tür immer offensteht. Es ist nicht selbstverständlich, dass wir den Freiraum haben eigenen Ideen nachzugehen und diverse Konferenzen im In- und Ausland besuchen zu können. Hinzu kommt deine verständnisvolle Unterstützung bei allem, was die Promotion direkt betrifft und auch allem darüber hinaus. Ich bin sehr froh, dass ich meine Doktorarbeit unter diesen hervorragenden Bedingungen in deiner Arbeitsgruppe anfertigen konnte.

Ebenfalls möchte ich mich bei meinem zweiten Betreuer Christopher Weidenmaier bedanken. Trotz der großen Entfernung konnte ich mich bei Fragen und Problemen immer an dich wenden.

Andreas Peschel möchte ich für das Erstellen des Zweitgutachtens danken.

Mein Dank gilt außerdem der gesamten Arbeitsgruppe Wolz, insbesondere Petra, Shilpa, Lisa, Carina, Esther, Andrea, Janina, Naty, Isa und Vitty sowie allen ehemaligen Mitarbeiterinnen und Studentinnen (vor allem Alejandra, Anna und Vanessa für ihre tatkräftige Unterstützung). Wir hatten gemeinsam viel Spaß, sei es im Labor, während der Pausen, im Bären, bei unseren Cooking-Days oder auf Konferenzen, wo wir gemeinsam verschiedene Städte erkundet haben. Ich werde gerne daran zurückdenken. Auch allen Doktoranden des SFB und GRK möchte ich danken. Ohne euch hätten die diversen Seminare, Tagungen und Symposien nur halb so viel Spaß gemacht.

Ein großer Dank geht auch an meine Freunde, die mich während der gesamten Studien- und Promotionszeit unterstützt haben. Ihr habt mich abgelenkt, wenn mein Kopf zu sehr mit wissenschaftlichen Inhalten beschäftigt war und mich aufgebaut, wenn Dinge anders liefen als erhofft. Das werde ich euch nie vergessen.

Abschließend möchte ich mich bei meiner Familie inklusive meiner Partnerin bedanken. Ihr habt mich mit viel Liebe, Geduld und Hilfsbereitschaft auf meinem bisherigen Weg begleitet und meine Entscheidungen immer respektiert und unterstützt. Ohne euch wäre ich heute nicht dort, wo ich bin.

Curriculum vitae

Eidesstattliche Erklärung

Ich erkläre hiermit, dass ich die zur Promotion eingereichte Arbeit mit dem Titel

„Regulation of cell wall glycopolymers in *Staphylococcus aureus*"

selbständig verfasst, nur die angegebenen Quellen und Hilfsmittel benutzt und wörtlich oder inhaltlich übernommene Stellen als solche gekennzeichnet habe. Ich erkläre, dass die Richtlinien zur Sicherung guter wissenschaftlicher Praxis der Universität Tübingen beachtet wurden. Ich versichere an Eides statt, dass diese Angaben wahr sind und dass ich nichts verschwiegen habe. Meine eigenen Beiträge zu Gemeinschaftsarbeiten habe ich im Abschnitt „Contribution to publications" dargestellt.

Tübingen, den